Electrochemical Characterization of Cobalt-Chromium-Molybdenum Alloy Hip Implants in Simulated Physiological Solutions

THESIS

submitted in partial fulfillment of the
requirements for the degree of

MASTER OF SCIENCE

in

MATERIALS SCIENCE AND ENGINEERING

by

Nedim Levi B.Sc.
born in Istanbul, Turkey

TUDelft

Delft University of Technology

Abstract

BIOMATERIALS play an essential role in the repair or replacement of bone tissue that has become diseased or damaged. Metals are more suitable candidates for load-bearing applications compared with ceramics or polymeric materials because they combine high mechanical strength and fracture toughness. However, the main limitation of these metallic materials is the release of the toxic metallic ions that can lead to various adverse tissue reactions and/or hypersensitivity reactions.

In this research, the biocompatibility and electrochemical behaviour of CoCrMo alloy were investigated under simulated physiological solutions at 37°C with different surface finish qualities and pH levels. Electrochemical techniques such as open circuit potential, potentiodynamic and potentiostatic polarization, cyclic voltammetry and electrochemical impedance spectroscopy were employed. Furthermore, optical microscopy, SEM-EDS and atomic force microscopy analysis of the alloy surface were carried out. In addition ICP-MS analytical technique was employed to trace released metal ions within the solutions.

It has been observed by the polarization curves, at higher potential values, the passive and the transpassive regions are protected by the chromium oxide film. Based on the ICP-MS results, the highest metal ion release has been seen after the oxidative dissolution of the chromium oxide film. Furthermore, the elemental analysis of the Ringer's solution for the different applied potential levels show that the highest ion release into the electrolyte is from the cobalt. Moreover the electrochemical impedance spectroscopy results show that the increase in the low frequency impedance values together with a more ideal capacitive behaviour with time indicate that the passive film on CoCrMo becomes more protective.

Acknowledgments

ALTHOUGH my name appears as the sole author of the thesis, in reality a number of people are responsible for the work. First and foremost, I would like to thank my thesis advisors, Dr. Arjan Mol from TU Delft and Dr. Mary Ryan from Imperial College London.

Dr. Mary Ryan gave the first inspiration about my research topic and showed the courtesy to be my supervisor while I was in Imperial College London under IDEA League collaboration. In addition, Dr. Arjan Mol has accepted to be my co-supervisor at TU Delft and encouraged me all the time about my research and always gave valuable criticisms.

I would like to thank my graduation committee members; Prof.dr.ir. J. Sietsma, Dr.ir. M.J.M. Hermans and Dr.ir. M. Janssen for their time and guidance.

Sincere thanks to Dr. Emanuele Cardilli, Dr. Yaiza Gonzalez-Garcia, Dr. Benoit Illy and Dr. Amy Cruickshank for their unlimited and kind cooperation to help and resolve research related problems.

It is my wish to thank Lambert Schipperheijn and Russell J. Stracey for their help in the laboratory work in the conducted research at TU Delft and at Imperial College London.

Many thanks for my colleague, Vanya Uluc for helping and analyzing the experimental work together with me.

My warmest thanks go to my friends, very specially, Sinan, Sertaç, Efe, Mert and Can for making me forget for brief periods of time about my thesis.

Further, I cannot forget to thank "Hillel House" crew, Adam, Vladimir, Lily, Nathan and Awital for their great deal of help during my stay in Netherlands and making me laugh all the time.

Finally, and most importantly, I would like to express gratitude to my family. Even thousands of kilometers apart, they have been present through every step of my life, providing support in difficult times. They have been a constant source of inspiration, and this thesis is dedicated to them.

Last but not least, thanks to my one and only love Meral for her unfailing encouragement and support.

Nedim Levi B.Sc.
Delft, The Netherlands
19 October 2011

v

Contents

List of Figures

List of Tables

Imagination is more important than knowledge. For knowledge is limited to all we now know and understand, while imagination embraces the entire world, and all there ever will be to know and understand.

<div style="text-align: right">

Albert Einstein

</div>

Introduction

1.1 Bio-Implants

BIOMATERIAL is a material used in implants or medical device, intended to interact with biological systems. The Clemson University Advisory Board for Biomaterials has formally defined a biomaterial to be "systemically and pharmacologically inert substance designed for implantation within or incorporation with living systems [1]". Black referred biomaterials as "a nonviable material used in a medical device, intended to interact with biological systems [2]". Other definitions have included "materials of synthetic as well as of natural origin in contact with tissue, blood, and biological fluids, and intended for use for prosthetic, diagnostic, therapeutic, and storage applications without adversely affecting the living organism and its components [3]" and "any substance (other than drugs) or combination of substances, synthetic or natural in origin, which can be used for any period of time, as a whole or as a part of a system which treats, augments, or replaces any tissue, organ, or function of the body [4]".

Therefore, it is a must that a biomaterial always has be considered in its final fabricated and sterilized form. Substitute heart valves and artificial hearts, artificial hip and knee joints, dental implants, internal as well as external fracture fixators, skin repair templates as well as dialysers to support kidney functions or intraocular lenses can be couple of numerous biomaterial examples. A material that can be used for medical application must possess a lot of specific characteristics, of which the most fundamental requirements are related with biocompatibility. Since the beginning of 21st century, considerable progress has been achieved in order to understand the interactions between the tissues and the materials. It has been acknowledged that there are profound differences between non-living (avital) and living (vital) materials.

Researchers have introduced the words "biomaterial" and "biocompatibility" to indicate the biological performance of materials. Thus, materials that are biocompatible can be considered as biomaterials, and the biocompatibility is a descriptive term which indicates the ability of a material to perform with an appropriate host response, in a specific application [5]. Researchers extended this definition and distinguished between surface and structural compatibility of an implant. Surface compatibility means the chemical, biological, and physical suitability of an implant surface to the host tissues. Structural compatibility is the optimal adaptation to the mechanical behavior of the host tissues [6]. Optimal interaction between biomaterial and host tissue can be talked about when both the surface and the structural compatibilities are opposed. Furthermore, it needs to be underlined that the success degree of a biomaterial in the body also depends on many other parameters such as surgical technique (degree of trauma imposed during implantation, sterilization methods, etc), health condition and activities of the patient. Ramakrishna et al. summarized several important factors that can be considered in selecting a material for a biomedical application at Table 1.1 [7].

The performance of materials in the body can be classified in many ways. First, biomaterials may be considered from the point of view of the problem area that is to be solved, as

Table 1.1: Various Factors in Material Selection for Biomedical Applications [7]

Factors	Descriptions		
	Chemical & Biological Characteristics	Physical Characteristics	Mechanical & Structural Characteristics
1st Level Material Properties	• Chemical Composition (Bulk and Surface)	• Density	• Elastic Modulus • Shear Modulus • Poissons Ratio • Yield Strength • Tensile Strength • Compressive Strength
2nd Level Material Properties	• Adhesion	• Surface Topology • Texture • Roughness	• Hardness • Flexural Modulus • Flexural Strength
Specific Functional Requirements	• Biofunctionality • Bioinert • Bioactive • Biostability • Biodegradation Behaviour	• Forms & Geometry • Thermal Expansion Coefficient • Electrical Conductivity • Color, Aesthetics • Refractive Index • Opacity	• Stiffness or Rigidity • Fracture Toughness • Fatigue Strength • Creep Resistance • Friction and Wear Resistance • Adhesion Strength • Proof Stress • Abrasion Resistance
Processing & Fabrication	Reproducibility, Quality, Sterilizability, Packaging, Secondary Process Ability		
Characteristics of Host: Tissue, Organ, Species, Age, Sex, Race, Health Condition, Activity			
Medical/Surgical Procedure, Period of Application/Usage			
Cost			

Table 1.2: Uses of Biomaterials [7]

Problem	Area Examples
Replacement of Diseased of Damaged Part	Artificial Hip Joint, Kidney Dialysis Machine
Assist in Healing	Sutures, Bone Plates, Screw
Improve Function	Cardiac Pacemaker, Intraocular Lens
Correct Functional Abnormality	Cardiac Pacemaker
Correct Cosmetic Problem	Augmentation Mammoplasty, Chin Augmentation
Aid to Diagnosis	Probes and Catheters
Aid to Treatment	Catheters, Drains

Table 1.3: Biomaterials in Organs [7]

Organ	Examples
Heart	Cardiac Pacemaker, Artificial Heart Valve, Total Artificial Heart
Lung	Oxygenator Machine
Eye	Contact Lenses, Intraocular Lenses
Ear	Artificial Stapes, Cochlea Implant
Bone	Bone Plate, Intramedullary Rod
Kidney	Kidney Dialysis Machine
Bladder	Catheter & Stent

in Table 1.2. Second, it can be considered on a tissue level, an organ level (Table 1.3), or a system level (Table 1.4). Third, materials can be classified as polymers, metals, ceramics, and composites as in Table 1.5.

The use of biomaterials did not become practical until the advent of an aseptic surgical technique developed by Dr. J. Lister in the 1860s. Earlier surgical procedures, whether they involved biomaterials or not, were generally unsuccessful as a result of infection. Problems of infection tend to raised up in the presence of biomaterials, since the implant can provide a region inaccessible to the bodys immunologically competent cells. The earliest successful

Table 1.4: Biomaterials in Body Systems [7]

System	Examples
Skeletal	Bone Plate, Total Joint Replacements
Muscular	Sutures, Muscle Stimulator
Circulatory	Artificial Heart Valves, Blood Vessels
Respiratory	Oxygenator Machine
Integumentary	Sutures, Burn Dressings, Artificial Skin
Urinary	Catheters, Stent, Kidney Dialysis Machine
Nervous	Hydrocephalus Drain, Cardiac Pacemaker, Nerve Stimulator
Endocrine	Microencapsulated Pancreatic Islet Cells
Reproductive	Augmentation Mammoplasty, Other Cosmetic Replacements

Table 1.5: Materials for Use in the Body [7]

Materials	Advantages	Disadvantages	Examples
Polymers • Nylon • Silicone Rubber • Polyester	• Resilient • Easy to Fabricate	• Not Strong • Deforms with Time • May Degrade	• Sutures, Blood Vessels, Hip Socket, Ear, Nose, Other Soft Tissues
Metals • Ti and Its Alloy • Co-Cr Alloys • Stainless Steels • Au • Pt	• Strong • Ductile • Tough	• May Corrode • Dense • Difficult to Make	• Joint Replacements, Bone Plates and Screws, Dental Root Implants, Pacer and Suture Wires
Ceramics • Aluminum Oxide • Calcium Phosphates • Hydroxyapatite	• Very Biocompatible • Inert • Strong in Compression	• Brittle • Not Resilient • Difficult to Make	• Dental, Femoral Head of Hip Replacement, Coating of Dental And Orthopedic Implants
Composites • Carbon-Carbon • Wire or Fiber Reinforced Bone Cement	• Strong • Tailor-Made	• Difficult to Make	• Joint Implants, Heart Valves

implants, as well as a large fraction of modern ones, were in the skeletal system. Table 1.6 lists notable developments relating to implants [8].

Also it can be seen at Figure 1.1 how biomaterials can take place within the body and compensate natural cells or bones functions.

METALS

Cranial Plates
 Ti, Ti Alloys
 316L Stainless Steel
 Ta

Orbit Reconstruction
 Co-Cr Mesh
 Ti Mesh

Maxillofacial Reconstruction
 Ti, Ti Mesh
 Ti, Al Valloy

Dental Implants
 316L Stainless Steel
 Co-Cr-Mo Alloys
 Ti, Ti Alloys

Bone Fracture Fixation
 316L Stainless Steel
 Co-Cr-Mo Alloys
 Ti, Ti Alloys

Harrington Road
(spinal manipulation)
 Co-Cr-Mo Alloy
 316L Stainless Steel

Prosthetic Joints
(hip, knee, shoulder,
elbow, wrist)
 316L Stainless Steel
 Co-Cr-Mo Alloys
 Ti
 Ti-Al-V-Alloys
Harrington Rods
 Co-Cr-Mo Alloys

BIOCERAMICS

Cranial Repair
 Bioactive Glasses
Karatoprostheses (Eye Lens)
 Al_2O_3
Otolaryngological Implants
 Al_2O_3
 HA
 Bioactive Glasses
 Bioactive Glass--Ceramics
Maxillofacial Reconstruction
 Al_2O_3
 HA
 HA-PLA Composite
 Bioactive Glasses
Dental Implants
 Al_2O_3
 HA
 Bioactive Glasses
Alveolar Ridge Augmentations
 Al_2O_3
 HA: TCP
 HA-Autogonous Bone Composite
 HA-PLA Composite
 Bioactive Glasses
Periodontal Pocket Obliteration
 HA
 HA-PLA Composite
 TCP
 Calcium and Phosphate Salts
 Bioactive Glasses
Percutaneous Access Devices
 Bioactive Glass-Ceramics
 Bioactive Glasses
 HA
 Pyrolytic Carbon Coating
Artificial Heart Valves
 Pyrolytic Carbon Coatings
Spinal Surgery
 Bioactive Glass-Ceramic
 HA
Disc Crest Repair
 Bioactive Glass-Ceramic
Bone Space Fillers
 TCP
 Calcium and Phosphate Salts
 Bioactive Glass Granules
 Bioactive Glass-Ceramic Granules
Orthopedic Load-Bearing Applications
 Al2O3
 Stabilized Zirconia
 Pe-HA Composite
Coatings for Chemical Bonding (Orthopedic
 Dental, and Maxillofacial Prosthesis)
 HA
 Bioactive Glasses
 Bioactive Glass-Ceramic
Orthopedic Fixation Devices
 PLA-Carbon Fibers
 PLA-Calcium Phosphate-Based Glass Fibers
Artificial Tendon and Ligamont
 PLA-Carbon-Fiber Composite

Figure 1.1: Clinical Uses of Inorganic Biomaterials [48]

Table 1.6: Notable Developments Relating to Implants [8]

Year	Investigators	Development
Late 18th-19th Century	——	Various Metal Devices To Fix Bone Fractures, Wires and Pins From Fe, Au, Ag and Pt
1860-1870	J. Lister	Aseptic Surgical Techniques
1886	H. Hansmann	Ni-Plated Steel Bone Fracture Plate
1893-1912	W.A. Lane	Steel Screws and Plates
1912	W.D. Sherman	Vanadium Steel Plates, First Developed for Medical Use, Less Stress Concentration and Corrosion
1924	A.A. Zierold	Introduced *Stellites*® (CoCrMo Alloy)
1926	M.Z. Lange	Introduced 18-8sMo Stainless Steel, Better than 18-8 Stainless Steel
1926	E.W. Hey-Groves	Used Carpenters Screw For Femoral Neck Fracture
1931	M.N. Smith-Petersen	First Femoral Neck Fracture Fixation Device Made of Stainless Steel
1936	C.S. Venable, W.G. Stuch	Introduced *Vitallium*® (19-9 Stainless Steel, Later Changed The Material to CoCr Alloy
1938	P. Wiles	First Total Hip Replacement Prosthesis
1939	J.C. Burch, H.M. Carney	Introduced Tantalum (Ta)
1946	J. and R. Judet	First Biomechanically Designed Femoral Head Replacement Prosthesis, First Plastics (PMMA) Used in Joint Replacement
1940s	M.J. Dorzee, A. Franceschetti	First Used Acrylics (PMMA) for Corneal Replacement
1947	J. Cotton	Introduced Ti and its Alloys
1952	A.B. Voorhees, A. Jaretzta, A.B. Blackmore	First Successful Blood Vessel Replacement Made of Cloth For Tissue Ingrowth
1958	S. Furman, G. Robinson	First Successful Direct Heart Stimulation
1958	J. Charnley	First Use of Acrylic Bone Cement in Total Hip Replacement on the Advice of Dr. D. Smith
1960	A. Starr, M.L. Edwards	First Commercial Heart Valves
1970s	W.J. Kolff	Total Heart Replacement

1.2 Materials Choice

1.2.1 Metals

Metals are used as biomaterials due to their excellent electrical and thermal conductivity and mechanical properties. The mobile free electrons act as the binding force to hold the positive metal ions together. This attraction is strong, as evidenced by the closely packed atomic arrangement resulting in high specific gravity and high melting points of most metals. Since the metallic bond is essentially non-directional, the position of the metal ions can be altered

without destroying the crystal structure resulting in a plastically deformable solid [9].

Some metals are used as passive substitutes for hard tissue replacement such as total hip and knee joints, for fracture healing aids as bone plates and screws, spinal fixation devices, and dental implants because of their excellent mechanical properties and corrosion resistance. Some metallic alloys are used for more active roles in devices such as vascular stents, catheter guide wires, orthodontic archwires, and cochlea implants [9].

The first metal alloy developed specifically for human use was the vanadium steel which was used to manufacture bone fracture plates (Sherman plates) and screws. Most metals such as iron (Fe), chromium (Cr), cobalt (Co), nickel (Ni), titanium (Ti), tantalum (Ta), niobium (Nb), molybdenum (Mo), and tungsten (W) that were used to make alloys for manufacturing implants can only be tolerated by the body in minimum amounts [10]. Sometimes those metallic elements, in naturally occurring forms, are essential in red blood cell functions (Fe) or synthesis of a vitamin B12 (Co), but cannot be tolerated in large amounts in the body [2]. The biocompatibility of the metallic implant is of considerable concern because these implants can corrode in an in vivo environment [11]. The consequences of corrosion are the disintegration of the implant material, which will weaken the implant, and the harmful effect of corrosion products on the surrounding tissues and organs.

1.2.2 Ceramics

Ceramics are defined as the art and science of making and using solid articles that have as their essential component inorganic nonmetallic materials [12]. Ceramics are refractory, polycrystalline compounds, usually inorganic, including silicates, metallic oxides, carbides and various refractory hydrides, sulfides, and selenides. Oxides such as Al_2O_3, MgO, SiO_2 and ZrO_2 contain metallic and nonmetallic elements and ionic salts, such as $NaCl$, $CsCl$ and ZnS. Exceptions to the preceding include covalently bonded ceramics such as diamond and carbonaceous structures such as graphite and pyrolized carbons [13]. Until recently, use of ceramics was somewhat limited because of their inherent brittleness, susceptibility to notches or microcracks, low tensile strength, and low impact strength. However, within the last 100 years, innovative techniques for fabricating ceramics have led to their use as "high tech materials ". In recent years, humans have realized that ceramics and their composites can also be used to augment or replace various parts of the body, particularly bone. Thus, the ceramics used for the latter purposes are classified as bioceramics.

Their relative inertness to the body fluids, high compressive strength, and aesthetically pleasing appearance led to the use of ceramics in dentistry as dental crowns. Due to their high specific strength as fibers and their biocompatibility, ceramics are also being used as reinforcing components of composite implant materials and for tensile loading applications such as artificial tendons and ligaments [13]. Unlike metals and polymers, ceramics are difficult to shear plastically due to the (ionic) nature of the bonding and minimum number of slip systems. Consequently, ceramics are very susceptible to notches or microcracks because instead of undergoing plastic deformation (or yield) they will fracture elastically on initiation of a crack. At the crack tip the stress could be many times higher than the stress in the material away from the tip, resulting in a stress concentration which weakens the material considerably [14]. The necessary properties for bioceramics can be explained by Billotte as following [15];

- should be non-toxic

- should be non-allergic

- should be biocompatible

- should be biofunctional for its lifetime in the host.

Ceramics used in fabricating implants can be classified as nonabsorbable (relatively inert), bioactive or surface reactive (semi-inert) and biodegradable or resorbable (non-inert) [16]. Alumina, zirconia, silicone nitrides, and carbons are inert bioceramics. Certain glass ceramics and dense hydroxyapatites are semi-inert (bioreactive), and calcium phosphates and calcium aluminates are resorbable ceramics [15].

1.2.3 Polymers

Synthetic polymeric materials have been widely used in medical disposable supplies, prosthetic materials, dental materials, implants, dressings, extracorporeal devices, encapsulants, polymeric drug delivery systems, tissue engineered products, and orthodoses like those of metal and ceramic substituents [17]. The real advantages of the polymeric biomaterials compared to metal or ceramic materials are ease of manufacturability to produce various shapes (latex, film, sheet, fibers, etc.), ease of secondary processability, reasonable cost, and availability with desired mechanical and physical properties. The required properties of polymeric biomaterials are similar to other biomaterials, that is, biocompatibility, sterilizability, adequate mechanical and physical properties, and manufacturability [18].

Although hundreds of different type of polymers are synthesized and could be used as biomaterials only a few kind of polymers are mainly used in medical device fabrications from disposable to long-term implants as given in Table 1.7 [18].

Table 1.7: Biomedical Application of Polymeric Biomaterials [18]

Synthetic Polymers	Applications
Polyvinylchloride (PVC)	Blood and Solution Bag, Surgical Packaging, Catheter Bottles, Connectors
Polyethylene (PE)	Pharmaceutical Bottle, Nonwoven Fabric, Pouch, Flexible Container, Orthopedic Implants
Polypropylene (PP)	Disposable Syringes, Blood Oxygenator Membrane, Artificial Vascular Grafts
Polymethymetacrylate (PMMA)	Blood Pump and Reservoirs, Implantable Ocular Lens, Bone Cement
Polystyrene (PS)	Tissue Culture Flasks, Roller Bottles
Polyethylenterephthalate (PET)	Implantable Suture, Artificial Vascular Grafts, Heart Valve
Polyetrafluoroethylene (PTFE)	Catheter and Artificial Vascular Grafts
Polyurethane (PU)	Film, Tubing and Components
Polymamide (Nylon)	Packaging Film, Catheters, Sutures

1.2.4 Composite Biomaterials

Composite materials are solids which contain two or more distinct constituent materials or phases on a scale larger than the atomic [19]. The term "composite" is usually reserved for

8

those materials in which the distinct phases are separated on a scale larger than the atomic, and in which properties are significantly altered in comparison with those of a homogeneous material. Accordingly, reinforced plastics such as fiberglass as well as natural materials such as bone are viewed as composite materials.. Natural biological materials tend to be composites. Natural composites include bone, wood, dentin, cartilage, and skin. Natural composites often exhibit hierarchical structures in which particulate, porous, and fibrous structural features are seen on different micro-scales [20]. Composite materials offer a variety of advantages in comparison with homogeneous materials. In biomaterials, it is important that each constituent of the composite should be biocompatible. Moreover, the interface between these different materials should not be degraded by the body environment. Some applications of composites in biomaterial applications can be counted as dental filling composites, reinforced methyl methacrylate bone cement and ultra-high-molecular-weight polyethylene and orthopedic implants with porous surfaces [19].

1.3 Hip Implants

1.3.1 General Background

Hip prosthesis or hip replacement surgery becomes necessary when the hip joint has been damaged from any cause such as arthritis, malformation of the hip since birth or abnormal development and damage from injury [21]. Figures 1.2 and Figures 1.3 show the anatomy of a natural hip. As it seems, a natural hip is composed of a femoral stem with a femoral head on top of it that articulates against the acetabular cup in the acetabulum. Cartilage is being existed between the acetabular cup and the femoral head in order to lubricate and facilitate the articulation [21]. In an arthritic hip joint, it can be said that the cartilage has been damaged, narrowed or even lost by a degenerative process or by inflammation. Figure 1.4 shows an illustration for damaged cartilage. This can create a pain for the patients while in move. If a part of the joint is damaged, a surgeon may be able to repair or replace only the damaged parts. On the other hand, if the entire joint is damaged a Total Hip Replacement (THR) or Total Hip Arthroplasty is suggested in which the damaged parts of the joint is being removed and replaced by an artificial prosthesis aimed for pain relief and restoration of movement. Figure 1.5 shows a hip arthroplasty, in which the damaged parts of the joint has been removed and replaced by an artificial prosthesis.

1.3.2 Design

Basically, the hip joint can be considered as three parts which are acetabular cup, cup-femoral head-articulating surface and femoral stem. Ducheyne stated that most frequent fixation problems about hip implants are related to infection, wear and wear particulate, migration and failure of implants and loosening of which the "long-term loosening"of the implant is especially important [22]. These problems can cause osteolysis in the bone bed which is the major reason of long-term loosening mostly for the femoral stem [23]. Some major factors related to late loosening are can be counted as stated by Park [24];

- mismatch of the physical properties between tissues and implant

- biocompatibility of the implant
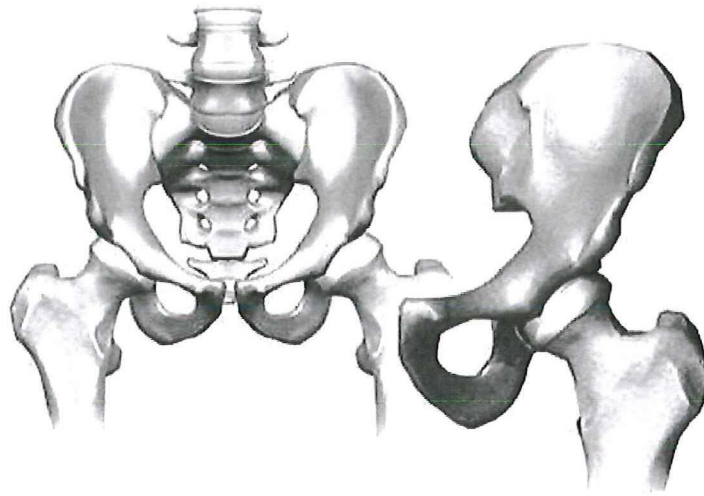
Figure 1.2: Anatomy of a Natural Hip Joint [21]
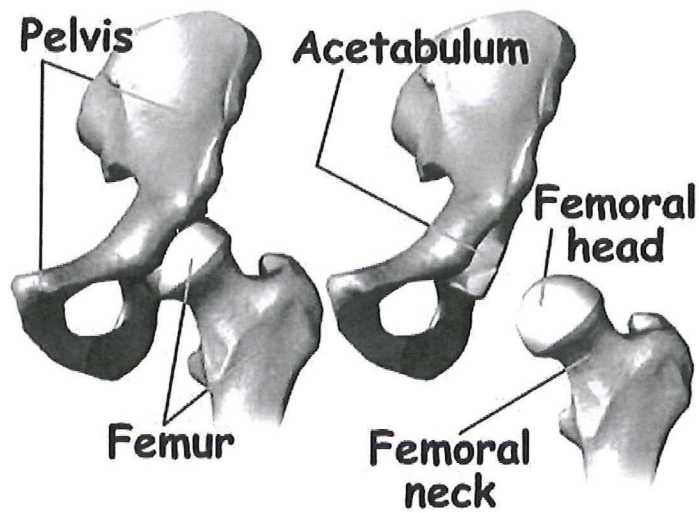
Figure 1.3: Close-up Illustration of the Anatomy of a Natural Hip Joint [21]

- deterioration of physical properties of implant materials

- surgical techniques

- design of the implant

- selection of patients

During the past century many different variations of materials and designs have been considered and developed to achieve an ideal painless, stable and freely mobile joint implant with a longer service time. Gluck in 1890, designed the first total hip replacement using ivory, holding prosthesis with glue. In 1919, Delbet used a rubber component instead of ivory, but these early attempts were unsuccessful. In 1939 Smith-Peterson described an

10
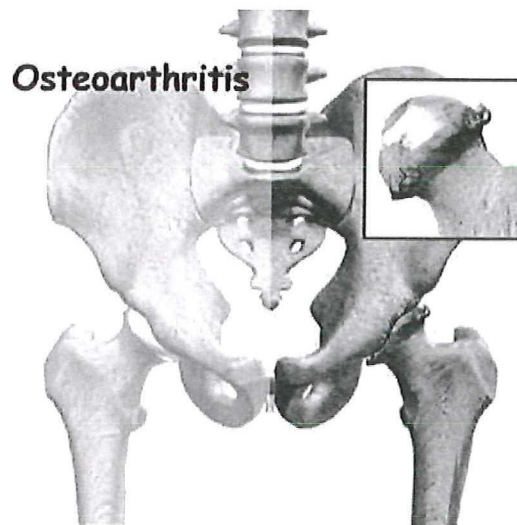
Figure 1.4: Anatomy of a Damaged Cartilage Arthritic Hip Joint [21]
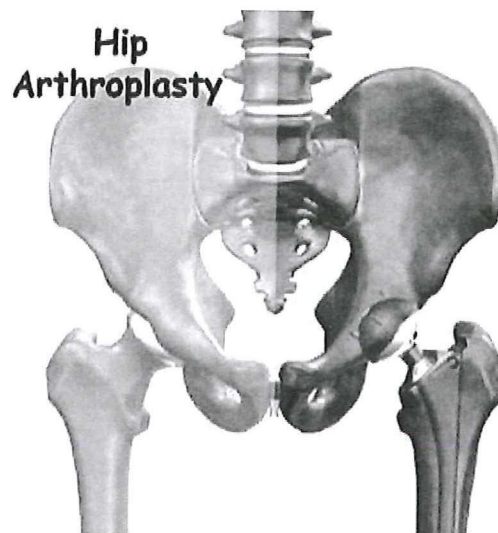
Figure 1.5: Hip Arthroplasty, the Damaged Parts of the Joint Have Been Removed and Replaced By an Artificial Prosthesis [21]

interpositional (mould) arthroplasty, which initially was made of glass, but then he modified it over a period of time to celluloid, Pyrex, Bakelite and finally Vitallium. The progress rate at 1960s has reached the peak point. In 1966, McKee and Watson Farrer introduced a metal on metal hip with stainless steel. Charnley in 1967, came out with an idea of a metal femoral component and a low-friction high molecular weight polyethylene acetabular cup. By 1968 the superiority of cobalt-chrome over any other steel components was found out. But meanwhile, Charnley introduced the concept of low friction arthroplasty using both cemented femoral and acetabular components, with a plastic bearing surface and polymethylmethacrylate (PMMA) for fixation. Even today, most of the THR has been designed based on that principle. In 1968 Ring underlined the disadvantages of using PMMA cements since poor bonding that

11

caused loosening of the acetabular component and its eventual failure of the implant. So he decided to developed cementless cup components with long pelvic anchoring screws. In 1976 Dipisa, Sih and Berman suggested that problem of loosening of hip replacement might be partly caused by thermal necrosis of bone in contact with polymerizing PMMA [25].

Also, sometimes the outcome of the THR may depend on the type of bone cement used. Some important properties of bone cements are;

- low vs. high viscosity

- plain vs. antibiotics impregnated

- low vs. high heat of polymerization cement

The physical properties of joint materials and bone are given at Table 1.8 [24].

1.3.2.1 Metal-on-Polymer Type Design

Metal on polymer type implants are the most commonly used hip replacements. The most often used bearing surface variation is metal on polyethylene. It helps to provide marked durability. One of the major disadvantages of this system is the movement at the interface of bone and cement but also fractures of cement cause PMMA debris and accelerated wear of other components. It may lead to granuloma formation, bone resorption and final bone-cement disintegration [23].

1.3.2.2 Metal-on-Ceramic Type Design

Ceramics are being used in total joint replacements, especially preferred to provide wear-resistant bearing surfaces. Thanks to ceramic materials high hardness level, ceramics can be polished until the very smooth surface finish. Therefore it can remain relatively scratch resistant while in service. The problem about the ceramic bearings is the poor performance against the fracture compare to the other type of materials. Ceramic bearings for patients with active lifestyles, sport life and high body weight, who can subject to repetitive impact, are not a good option for that kind of a design [26].

1.3.2.3 Metal-on-Metal Type Design

Metal-on-metal (MoM) type design total hip replacement joints have been developed to function in the absence of polymer or ceramic materials. Those implants do not perform wear as quickly as the metal on polymer design, longer service duration time and less inflammatory osteolysis can be satisfied which make that design great option for with young, active patients on the contrary of metal on ceramic and metal on polymer designs. They may need one or more revisions during their lifetime. The biggest concern about that design is the possibility of release of the microscopic metal particles that can lead to inflammation and loosening. Some scientific research has been found out elevated levels of metal ions in the blood [26]. Ultimately, the development metal on metal total hip replacement prosthesis has been focused on reducing the material degradation caused via released metal ions and metallic wear debris. Elevated level of metal ions can be traced in blood and urine for patients who have MoM artificial joint replacements. Some research has shown the risks of adverse tissue reactions, cytotoxicity and tissue necrosis and adverse immunological reactions and hypersensitivity [27].

12

Table 1.8: Physical Properties of Materials Used For Joint Prosthesis and Bone [24]

Materials		Young Modulus (GPa)	UTS (MPa)	Elongation	Density (g/cm^3)
Metals	316L SS (Wrought)	200	1000	9	7.9
	CoCrMo (Cast)	230	660	8	8.3
	CoNiCrMo (Wrought)	230	1800	8	9.2
	Ti6Al4V	110	900	10	4.5
Ceramics	Alumina	400	260	<0.1	3.9
	Glass-Ceramic	200	200	-0.1	2.5
	Calcium Phosphate	120	200	-0.1	3.2
Polymers	PMMA Bone Cement	2	30	3	1.1
	UHMW Polyethylene	1	30	200	0.94
	Polysulfone	2.5	70	50	1.24
Fibers & Wires	Aramid (Kevlar)	130	2700	2	1.45
	Carbon	400	2500	1	2
	Nylon	5	500	10	1.07
Bone	Femur (Long Axis)	17	130	3	2
	Femur (Tangential)	12	60	1	2
	Spongy Bone	0.1	2	2.5	1.0

Although researchers are constantly looking ways to improve implant design and durability, today there is no such a total hip replacement can be viewed as perfect. The properties of these different bearing combinations are summarized in Table 1.9 [28].

1.3.3 Components of THR

As mentioned in the introduction, a total hip replacement includes the two major components of femoral and acetabular cup. The femoral component is including femoral head, femoral neck, femoral collar and femoral stem. Each of these parts of femoral has a important role in handling load and providing a smooth movement. Femoral component needs to be attached to the adjacent bone using various fixations in order to handle the applied load. Femoral fixation can be categorized under two general groups which are using polymethylmethacrylate

13

Table 1.9: Properties of Various Bearing Combinations [29]

Material Properties		Ceramic on Ceramic	Metal on Metal	Metal on Polymer
Mechanical Properties	Hardness (MPa)	2300	350	Low
	Scratch Resistance	High	Low	Low (Cup) / Low (Head)
	Bending Strength (MPa)	550	950	NA (Cup) / 950 (Head)
	Fracture of Components	Reported	NA	NA
Tribology	Running-in Wear	$0.1\mu m$	$25\mu m$	$100\mu m$ (Creep)
	Steady-State Wear	$03\mu m$	$5\mu m$	$1020\mu m$
	Runaway Wear	Not Reported	Reported	Not Reported)
	Particle Size (Mean)	$0.2\mu m$	$0.05\mu m$	$0.5\mu m$
	Friction	Low	High	Low
	3-Body Wear	Not Reported	Reported	Reported
	Self-Polishing	Not Reported	Reported	N/A
	Metal Ion Level In Body Fluids in Well-Fixed Prosthesis	Not Increased	Increased In Blood and Urine	Not Increased
Corrosion	Passive Layer	N/A	Worn Every Cycle	N/A
	Surface Corrosion	N/A	Reported	N/A
	Interface Corrosion	Not Reported	Reported	Head / Trunnion
Biological Effects	Cell Toxicity	No	Yes	No
	Local Tissue Reaction	Low	Low	Low
	Systematic Effects	Not Reported	Reported	Not Reported
	Unexplained Pain	Not Reported	Reported	Not Reported
	Hypersensitivity	Not Reported	Reported	Not Reported
	Carcinogenicity	Not Reported	Consideration	Not Reported
Other Considerations	Squeaking	Not Reported	Reported	Not Reported
	Clicking	Not Reported	Reported	Not Reported
	Seizing	Not Reported	Reported	Not Reported
	Clinical Introduction	1970	Restarted 1988	1998

(PMMA) bone cement (cemented) or non-cemented options. Also it has been claiming a third category of artificial hip that uses cement on the ball side and non-cemented on the socket side. Figure 1.6 shows various components of a THR. Successful joint surgery requires that the replacement joint be painless, stable and freely mobile with an acceptable service lifetime [24]. Ideally, the new artificial joint must exactly match and satisfy the geometry and performance of the natural hip. In any joint replacement surgery, three key variables are always valid which geometry, choice of material and operative procedures are [29].

14

Figure 1.6: Various Components of a THR [21]

1.3.3.1 Socket or Acetabular Cup

The artificial socket is used to replace and compensate the function of the natural acetabular cup of the hip joint and to house the ball portion of the joint. Acetabular cup is one of the major part of total hip replacement prosthesis in order to satisfy the durability. The hip joint can be pictured as a ball that fits into a socket. The socket part of the hip is being called the acetabulum. The femoral head at the top of the thigh bone (femur) rotates within the curved surface of the acetabulum. In hip replacement surgery, the acetabular cup usually combined of a metal shell with a polyethylene liner. The sockets for use with cement are generally made of UHMW polyethylene, which is very tough, and slippery particularly when wet. It has ridges on the outer part and a wire marker since its position can be followed on the X-ray. The ridges are designed to improve the fixation of the acetabular cup by the cement. It is implanted into the natural hip socket by first filling the cavity with the bone cement and then pushing in the artificial cup. Thus the cup is held still while the cement sets. The socket for use without cement is made of metals. Outer side is designed with porous surface in order to encourage bone growth into it. However, it is crucial that the artificial socket must be placed firmly since the healing process can take 6-12 weeks. So during the surgeries, machining the natural socket and using an artificial socket that is precisely 1-2 mm bigger than the natural one can provide the initial fit. The acetabular cup is then forcibly jammed into the accurate position. Further fixation can be satisfied if necessary by using additional screws. The next stage is to place a plastic insert within the metal shell against which the artificial ball will form the joint [24].

1.3.3.2 Femoral

Ball The ball portion of the artificial hip consists of a short metal stem and on top of it a metal ball. It is attached with an angle that to mimic the shape of the human thigh-bone top end. [24].

15

Table 1.10: List of Design and Fixation Related Variables in THR [24]

Part	Materials	Fixation Methods
Cup	All PE	Cemented
	Metal-Backed	Uncemented (Mechanical)
	Porous-Coated	*Uncemented (Mechanical)*
	Screw-Holed	*Uncemented (Mechanical)*
	All Ceramic	Cemented / Uncemented
Articulated Surfaces	PE/Metal	No Fixation Required
	PE/Ceramic	
	Ceramic/Ceramic	
	Metal/Metal	
Femoral Stem	Metal	Cemented/Uncemented
	Composite	Uncemented
	Smooth	*Threaded (Rare)*
	Textured	*Uncemented*
	Porous-Coated	*Uncemented*
	PMMA-Coated	*Cemented*
	HA-Coated	*Uncemented*
Head	Metal	Fixed
	Ceramic	Rotated (Trunnion/Modular)

Stem In general there have been three different types of femoral stems used in THR in the material of view. The Charnely stem was manufactured from stainless steel. Later on, other materials such as titanium alloys (Ti-6Al-4V) and CoCr alloys were used to manufacture the stem and other parts of THR [24]. The design of the femoral stem also involves the articulating surface with the acetabular cup since it is an important factor for the durability of the stem function. The fixation of the stem can be divided into two categories, i.e., cemented and uncemented. The uncemented can be classified into interference fit and porous-coated for tissue ingrowth fixation. The porous-coated type can be further coated with a hydroxyapatite layer to help tissue ingrowth [24]. Table 1.10 gives design and fixation related variables for total hip replacement, while Figure 1.7 shows examples of cemented and uncemented hip prosthesis [24].

From the general viewpoint, in comparison of cemented implants with uncemented components, it can be said that uncemented version can offer advantages such reduced operating time, reduced initial trauma to endosteal bone surfaces, long term interface stability, less foreign material.

Total Hip Replacement Design variation include different types such as modular approach, straight stem, curved stem, platforms and no-platforms, holes and no-holes in the femoral stem and so on [30]. The type of THR design for the patient has been decided by surgeon based on some parameters like age, body condition, activity level and budget. A lifetime for artificial hip joint is about 20-25 years. Although that amount of time reasonable for many elderly patients, but still it is not good enough for younger recipients with a more active life style. In such cases hip replacement may end up with loosening or even failure that eventually requires revision surgery. Revision surgeries are become inevitable after some major problems such as related to osteolysis or in some cases infection. Osteolysis is a simply biological reaction to the debris from the bearing surfaces of implant as components of implants rub against each other during daily life activities. The other problem which is infection of the prosthesis occurs in

(a) Uncemented THR   (b) Cemented THR
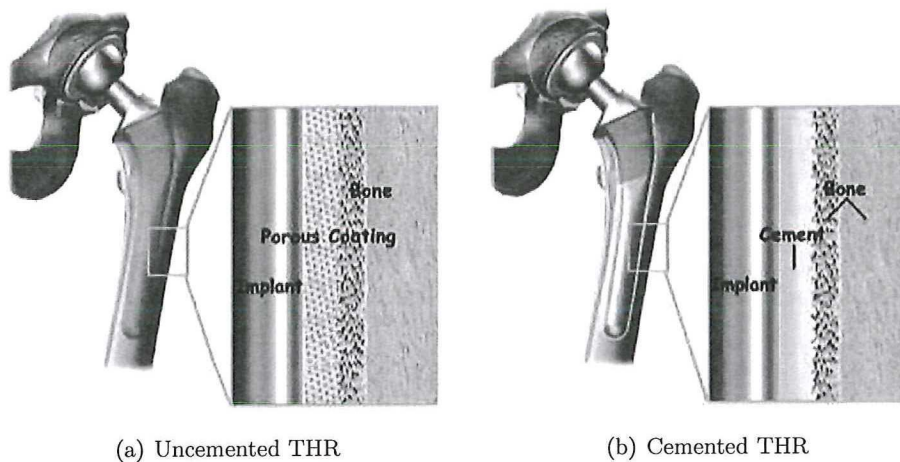
Figure 1.7: Illustration of the Bone-Implant Interfaces [24]

only a very small ratio of, but that kind of complication may be resulted in pain, immobility, failure and loss of prosthesis, reoperation, and in some worse cases loss of limb or life [31]. Other factors that can trigger stem loosening include bone resorption, degradation of bone cement, and unfavorable positioning of the prosthesis. Its really important to understand of the important phenomena contributing to infection and loosening of joint implants. It has been reported that due to systematic and/or local antibiotic treatment and other preventive measures, the incidence of deep hip prosthetic infections in Scandinavia appears to be less than 1% [24]. Despite that development, long term aseptic loosening of joint prosthesis is a increasing problem that cause revisions. Aseptic loosening is related with osteolysis which caused because of the wear debris of UHMWPE. Malchau et al. claimed that aseptic looseing problem is the primary cause of failure of THR and accounts for almost seventy five percent of all revision operations [32]. The evolution of arthroplastic devices for the hip joint can be seen at Figure 1.8 [33].

1.3.4 Tissue-Implant Interaction

The aim of medical devices is to serve patients as long as possible and satisfy maximum health conditions for a problem within the body and improve life quality. Yet, some implants can face different kind of complications that help device failure. As a result, it may cause some troubles for the patient. All the implants have interactions with the tissue environment at different extents depends on their position within the body. Most frequent biomaterials-tissue interactions are summarized in the Table 1.11 [34]. The major complications of medical devices are generally reasoned by biomaterials-tissue interactions that include both way effects of the implant on the host tissues and effects of the host on the implant.

Schoen stated that these interactions comprise aberrations of physiological biomaterial-tissue interactions processes that function as common host defense mechanisms such as inflammation or thrombosis [33]. Inflammation, wound healing and foreign body responses are generally considered as parts of the tissue or cellular host responses to injury.

Table 1.12 lists the sequence of the in-vivo events following injury [34]. Injury can be defined by biomaterials point of view, positioning a biomaterial within the body have necessary

17
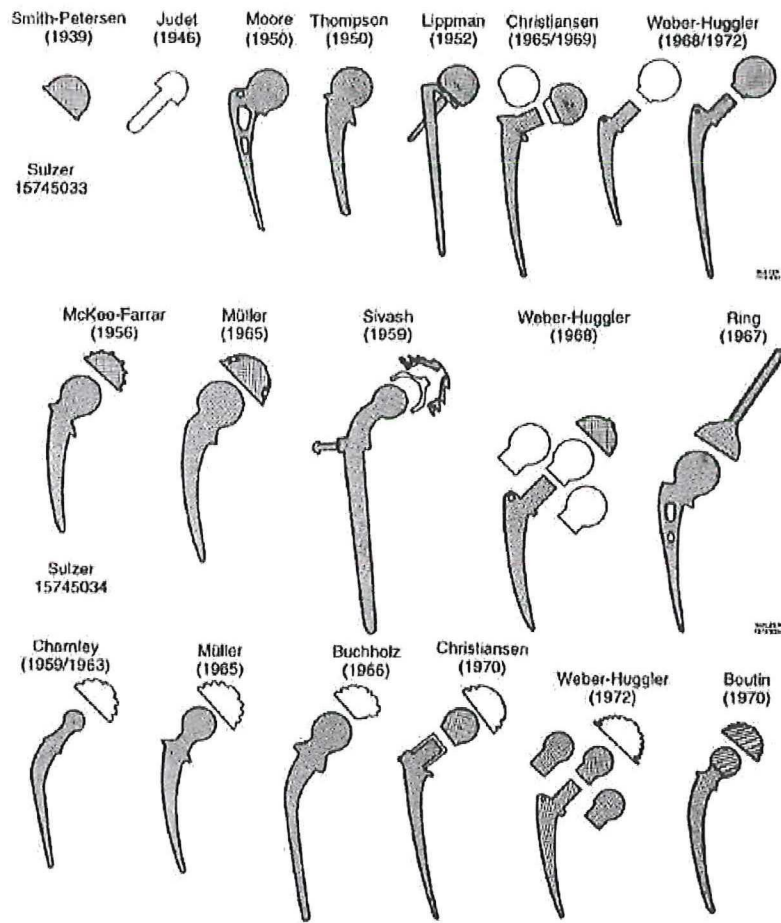
Figure 1.8: The Stages in The Development Arthroplastic Devices For The Hip Joint [33]

steps such as injection, insertion, or surgical implantation. As a result tissues or organs which are involved the procedure will be injured. Placing the biomaterial step initiates a response by the body since body is injured and homeostasis must be maintained. The degrees of how homeostatic mechanisms are disturbed and the pathophysiologic conditions are raised and resolved are a measure of the host's reaction to the biomaterial [35]. Nevertheless, homeostatic mechanisms can be divided into blood-material or tissue-material interactions basically, it must be underlined that the different components or mechanisms involved in homeostasis maintenance are present in both blood and tissue and are a part of the physiologic continuum. Furthermore, host reactions can be based on tissue, organ or species. Therefore, the degree of injury is implantation-depended [34].

The sequence of events following implantation of a biomaterial is illustrated in Figure 1.9. The size, shape, and chemical and physical properties of the biomaterial are some major reasons on impact on the intensity and duration of the inflammatory or wound-healing process. Therefore, inflammatory reaction response may give clues about the biocompatibility of a biomaterial.

While injury step initiates the inflammatory response within the body, the chemicals released from plasma, cells, and injured tissue mediates the response as seen in Table 1.13.

18

Table 1.11: Interaction Between Biomaterial and Tissue [34]

Effect of the Implant on the Host			Effect of the Host on the Implant	
Local	Blood-Material Interactions	Protein Absorption	Physical-Mechanical Effects	Abrasive Wear
		Coagulation		
		Fibrinolysis		
		Platelet Adhesion, Activation, Release		Fatigue
		Complement Activation		
		Leukocyte Adhesion/Activation		Stress
		Adhesion/Activation		Corrosion Cracking
	Toxicity			
	Modification of Normal Healing	Encapsulation		Corrosion
		Foreign Body Reaction		
		Pannus Formation		Degeneration and Dissolution
	Infection			
	Tumorigenesis			
Systemic and Remote	Embolizations	Thrombus	Biological Effects	Absorption of Substances From Tissues
		Biomarerial		
	Hypersensitivity			Enzymatic Degradation
	Elevation of Implant Elements on Blood			Calcification
	Lymphatic Particle Transport			

Table 1.12: Sequence of Local Events Following Implantation [34]

Injury
⇓
Acute Inflammation
⇓
Chronic Inflammation
⇓
Granulation Tissue
⇓
Foreign Body Reaction
⇓
Fibrosis

Released chemical mediators are quickly inactivated or destroyed. Thus, influence is predominantly local. Furthermore, it has been noted that lysosomal proteases and oxygen-derived free radicals produce the most significant damage or injury. Also they are partly responsible for the degradation of biomaterials [34].

Table 1.13: Important Chemical Mediators of Inflammation Derived From Plasma, Cells and Injured Tissue [34]

Mediators		Examples	
Vasoactive Amines		Histamines, Serotonin	
Plasma Proteases	Kinin System	Bradykimin, Kallikrein	
	Complement System	C3a, C5a,C3b, C5b-C9	
Coagulation/Finrinolytic System		Fibrin Degradation Products	
Arachidonic Acid Metabolites	Prostaglandins	PGI2, TxA2	
	Leukotrienes	HETE, Leukotriene B4	
Lysosomal Proteases		Collagenase, Elastase	
Oxygen-Derived Free Radicals		H_2O_2, Superoxide Anion	
Platelet Activating Factors		Cell Membrane Lipids	
Cytokines		Interleukin 1 (IL-1); Tumor Necrosis Factor (TNF)	
Growth Factors		Platelet-Derived	(PDGF); Fibroblast Growth Factor
		Growth Factor	(FGF); Transforming Growth Factor (TGF$-\alpha$ or TGF-β)
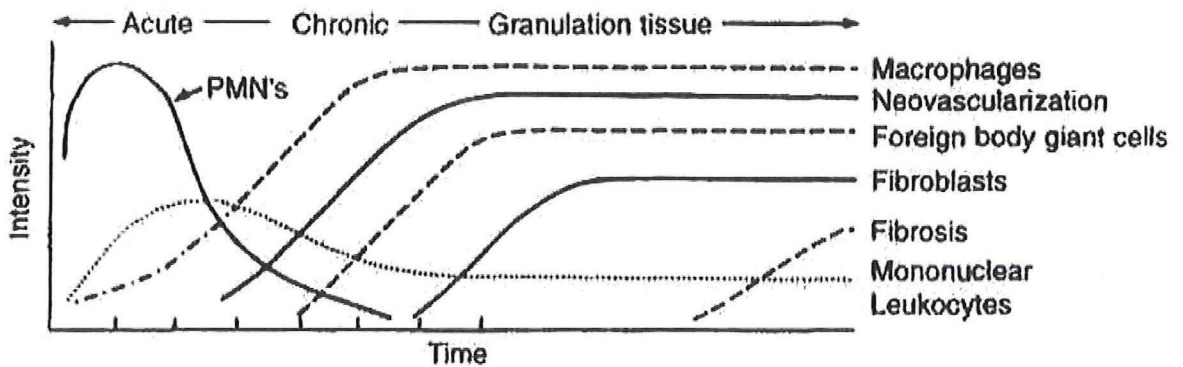
Figure 1.9: The Temporal Variation in the Acure Inflammatory Response, Chronic Inflammatory Response, Granulation Tissue Developlement and Foreign Body Reaction to Implanted Biomaterials [34]

20

Hip Implants

2

2.1 General Background

THE correct choice of implant depends on various parameters such as patients age, lifestyle and activity level. Also it should be considered that whether the hip replacement is being done for the first time or revision for a previously carried out artificial. So far there are four different material combinations has been preferred in practical use which are a metallic femoral head in polymeric acetabular cup; a ceramic head in a polymeric cup; a ceramic head in a ceramic cup; and a metallic head in a metallic cup. The metals used for bearing surfaces are generally Co-Cr-Mo alloys, the polymer Ultra-High-Molecular-Weight Polyethylene (UHMWPE), and the ceramic high purity alumina, or in the case of ceramic on polymer joints only, in some cases partially stabilized zirconia [36]. Modular designs, where the stem and ball are of two different materials, are very common in THR [28]. Table 2.1 summarized some of the femoral head to socket combinations that have been used for total hip replacement arthroplasty in practice nowadays [30]. Cobalt base alloys are the most commonly used metals for current metal-on-polymer implants.

It should be underlined the reason of excessive wear titanium alloy femoral heads to the UHMWPE acetabular cups. The polymeric wear debris produced after a few years of using the prosthesis can trigger adverse pathological reaction in the surrounding tissues, which can be ended up with osteolysis and joint loosening although the metal on polymer hip prosthesis showed relatively low wear rate compare to other materials combinations [36]. Wang et al., indicated that cross linking the polymer chains can have better results on minimizing the wear rates compared to the very smooth ceramic femoral heads applications instead of metal heads [37].

Table 2.1: Materials Combination in Total Hip Replacement Prosthesis [30]

Femoral Component	Socket Component	Results
Co-Cr-Mo	Co-Cr-Mo	Early High Loosening Rate and Limited Use; New Development Show Lowest Wear Rate
Co-Cr-Mo	UHMWPE	Widely Employed; Low Wear
Alumina/Zirconia	UHMWPE	Very Low Wear Rate; Zirconia More Impact on Resistant
Alumina	Alumina	Minimum Wear Rate (Components Matched)
Ti-6Al-4V	UHMWPE	Reports of High UHMWPE Wear Due to Breakdown of Titanium Surface
Surface Coated Ti-6Al-4V	UHMWPE	Enhanced Wear Resistance to Abrasion; Only Thin Treated Layer Achieved

2.2 Cobalt-Chromium-Molybdenum Alloy

Cobalt-chromium alloys can be divided into two groups basically; the castable CoCrMo alloy and the CoNiCrMo alloy which is usually wrought by (hot) forging. The castable CoCrMo alloy has been used for many years at biomaterial industry such as in dentistry and, relatively recently, in making artificial joints. The wrought CoNiCrMo alloy is relatively new, now used for making the stems of prostheses for heavily loaded joints such as the knee and hip. The ASTM lists four types of Co-Cr alloys which are recommended for surgical implant applications which are cast CoCrMo alloy (F75), wrought CoCrWNi alloy (F90), wrought CoNiCrMo alloy (F562), and wrought CoNiCrMoWFe alloy (F563) [10]. The chemical compositions of each different variation have been showed in Table 2.2 [39]. The castable CoCrMo and the wrought CoNiCrMo alloy are most two extensively used materials in todays medical sector. As Table 2.2 shows, the compositions are quite different from each other. The two basic elements of the Co-Cr alloys form a solid solution of up to 65% cobalt. The molybdenum is added to produce finer grains. Thus it results in higher strengths after casting or forging procedures. The chromium helps to increase the corrosion resistance as well as solid solution strengthening of the alloy. The CoNiCrMo alloy originally called MP35N contains approximately 35% cobalt and nickel each. The alloy is highly corrosion resistant to seawater (containing chloride ions) under stress. Cold working can increase the strength of the alloy considerably. However, there is a considerable difficulty of cold working on this alloy, especially when making large devices such as hip joint stems. Only hot-forging can be used to fabricate a large implant with the alloy. It has been noted that the abrasive wear properties of the wrought CoNiCrMo alloy shows quite similar results with the cast CoCrMo alloy [38]. Wear rate is about 0.14 mm per year in joint simulation tests with ultra-high molecular weight polyethylene acetabular cup. But regardless of that fact, the cast CoCrMo alloy is not recommended for the joint prostheses bearing surfaces since its poor frictional properties with itself or other materials [36]. The superior fatigue and ultimate tensile strength of the wrought CoNiCrMo alloy make it a great candidate for the applications which require longer performance life without any mechanical failure such as the stems of the hip joint prostheses [36]. The mechanical properties required for CoCr alloys are given in Table 2.3. As with the other alloys, the increased strength is accompanied by decreased ductility. Both the cast and wrought alloys have excellent corrosion resistance [40].

2.2.1 Cast CoCrMo (ASTM F75)

CoCrMo alloys cast to a final form (high Carbon) are made by investment casting procedures. This step involves the simultaneous casting of different components (e.g., femoral stem or ball components for hip implants) onto so called "casting tree". Then it has been followed by cutting components from the "tree" and grinding, welding if necessary, honing or otherwise surface finishing to achieve the final implant form. The high carbon alloy is the most wear resistant clinically used metallic biomaterial. Mostly, chemical compositions are like $M_{23}C_6$ (mainly), M_7C_3, and M_6C carbides, where M is primarily chromium [41]. Those forms can be observed during solidification at the structure (Fig. 2.1) [42]. Post solution treatment displays a high rate of work hardening as can be seen at Figure 2.1b. That situation also helps the alloy to enhance wear resistance. This phenomenon can be explained by the result of localized hardening of the surrounding Co-based matrix phase during functional loading. Depends on composition, alloy melts between 1350 °C and 1450 °C. It has been observed that it forms

24

Table 2.2: Chemical Composition of CoCr Alloys [39]

Element	CoCrMo (F75)		CoCrWNi (F90)		CoNiCrMo (F562)		CoNiCrMoWFe (F563)	
	Min.	Max.	Min.	Max.	Min.	Max.	Min.	Max.
Cr	27.0	30.0	19.0	21.0	19.0	21.0	18.0	22.0
Mo	5.0	7.0	—	—	9.0	10.5	3.0	4.0
Ni	—	2.5	9.0	11.0	33.0	37.0	15.0	25.0
Fe	—	0.75	—	3.0	—	1.0	4.0	6.0
C	—	0.35	0.05	0.15	—	0.025	—	0.05
Si	—	1.0	—	1.0	—	0.15	—	0.5
Mn	—	1.0	—	2.0	—	0.15	—	1.0
W	—	—	14.0	16.0	—	—	—	4.0
P	—	—	—	—	—	0.015	—	—
S	—	—	—	—	—	0.01	—	0.01
Ti	—	—	—	—	—	1.0	—	3.5
Co	Balance							

Table 2.3: Mechanical Property Requirements of CoCr Alloys [40]

Materials / Property	Cast CoCrMo (F75)	Wrought CoCrWNi (F90)	Wrought CoNiCrMo (F562)	
			Solution Annealed	Cold-Worked & Aged
Tensile Strength (MPa)	655	860	793 - 1000	1793 (Min.)
Yield Strength (0.2% Offset) (MPa)	450	310	240 - 655	1585
Elongation (%)	8	10	50	8
Reduction of Area (%)	8	—	65	35
Fatigue Strength (MPa)	310	—	—	—

a typical as-cast, cored structure on solidification with the major phase being face-centered cubic (FCC) austenite designated as either γ- or α-phase and the interdendritic zones being enriched in chromium, molybdenum and carbon. The γ-phase forms at temperatures above 890 °C while a hexagonal close-packed (HCP) structure is stable below this temperature. But, since the sluggish nature of the FCC to HCP transformation, a metastable FCC phase can be normally retained to room temperature [43].

Scanning electron micrographs in Figure 2.1 showing microstructures of (a) a polished sample of as cast high carbon CoCrMo alloy with the relatively large grains, the heterogeneous composition evident from the different response to chemical etching used to show the microstructure where the darkest regions correspond to carbides dispersed throughout. At (b) discontinuous $M_{23}C_6$ forming from γ-phase grain boundary region.For (c) solution annealed CoCrMo alloy has been observed which showed more homogeneous structure but with some retained carbides throughout.

Aging at between 650 °C and 850 °C favors $M_{23}C_6$ precipitation in the HCP zones but
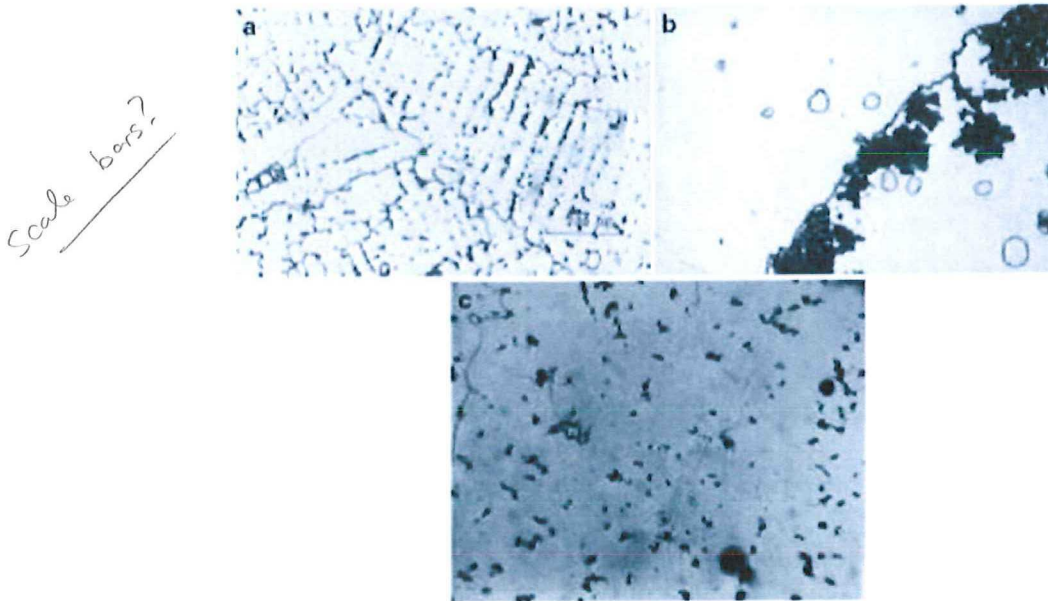
Figure 2.1: Microstructure Investigation Under Scanning Electron Microscope (SEM) [42]

while this does increase yield strength, it also reduces the materials ductility to unacceptable levels, making such an aging treatment impractical [44]. During solidification, a highly cored structure forms with interdendritic Cr-, Mo- and C-rich regions forming extensive carbide networks and other brittle intermetallic phases (σ-phase). That development results in low ductility. In order to homogenize partially the structure, the as-cast alloy is treated with a short (1 hour) solution anneal at between 1200 °C and 1225 °C. Then, the alloy is cooled rapidly through the 1100-800 °C temperature range. The reason for that is avoiding precipitation of embrittling $M_{23}C_6$. The 1 hour solution annealing treatment results in only partial homogenization of the cored structure but it is enough for acceptable ductility levels (11-17 % elongation). In order to understand the heat treatment steps, phase diagram has been shown in Figure 2.2. According to Thermo-Calc (coupled with PBIN thermodynamic database), the following five phases are present in cobalt-chromium binary system above 800 °C [45];

- Liquid Phase

- Cobalt-Rich Face-Centered Cubic (FCC) Phase

- Cobalt-Rich Hexagonal Close-Packed (HCP) Phase

- Sigma Phase

- Chromium-Rich Body-Centered Cubic (BCC) Phase

The biggest drawback of the cast and solution annealed CoCrMo alloy is its relatively low mechanical properties besides than wear resistance. Mechanical and chemical properties of cobalt based alloys are shown in Table 2.4 and Table 2.5 respectively [46],[47].

Major reasons for that problem are coarse grain structure, inherent casting defects and shrinkage porosity and relatively slow casting cooling rate. Furthermore, the carbides that

26
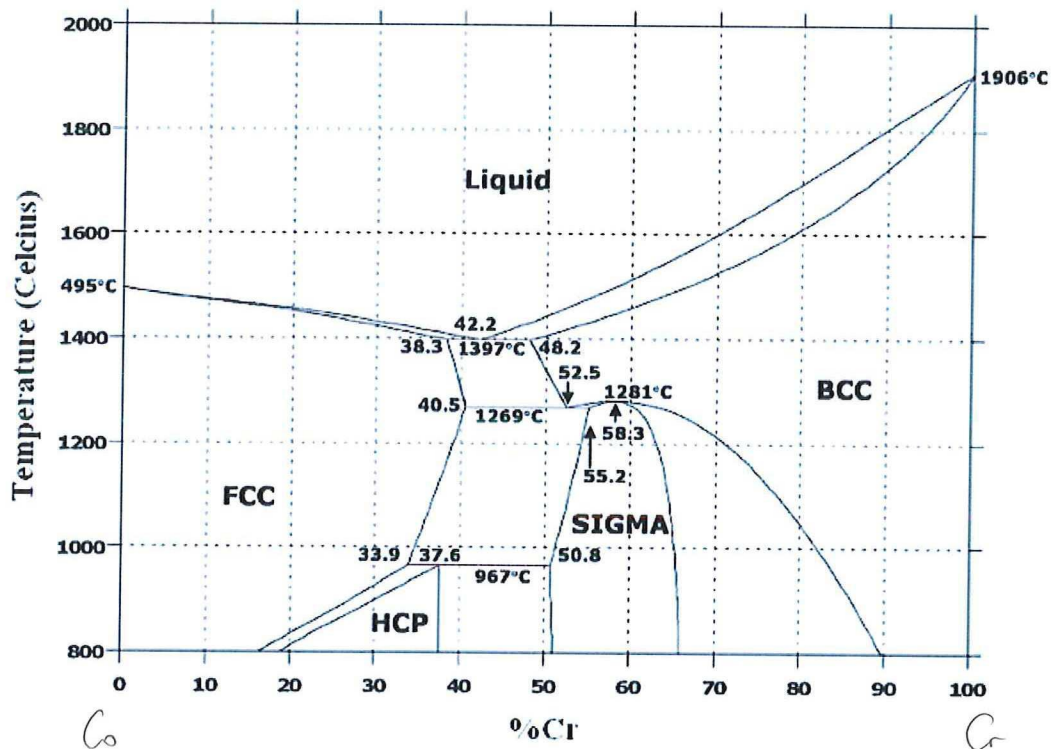
Figure 2.2: Phase Diagram of Cobalt-Chromium Binary Alloys [45]

Table 2.4: Mechanical Properties of CoCr and CoNi Alloys after Different Treatments [46]

Process Description	σ_{yield} (MPa)	σ_{uk} (MPa)	% Elongation	$\sigma_{fatigue}(10^7)$
CoCrMo Alloys				
F75 - Cast + Solution Annealed	450 - 530	655 - 890	11 - 17	207 - 310
F75 - Cast + Porous-Coated	$\sim$ 490	$\sim$ 735	$\sim$ 11	150 - 207
F799 - Forged (Low Carbon)	875 - 995	1320 - 1450	19 - 26	670 - 800
F799 - Forged (Low Carbon) + P-C	$\sim$ 410	$\sim$ 815	$\sim$ 33	——
F799 - Forged (High Carbon)	$\sim$ 1175	$\sim$ 1510	$\sim$ 10	——
F799 - Forged (High Carbon) + P-C	600 - 840	1030 - 1280	$\sim$ 18	$\sim$ 240
P/M D-S (As-Forged)	840	1280	——	690 - 895
P/M D-S + P-C	——	——	——	345
CoNi Alloy (MP35N) - F562				
Annealed (1050 °C)	300	800	40	340
Cold-Worked (%50 Red. in Area)	650	1000	20	435
Cold-Worked + Aged	1900	2050	10	405
Other Co Alloys				
F1058 C-W + Aged (Wire)	1240 - 1450	1860 - 2275	——	——
F563 C-W + Aged	827 - 1172	1000 - 1310	12 - 18	——

27

Table 2.5: Chemical Composition (%m/m) of Alloys Used for Metal-Metal Hip Bearings [47]

Element	ASTM F75 Casting Alloy	BS/ISO 7252-4 Casting Alloy	ASTM F1537 Alloy 1 (Low Carbon) Forged	ASTM F1537 Alloy 2 (High Carbon) Forged	ASTM F1537 Alloy 3 (Dispersion Strengthened) Forged
Chromium	27 - 30	26.5 - 30	26 - 30	26 - 30	26 - 30
Molybdenum	5 - 7	4.5 - 7	5 - 7	5 - 7	5 - 7
Carbon	0.35 Max.	0.2 - 0.35	0.14 Max.	0.15 - 0.35	0.14 Max.
Nickel	0.5 Max.	1 Max.	1 Max.	1 Max.	1 Max.
Iron	0.75 Max.	1 Max.	0.75 Max.	.75 Max.	0.75 Max.
Manganese	1 Max.	1 Max.	1 Max.	1 Max.	1 Max
Silicon	1 Max.	1 Max.	1 Max.	1 Max.	1 Max
Tungsten	0.2 Max.	N/S	N/S	N/S	N/S
Phosphorus	0.02 Max.	N/S	N/S	N/S	N/S
Sulphur	0.01 Max.	N/S	N/S	N/S	N/S
Nitrogen	0.25 Max.	N/S	0.25 Max.	0.25 Max.	0.25 Max.
Aluminum	0.1 Max	N/S	N/S	N/S	0.3 - 1
Titanium	0.1 Max	N/S	N/S	N/S	N/S
Boron	0.01 Max	N/S	N/S	N/S	N/S
Lanthanum	N/S	N/S	N/S	N/S	0.03 - 0.2
Cobalt	Balance				

are retained after the solution anneal, while beneficial for wear resistance, create sites for easy crack initiations. Internal porosity can be disappeared by hot isostatic pressing (HIP). However, this process is not as solution for surface connected defects therefore still those defects can act as preferred sites for early crack initiation. Corrosion resistance is dependent on the formation of a passive chromium and molybdenum containing oxide layers. By nitric acid solution treatment, passive oxide layer is normally formed as a final step in implant manufacture [46].

2.2.2 Wrought CoCrMo (ASTM F799, F1537)

Warm or hot forging of cast CoCrMo billets have significantly higher mechanical properties. The lower carbon content results in fewer and smaller carbides throughout the structure. Therefore it enhances the alloys formability but on the other hand it is a sacrifice which results in reducing wear resistance. For hot forging, billets are heated to temperatures between 1000 °C and 1150 °C. Re-annealing at stages during the forging process is used in order to prevent edge cracking during deformation. Final implant shapes can be formed by closed-die forging and a series of forging and re-annealing following that step [42]. A lower temperature finish forging operation is used to achieve a degree of strain hardening of the alloy and a final form with desirable mechanical properties. Yield, ultimate and fatigue strengths are significantly higher than compare to high carbon version cast alloy despite the lower carbide content since as a result of much finer grain size, possible stacking fault or HCP band formation, and strain hardening. The wear resistance of the low carbon alloy is poor compared with the higher carbon cast alloy thereby it is limiting the use for femoral ball or
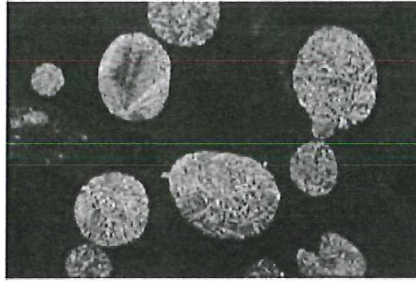
Figure 2.3: Scanning Electron Micrograph of Atomized CoCrMo Powder [46]

other surface bearing components for that type of alloy. Closed-die forging of high carbon CoCrMo alloys is also possible despite it is rather difficult and needs very close control on forging and reannealing stages [42]. Whether cast or high carbon wrought cobalt based alloys provide superior wear resistance remains controversial. The fine carbide distribution does allow improved surface finishing of components and this may contribute to better wear characteristics. Fine-grained, high carbon bar stock that is suitable for subsequent closed-die forging to final shape can also be formed using a powder metallurgy processing route. High carbon CoCrMo alloy powders are formed by atomization either by inert gas atomization or by a rotating electrode process by powder metallurgy. Then formed powders rapidly solidified "micro-castings" so while retaining carbides and a cored structure, small and finely distributed throughout the atomized powder (Fig. 2.3) [46]. After atomization step, the powders are sized by screening process. Then those powder are accumulated in a suitable containment vessel that is evacuated, sealed and hot isostatically pressed (at around 1100 °C for 1 hour at 105 MPa pressure) or hot forged, to form full density CoCrMo alloy. During the period at elevated temperature, some grain coarsening occurs but it is limited in extent because of the grain growth inhibition effect of the finely distributed carbides. The fine microstructure permits easier hot or warm forging to a near final form. Implants of relatively high strength, with good honing and polishing characteristics and good wear resistance can be formed using metal powder-formed material [46].

Another method for forming near final shapes from CoCrMo alloy powders is metal injection molding (MIM). The process follows mixing fine atomized powders with an organic binder, and extruding steps which results slurry to form pellets.

2.2.3 Surface Modification of CoCrMo Implants

In order to achieve strong implant-to-bone fixation without the use of acrylic bone cement, cast CoCrMo implant surfaces can be modified by either sintering CoCrMo powders to the bone-interfacing surfaces or plasma spray coating the surfaces. For the sintered coatings, typically 250 - 350 μm size powders (-45/+60 mesh) are used to form porous coatings of approximately 50-70 % density (i.e., vol.% porosity ~30-50 %) [42]. Sufficient strength particle-to-particle and particle-to-substrate core bonding is accomplished by sintering CoCrMo alloy powders at around temperature of 1300°C for a period of 1 hour or so. This high temperature sintering anneal can have influence on the microstructure and mechanical properties of both cast and wrought CoCrMo alloys dramatically. It has been observed that for cast alloys, localized melting of the chromium, molybdenum and carbon rich interdentritic zones occurs at approx-

29

imately 1235°C, the eutectic temperature for the solute enriched interdentritic region. Upon cooling, eutectic phase structures, (γ-phase + $M_{23}C_6$ carbides + possibly some α-phase), form integranularly and intragranularly (Fig. 2.4a,b) [46]. These eutectic structures develop as networks at sinter neck regions and along the solid substrate grain boundaries. Therefore they can form pathways for easy crack propagation that can reduces ductility and fracture resistance of porous-coated implants (Fig. 2.4). However, undesirable effect can be eliminated by slow cooling from the normal sintering temperature ($\sim$1300°C) to below the incipient eutectic melting temperature (1235°C) [46]. At early stage sintered porous coatings was limited to cast CoCrMo compositions since concerns of recrystallization and grain growth during sintering of wrought CoCrMo alloys. But with the development of high carbon and dispersion strengthened wrought cobalt based alloys with fine non-metallic dispersoids throughout that inhibit grain growth, now it is possible and practical to porous coat these alloys and retain relatively small grains (60-150µm size range) [42].
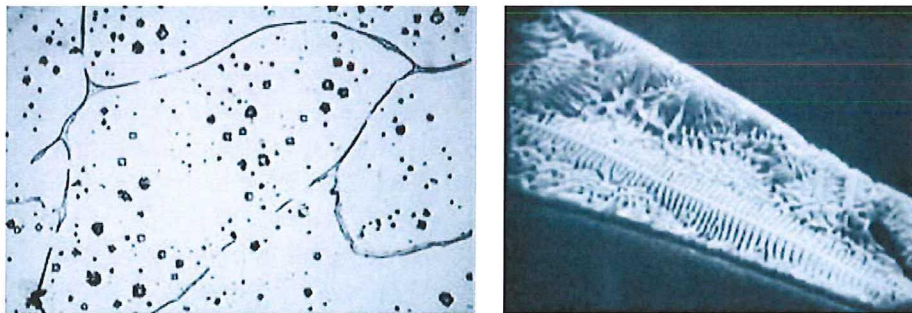
(a) Grain Boundaries with Eutectic Structure ($M_{23}C_6$ + γ-Phase Primarily)

(b) Higher Magnification View of the Grain Boundary Microstructure; The Lamellar Eutectic Structure of $M_{23}C_6$ + γ-Phase Lamellae

Figure 2.4: Scanning Electron Micrographs of Polished CoCrMo Samples Following a 1300°C 1h Sinter Annealing Treatment Followed by a Normal Furnace Cooling to Room Temperature [46]

Biological Environment

3.1 Simulated Physiological Solutions

THE human body is more likely an aggressive environment for different kind of materials especially for metals and its alloys. Body fluid is in an oxygenated saline solution with salt content of about 0.9% at pH 7.4, and temperature of 37.1°C [48]. After the moment that orthopaedic implant is surgically introduced into the human body, it is constantly bathed in extracellular tissue fluid. All the implantable metallic materials undergo chemical or electrochemical dissolution at different rates without regard to materials corrosion-resistantance, due to the complex and corrosive environment of the human body [49]. Artificial body fluids can be found at Table 3.1 [50]. The body fluid consists of water, complex compounds, dissolved oxygen and large amounts of sodium (Na^+), chloride (Cl^-) ions and other electrolytes like bicarbonate and small amounts of potassium, calcium, magnesium, phosphate, sulphate and amino acids, proteins, plasma, lymph, etc [49]. Another function of these ionic species is to keep the homeostasis or maintenance of the pH level of body and participation in the electron transfer reactions [51]. Kamachi et al., stated that on surgical implantation, the internal body environment is greatly disturbed. Instability develops in fluid compartment and transport of ions and non-uniform changes normally accompany disease states [48]. From an electrochemical viewpoint, the initiation of corrosion can be activated because of the new conditions has come out due to implant surface. These conditions may be responsible for the formation of electrochemical cells with active metal dissolution at localized spots at the implant-body fluid interface. These factors can have big influence for unbalancing the local environmental body conditions which can trigger various forms of corrosion and/or failure of the implant. An orthopedic implant is accepted as unsuccessful if the result is premature removing from the body in case of severe paining, inflammation and other reactions with the body like corrosion and wear.

Table 3.1: Simulated Physiological Solutions Used in Immersion Test [50]

Solutions	pH	Compositions (g/l)
α-Medium	7.5	NaCl: 6.8 KCl: 0.4 Na$_2$HPO$_4$: 1.15 NaH$_2$PO$_4$.H$_2$O: 0.2 Amino Acids and Vitamins: 0.27, Fetal Bovine Serum (10 % Vol), 7.5 % NaHCO$_3$ Solution (1 Vol %)
PBS (-)	7.5	NaCl: 8, KCl: 0.2, NaH$_2$PO$_4$: 0.14, KH$_2$PO$_4$: 0.2
Calf Serum (Membrane Filtered)	7.4	——
Artificial Saliva	6.4	NaCl: 0.844, KCl: 1.2, CaCl$_2$: 0.146, MgCl$_2$: 0.052, K$_2$PO$_4$: 0.342
Ringer's Solution	6.4	NaCl: 8.36, KCl: 0.3, CaCl$_2$: 0.15
Hank's Solution	6.9	NaCl: 8, KCl: 0.4, NaHCO$_3$: 0.35, NaH$_2$PO$_4$.H$_2$O: 0.25, Na$_2$HPO$_4$.2H$_2$O: 0.06, CaCl$_2$.2H$_2$O: 0.19, MgCl$_2$: 0.19, MgSO$_4$.7H$_2$O: 0.06, Glucose: 1.0
0.9 / 4.5 % NaCl	5.6 / 5.4	NaCl: 9 / 4.5
0.9 NaCl + HCl	2 / 2.9 / 3.9 / 4.9	NaCl: 9, HCl Added to Adjust pH
4.5 NaCl + HCl	1.9	NaCl: 4.5, HCl Added to Adjust pH
0.02 (% 1 Lactic Acid)	3.5 / 3 / 2.2	——
% 1.2 L-cysteine	2.1	HSCH$_2$CH(NH$_2$)COOHHC1H$_2$O: 17.6
0.01 % HCl (0.05 vol % Concetrated HCl)	2	——

Degradation Phenomena

4

THE most important requirement for the choice of the biomaterial is its acceptability by the human body which can be described as biocompatibility. The implanted material should not cause any complications like allergy, inflammation and toxicity either immediately after surgery or under post-operative conditions. The success of a biomaterial is highly dependent on different factors as mentioned on other sections such as the mechanical, chemical and tribological, biocompatibility of the implant, the health condition of patient, and the competency of the surgeon. Any dysfunction of those factors can accelerate degradation within the body.

Implants should be subjected to both in vitro and in vivo studies for their applications. In vitro tests which are performed in simulated body condition in order to have an overview of the behavior of the material under the given condition and can be considered as the first step. The in vivo tests which are performed using animal models evaluate the actual performance of the materials and these tests are required in order to get an approval by different council such as FDA or CE [52]. In vitro corrosion studies on orthopedic biomaterials are mostly carried out either in Hank's solution or Ringer's solution which chemical compositions are given in Tables 2.5 on previous chapter.

Dee, Puleo and Bizios has explained corrosion of biomaterials as the gradual degradation of materials by electrochemical attack is of great concern particularly when a metallic implant is placed in the hostile electrolytic environment of the human body. The implants face severe corrosion environment which includes blood and other constituents of the body fluid which encompass several constituents like water, sodium, chlorine, proteins, plasma, amino acids along with mucin in the case of saliva [53].

The reaction of the metallic ions due to corrosion in the human body can contribute many different factors. As corrosion starts on the surface of the implant, the dissolution of metal will lead to erosion. It will cause to brittleness and fracture of the implant. Once fracture occurs, corrosion rate will accelerate since two reasons. Firstly, the amount of exposed surface area will increase and secondly protective oxide layer will be destroyed. If the metal fragments are not surgically extracted, further dissolution and fragmentation can occur, which may result in inflammation of the surrounding tissues [52]. Table 4.1 illustrates the effects of corrosion in human body due to various biomaterials. Williams have reported that the release of corrosion products will obviously lead to adverse biological reactions in the host, and several authors have reported increased concentrations of corroded particles in the tissue near the implants and other parts of the human body [54]. Cobalt-chromium alloy which is a commonly used biomaterial consists of the elements cobalt, chromium, nickel and molybdenum. It has been noted that corrosion of cobalt-chromium in the wet and salty surroundings of the human body, releases toxins into the body which in turn leads to the formation of cancerous tumors [55]. It can be illusional that the number of tumors near the implant formed may be less, but there is always a possibility that many could exist at other parts of the human body because of the released ions.

The oxide layer on the surface majorly contributed in order to inhibits the dissolution of

Table 4.1: Effects of Corrosion in Human Body Due to Various Biomaterials [54]

Metals	Effect of Corrosion
Nickel	Affects Skin - Such as Dermatitis
Cobalt	Anemia B Inhibiting Iron From Being Absorbed into The Blood Stream
Chromium	Ulcers and Central Nervous System Disturbances
Aluminum	Epileptic Effects and Alzheimers Disease
Vanadium	Toxic in The Elementary State

metal ions. However it is not always stable in the human body. When the surface oxide film of a metallic material is disrupted, corrosion proceeds and metal ions are released continuously unless the film is regenerated. The interaction between physiological environment and the material have the major influence on reformation and repassivation of the oxide layer. The time taken for repassivation is different for every kind of materials being used within the body. The corrosion rate and the amount of released metal ions are dependent on regeneration time. The analysis of the surface oxide film on various metallic biomaterials is given in Table 4.2 [52].

To minimize these problems, better understanding of some of the basic principles involved in the degradative process of corrosion is required. Shreir indicated that corrosion of implants in the aqueous medium of body fluids takes place via electrochemical reactions and it is necessary to appreciate and understand the electrochemical principles that are most relevant to the corrosion processes [56]. The electrochemical reactions that occur on the surface of the implant have the same principles with any kind of corrosion degradations. The metallic components of the alloy are oxidized to their ionic forms and the dissolved oxygen is reduced to hydroxyl ions. During corrosion process, the total rates of oxidation and reduction reactions must be equal so as electron production and electron consumption. The overall reaction rate is controlled by the slowest step of these two processes [57]. The types of corrosion that are pertinent to the currently used alloys are pitting, crevice, galvanic, intergranular, stress-corrosion cracking, corrosion fatigue and fretting corrosion.

4.1 Types of Corrosion

4.1.1 Pitting Corrosion

Pitting corrosion is a localized form of corrosion that results in extensive damage and release of significant amounts of metal ions [48]. Pitting refers to the formation of small cavities or holes on materials surface, which is protected otherwise by the presence of an adherent, tenacious and self-healing thin passive film. Each pit has been formed is enhancing the interaction level of certain aggressive ions with the film at locations. The pits may be visible to the naked eye in some cases. However it is not always the case. Mostly they are invisible and dangerous since that kind of an error on the surface may allow the formation of stress corrosion cracking (SCC) or fatigue cracks. Thus, a small, narrow pit with minimal overall metal loss can lead to the failure of an entire engineering system. Pitting may occur when localized chemical or mechanical damage to the protective oxide film has been done. As an example water chemistry factors which can cause breakdown of a passive film are acidity due to low dissolved oxygen concentrations (which tend to render a protective oxide film

Table 4.2: Analysis of the Surface Oxide Film on Various Metallic Biomaterials [52]

Metallic Biomaterial	Surface Oxides	Surface Analysis
Titanium(Ti)	Ti^{0+}, Ti^{2+}, Ti^{3+}, Ti^{4+}	Ti^{2+} oxide thermodynamically less favorable than Ti^{3+} formation at the surface. Ti^{2+} and Ti^{4+} oxidation process proceeds to the uppermost part of the surface film and Ti^{4+} observed on the surface outer most layer.
Titanium Alloys; • Ti-6Al-4V • Ni-Ti • Ti-56Ni • Ti-Zr	TiO^{2+} TiO^{2+} - Based Oxide Titanium and Zirconium Oxides	- Surface consists of small amount of Al_2O_3, hydroxyl groups, and bound water and the alloying element Vanadium was not detected. - Minimal amounts of nickel in both oxide and metal states. - Very low concentrations of metallic nickel, NiO, hydroxyl groups and bound water on the surface were detected. - Titanium and zirconium are uniformly distributed along the depth direction. The thickness of the oxide film increases with increase in zirconium content.
Stainless Steel; • Austenitic Stainless Steel • 316L	Iron and Chromium Oxides of Iron, Chromium, Nickel, Molybdenum and Manganese	- Only very less amount of molybdenum was observed on the surface and nickel was absent when tested in both the air and in chloride solutions. - The surface film contains a large amount of OH-, that is, the oxide is hydrated or oxyhydroxide. Iron is enriched in the surface oxide film and nickel, molybdenum, and manganese are enriched in the alloy substrate just under the surface oxide film.
Co-Cr-Mo Alloy; • Co-36.7Cr-4.6Mo	Oxides of Cobalt and Chromium Without Molybdenum	- Surface contains large amount of OH-, that is the oxide is hydrated or oxyhydroxidized. - Chromium and molybdenum distributed more at the inner layer of the film.

less stable) and high concentrations of chloride (as in seawater). Also poor application of, a protective coating can be a reason for pitting corrosion. Furthermore the presence of non-uniformities in the metal structure of the component can form pits on the surface. Kamachi et al. reported that once the pit is initiated, the metal ions form precipitates at the top of the

pit and often form a film covering the pit. The film restricts entry of the solution and oxygen into the pit, and repassivates, which could renew the protection [48]. Also he has underlined that the importance of assessing pitting corrosion resistance by determining pit propagation rate (PPR) curves [58]. For biomedical applications, pitting corrosion is a problem often on the underside of screw heads. It is more like to observe that kind of attack in media containing chloride ions [59]. Sivakurmar et al. well established that the resistance to pitting in saline environment can be enhanced by molybdenum addition and by keeping the inclusion level at minimum level.

4.1.2   Crevice Corrosion

Crevice Corrosion refers to the localized attack on a metal surface at, or immediately adjacent to, the gap or crevice between two joining surfaces thus it is related to structural details. The gap or crevice can be formed between two metals or a metal and non-metallic material. Outside the gap or without the gap, both metals are resistant to corrosion. The damage is normally confined to one metal at localized area within or close to the joining surfaces [48]. By biomedical point of view, the phenomena usually encountered beneath the screw head that holds the plate or in similar locations such as the intersection of the components of two pieces, hip nail [53]. Some researchers showed that, 316L stainless steel is highly susceptible to crevice corrosion attack as compared to the other commonly used metallic implant material [60]. On the bone plate and screws made of stainless steels, corrosion can form at the contact area of screw heads and the counter sinks hole. However, crevice corrosion problem can be solved by appropriate design of device and proper choice of the material.

4.1.3   Galvanic Corrosion

Galvanic corrosion or bimetallic corrosion is defined as the accelerated corrosion of a metal because of corrosion damage induced when two dissimilar materials are coupled in a corrosive electrolyte. For implants, it can be the case when two different kinds of metals are in physical contact in an ionic conducting fluid medium such as serum or interstitial fluid. The differential composition or process variables of a plate and the adjoining screws can be galvanic couple, which results in galvanic corrosion [48]. Galvanic corrosion is a function of different factors such as relative areas of electronic and ionic contact, as well as the actual metal pair involved. However, for galvanic corrosion it is always safe to assume that some that kind of corrosion will occur in any dissimilar metal pair no matter corrosion resistivity in acidic pH. For surgical implants, galvanic corrosion can occur if bone plate and bone screws are made of dissimilar metals or alloys. Corrosion effects can be observed mostly between the plate and bottom side of the screw holes.

4.1.4   Corrosion Fatigue

Corrosion fatigue is the result of the combined action of an alternating or cycling stresses and a corrosive environment. Corrosion fatigue resistance is an important factor of consideration for load-bearing surgical implant metals or for metals used in cyclic motion applications. The fatigue process can cause rupture of the protective passive film, upon which corrosion is accelerated.If the metal is simultaneously exposed to a corrosive environment, the failure can take place at even lower loads and after shorter time. Cracks, which can initiate from hidden

Table 4.3: Types of Corrosion in the Conventional Materials Used For Biomaterial Implants [63]

Type of Corrosion	Material	Implant Location
Pitting	304 SS, Cobalt Based Alloy	Orthopedic & Dental Alloys
Crevice	316L SS	Bone Plates & Screws
Stress Corrosion Cracking	CoCrMo, 316L SS	Only in vitro
Corrosion Fatigue	316 SS, CoCrNiFe	Bone Cements
Fretting	Ti6Al4V, CoCrSS	Ball Joints
Galvanic	304 SS / 316 SS CoCr / Ti6Al4V 316 SS / Ti6Al4V or CoCrMo	Oral Implants Screws and Nuts
Selective Leaching	Mercury From Gold	Oral Implants

imperfections, surface damage, minute flaws and chemical attack can cause failure. The corrosive attack can be affected by solution type, solution pH, oxygen content and temperature. The body fluid environment may well decrease the fatigue strength of the implant. Fatigue striations on the fractured surface of the implants with colored "beach marks" are indicative of corrosion fatigue. The presence of corrosion pit or pits could induce the fatigue to develop [59]. Hu et al. reported that failures of mechanical origin in orthopaedic implants are most commonly due to fatigue or environmentally assisted fatigue. In some instances, however, the mechanism responsible for crack initiation and crack propagation may be different [61].

4.1.5 Fretting Corrosion

Kamachi et al., defined fretting corrosion when it is the case of two opposing surfaces such as bone plates and the screw heads of the prosthetic devices rub each other continuously in an oscillating fashion in the body environment [48]. It is the result of small relative movements between the contacting surfaces in a corrosive medium. Syrett et al. reported that clinical significance of fretting attack is because of the risk that it can rise up corrosion products in adjacent tissues to a large amount of and it might be the one of a main reason for crack initiation and fracture failure of an implant [62]. Quantification of weight loss of the implant due to fretting corrosion has been well researched at literature and it can be seen that phenomena is directly proportional to the load transmitted across the surfaces, the number of cycle fretted and the amplitude of stresses. As a result, it has been reported that the weight loss is inversely proportional to the hardness of the material and the frequency of stroke. [62].

Different the types of corrosion for the conventional materials are introduced in Table 4.3 [63].

4.2 Corrosion Of Cobalt-Based Alloys

Cobalt based alloys have wide superior properties on traditional stainless steels such as higher mechanical strength, elastic modulus, abrasion resistance and enhanced corrosion resistance. Chromium is the major contributor for that kind of alloys in order to increase corrosion resistance like in stainless steel. However in addition to the stainless steel corrosion resistance, element of cobalt also contributes to the corrosion resistance and that extra contribution put cobalt-chromium based alloys a step forward on the basis of corrosion resistance [64]. As mentioned above, their better mechanical properties, apart from these alloys being used for the fabrication of removable partial dentures, make them a great candidate for implants since requirements of biomaterial framework constructions [65]. Cobalt-based alloys have been widely used for orthopaedic application but biocorrosion of this alloy is one of the most important problems to be solved since large amount of released metal ions which causes adverse effects become that kind of alloy suspicious [66]. As mentioned on previous chapters, CoCrMo alloy is used as a femoral head of joint prostheses in conjunction with an ultra-high molecular weight polyethylene (UHMWPE) cup in order to obtain high wear and corrosion resistance via help of cobalt based alloys. The problem with other kind of designs such as the metal-on-metal couple is that the release of metal ions is higher than that of the polymer-on-metal couple in in vivo, which will, over many years lead to toxicity problem. Sachiko et al. stated that the metal ions dissolved from CoCrMo alloy powder can bind serum proteins to a much greater level compared to that of Ti6Al4V alloy [67].

4.3 Metal Release of Cobalt-Chromium Alloy

Osteolysis and aseptic loosening or loosening in the absence of infection are the most important reasons of failure of total hip replacements. Particles released from the implant as the femoral head articulates against the acetabular cup during movement have been found to be of a clinically relevant size (0.110 μm) that activates macrophages [66]. Macrophages are monocytes, which are actually member of leukocyte type that grow and settle in tissues instead of remaining in the bloodstream where they become tissue macrophages and make up the bodys first line of defense. The main components of the immune response are leukocytes. Leukocytes, or in other name white blood cells, consist of 5 different types. Three of which are granulocytic leukocytes and the other two of which are agranulocytic. The three granulocytic leukocytes are neutrophils, eosinophils and basophils because of they have granules in their nuclei. The two agranulocytic leukocytes are monocytes and lymphocytes [68].

MacDonald et al. indicated that biological risks of metal ions include wear debris, colloidal organometallic complexes, free metal ions, and inorganic metal salts or oxides formed. Organometallic complexes are formed by metal ions binding to proteins. Because of proteins are Zwitter ions, most of them are negative charged carrier within the bodys pH level which is 7.4. Positively charged metal ions, such as cobalt, chromium, and nickel bind to proteins, changing the pH level. Proteins rise up kinetics of corrosion of an implant since it increases the dissolution of metals, especially cobalt and chromium. Cobalt and chromium have the same affinity for proteins, but nickel significantly competes for cobalt and chromium binding areas. The mechanism by which cobalt induces genotoxicity, mutagenicity, carcinogenicity and apoptosis [69].

Once a metal is bound to a protein, it can be systemically transported and either stored or

40

excreted. Cobalt is transported from tissues to the blood and eliminated in the urine within 48 hours, while chromium builds up in the tissues and red blood cells [70].

Shrivastava et al. discussed that large number of biologically active substances, including heavy metals, may have direct, primary or secondary effects on the immune system. On one hand there are various metals that responsible for many biochemical, immunological and physiological activities of the body as micronutrients that promote the action of insulin in body tissues so that the body can use sugars, proteins and fats. But on the other hand some of them can give rise to disordered functions of the immune system resulting in increased susceptibility to infection [71]. Heavy metals have a big influence on altering the immune response by immunostimulatory or immunosuppressive mechanisms.

Chromium is a naturally occurring heavy metal found in the environment commonly in trivalent, Cr(III) and hexavalent, Cr(VI), forms. The reduction of Cr(VI) to Cr(III) results in the formation of reactive intermediates that together with oxidative stress and oxidative tissue damage and a cascade of cellular events including modulation of apoptosis regulatory gene p53 contribute to the cytotoxicity, genotoxicity and carcinogenicity of Cr(VI)-containing compounds. Some research shows that Cr(III) is unable to enter into the cells but form of Cr(VI) enters through membrane anionic transporters. Intracellular Cr(VI) is metabolically reduced to Cr(III). Cr(VI) does not react with macromolecules such as DNA, RNA, proteins and lipids. However, both Cr(III) and the reductional intermediate Cr(V) are capable of co-ordinate, covalent interactions with macromolecules [72]. The chromium genotoxicity can come out as several different types of DNA lesions, gene mutations and inhibition of macromolecular synthesis. Further, chromium exposure may initiate some diseases such as apoptosis, premature terminal growth arrest or neoplastic transformation. Chromium-induced tumor suppressor gene p53 and oxidative processes are some of the major factors that may determine the cellular outcome [71]. Clinical and laboratory evidences show that hexavalent chromium, Cr(VI), is responsible for most of the toxic actions [72]. Exposure to Cr(VI) can cause various point mutations in DNA and to chromosomal damage, as well as to oxidative changes in proteins. [71].

4.3.1 Chromium

Bagchi et al., stated that the reduction of Cr(VI) to Cr(III) yields reactive intermediates, which in combination with oxidative stress, oxidative tissue damage, and a cascade of cellular events leads to activation of the p53 apoptosis regulatory gene, causes cytotoxicity, genotoxicity, and carcinogenicity associated with Cr(VI) [73]. In patients with loosening, Cr(VI) increases the expression of CD3, and CD69. CD69 is an activation antigen on CD3/T lymphocytes. Thus chromium that has been released from the implant is responsible for lymphocyte sensitization, which initiates a localized immune response and failure of the implant [74]. Chromium (VI) initiate the dose-dependent activation of the nuclear transcription factors NF-jB and p53, and damages DNA, induces cell apoptosis, and inhibits cell proliferation. NF-jB inhibits apoptosis by transcriptional activation of genes and induction of proliferation [75]. Although Cr(VI) is more toxic than Cr(III), the latter also has adverse physiological effects. Trivalent chromium is a highly reactive and short-lived molecule that interacts with subcellular organelles and induces apoptosis and necrosis [76]. It also has a influence on decreasing the viability and/or proliferation rate of eukaryotic cells by damaging DNA and inhibiting topoisomerase DNA relaxation [77]. Yet, trivalent chromium is essential for proper insulin function and is required for normal protein, fat, and carbohydrate metabolism

[73]. Pentavalent chromium (Cr(V)) is a highly reactive intermediate which is formed during the reduction of Cr(VI) to Cr(III). This intermediate is stabilized by sialoglycoproteins and carbohydrates and initiates genotoxicity of the cell [78].

4.3.2 Cobalt

Cobalt has a potential to behave as carcinogenic because it inhibits the repair of damaged DNA. When H_2O_2 was present in the environment, cobalt directly caused site-specific DNA damage [79]. Catelas et al. found out that Co(II) is more toxic than Cr(III) since higher amount of TNF-α was released upon exposure to a lower concentration of Co(II) compare to Cr(III) [80]. Jones et al. found that patients with McKeeFarrar prostheses were Co(II) positive on patch nesting, but nickel and chromium negative. The patients had symptoms of pain, instability, and spontaneous dislocation and showed necrosis of bone, muscle, and the joint capsule [81].

4.3.3 Oxidative Damage

Transition metals in toxic doses such as chromium and nickel, alter the bodys oxidationreduction balance. This disturbance damaged redox-sensitive signaling molecules, such as nitric oxide, S-nitrosothiols, AP-1, NF$-\kappa$B, I$-\kappa$B, p53, p21ras and others via oxidative stress. Damage to these molecules, prevents normal cell signaling and gene expression, which initiates toxicity and carcinogenicity [82]. By participating in oxidation-reduction reactions, metal ions can cause shifts in the bodys pH [83]. They also cause hydrolysis of oxidehydrates to form metalorganic complexes. Study of Carter shows that iron, copper, chromium and cobalt ions combine with oxygen species, including molecular dioxygen, superoxide and hydrogen peroxide to produce many different redox reactions [83]. In the presence of hydrogen peroxide (H_2O_2), Cr(VI) increases oxidative damage by generating hydroxylradicals (-OH) via Fenton-type and HaberWeisstype reactions [84].

$$M^{n+} + H_2O_2 \rightarrow M^{n+1} + {}^-OH + {}^{\bullet}OH \tag{4.1a}$$

$$M^{n+1} + O_2^{\bullet -} \rightarrow M^{n+} + O_2 \tag{4.1b}$$

$$H_2O_2 + O_2^{\bullet -} \xrightarrow{M^{n+}/M^{(n+1)+1}} O_2 + {}^-OH + {}^{\bullet}O \tag{4.1c}$$
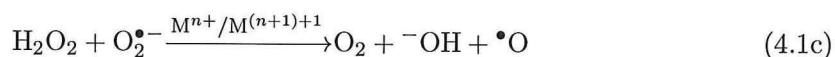
Harris et al. used the Equation 4.1 as showed above in order to demonstrate how redox cycling results in rapid production of large amounts of highly toxic hydroxyl radicals [84]. Equation 4.1a is a Fenton-type reaction in which a metal is oxidized as hydrogen peroxide dissociates. In Equation 4.1b, superoxide reduces an oxidized metal by donating one electron. Together, Equation 4.1a and Equation 4.1b form the HaberWeiss reaction in Equation 4.1c.

4.4 Immune Response To Metal Particles

The response to wear debris produced by implants is classified as a Type IV T-cell mediated hypersensitivity reaction [85]. The presence of metalprotein complex specific antibodies detected in serum indicates the formation of antibodies against metals, suggesting involvement

of humoral immunity as well. Cobalt-chromium-molybdenum and titanium-alloy degradation products are immunologically reactive since they can become complexed with high molecular weight serum proteins, especially immunoglobulins [86]. A disturbance of the immune system was directly linked with an increase in metal ions released in the blood. Donati et al. indicated that the toxic action of metal ions, in conjunction with the compartmentalization of lymphocytes in periprosthetic tissues, is responsible for the observed decrease in the components of the immune system [85]. A recent study has indicated that, patients with infection in the periprosthetic tissue around their implants showed an increased rate of allergic reactions to cobalt and nickel compared to patients with implants who do not have any infection and to persons without implants. Figure 4.1 shows ion concentration versus the time transformations [87].
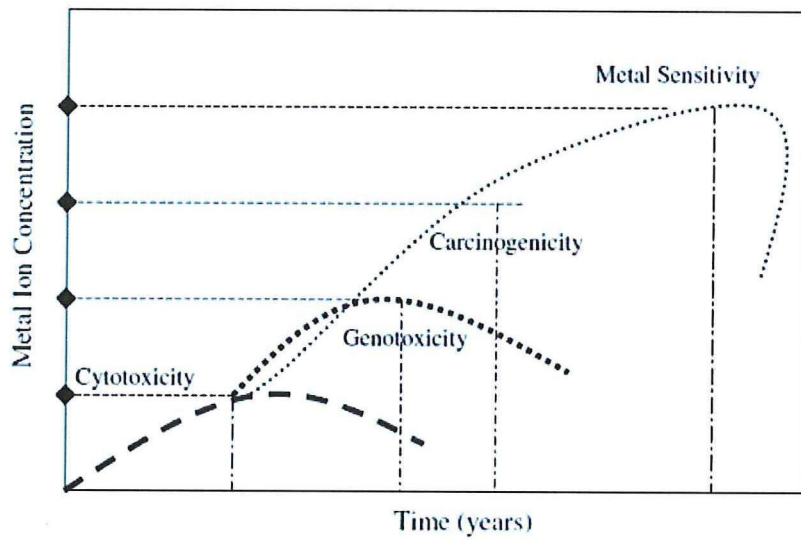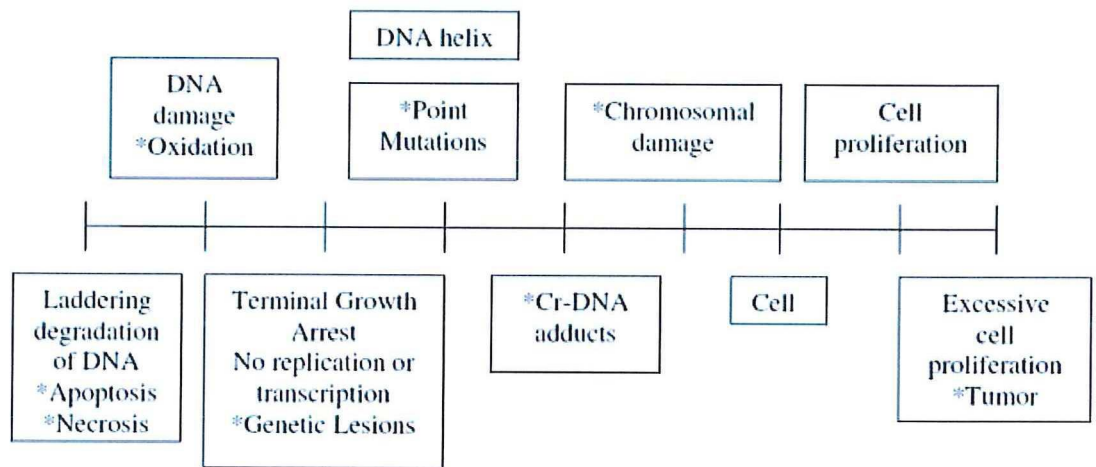
Figure 4.1: Scanning Taxonomy of Metal Ion Concentrations [87]

44

Research Approach 5

A Renewed interest in metal-on-metal prosthesis bearings has been considered and developed since the early 1990s. This has been mainly due to the problems of polyethylene wear debris induced osteolysis from the widely used polyethylene-on-metal total joint arthroplasty as been described in details on previous chapters. Cobalt-chromium based alloys play an essential role for orthopedical implants in assisting with the repair or replacement of bone tissue that has become diseased or damaged. Those alloys are more suitable for load-bearing applications compared with ceramics, polymeric and even other metallic materials because they combine high mechanical strength and fracture toughness. However, metal-on-metal joint replacements are not used by surgeons without concerns, especially if cobalt-chromium based alloy is the case since the main limitation of these alloys is the release of the toxic metallic ions. Those released metal ions from metal-on-metal pairs may cause cytotoxicity, tissue necrosis, adverse immunological reactions and hypersensitivity.

The conducted research has been widely inspired by a real case study. In 2010, Johnson & Johnson unit DePuy Orthopaedics issued a global recall of two hip-replacement systems. DePuy, which has sold about 93,000 units of its ASR XL Acetabular System and the ASR Hip Resurfacing System, said recent data received by the company showed an increase in the number of people who have had a second hip replacement surgery, also called a revision surgery. The ASR XL Acetabular Head System and ASH Hip Resurfacing System were designed for metal-on-metal construction which is made of chromium based alloys. The main reason for the recall was the increase of metal ions within the blood due to wear products of the design.

When cobalt-chromium alloys are used as implants, a comprehensive knowledge of their effect on the surrounding tissues is required. The oxidation of cobalt, chromium and molybdenum may produce soluble cobalt and chromium species, which can be released to the neighboring tissues. Depending on the nature and concentration of such chemical species, several adverse reactions may take place, including allergic and carcinogenic effects when used as orthopedical implants. Therefore, without any doubt it is important to have a better understanding of the metal ion release processes for cobalt-chromium based orthopaedic implant materials.

Surface oxide films on metallic materials play an important role as an inhibitor of ion release and they change with the release in vivo. Low concentration of dissolved oxygen, inorganic ions, proteins and cells may accelerate the metal ion release. The regeneration time of the surface oxide film after disruption also governs the amount of released ion.

The aim of the conducted research was to provide a better understanding of the electrochemical behaviour and the corrosion resistance of the cobalt based alloys at in vitro physiological environments. More specifically, the relevant mechanisms in the passive and transpassive states were investigated in detail. F1537 CoCrMo Alloy, 316L Stainless steel, pure cobalt, pure chromium and pure molybdenum studied in simulated physiological solution, Ringer's solution, at 37°C, without and with the addition of other chemical additions. The experiments were employed using electrochemical techniques: open circuit potential, anodic

potentiodynamic and cathodic potentiodynamic measurements, potentiostatic experiments, cyclic voltammetry and electrochemical impedance spectroscopy. In addition inductively coupled plasma - mass spectroscopy (ICP-MS) analysis has been carried out in order to observe and have a good understanding of ion release phenomena. Further, the microstructure and surface condition measurements were evaluated by optical microscopy, AFM and SEM-EDX.

Experimental Plan

6

6.1 Introduction

DURING the conducted research, different parameters such as pH level difference, surface finish and materials selection, have been applied to each of the experimental setup. In order to have a better understanding, the block diagram of experimental plan is shown in Figure 6.1.

6.2 Materials

6.2.1 Cobalt-Chromium-Molybdenum Alloy

Low carbon wrought Co-Cr-Mo alloy (ASTM F1537) rod was supplied by Böhler Edelstahl and used as a working electrode and the main target material during the research. Its nominal chemical composition is shown in Table 6.1. Hardness value of the alloy was 47.5 HRC. Samples were cut into the cylinders of 8 mm in diameter and 15 mm thick.

Table 6.1: Composition (wt. %) of Low Carbon Wrought Alloy

Percent	C	Si	Mn	P	S	Cr	Mo	Ni	Co	Fe	N
(wt. %)	0.039	0.41	0.57	0.003	0.0003	27.45	5.15	0.19	65.69	0.19	0.193

6.2.2 Chromium

Pure chromium (99.7% purity) rod was provided by Goodfellow Cambridge Limited and used as a working electrode in order to have a comparison with cobalt-chromium-molybdenum alloy. Samples were cut in form of cylinders 5 mm in diameter and 10 mm thick.

6.2.3 Cobalt

Pure cobalt (99.9% purity) rod was provided by Goodfellow Cambridge Limited and used as a working electrode in order to have a comparison with cobalt-chromium-molybdenum alloy. Samples were cut in form of cylinders 6.35 mm in diameter and 10 mm thick.

6.2.4 Molybdenum

Pure molybdenum (99.9% purity) rod was provided by Goodfellow Cambridge Limited and used as a working electrode in order to have a comparison with cobalt-chromium-molybdenum alloy. Samples were cut in form of cylinders 5 mm in diameter and 10 mm thick.
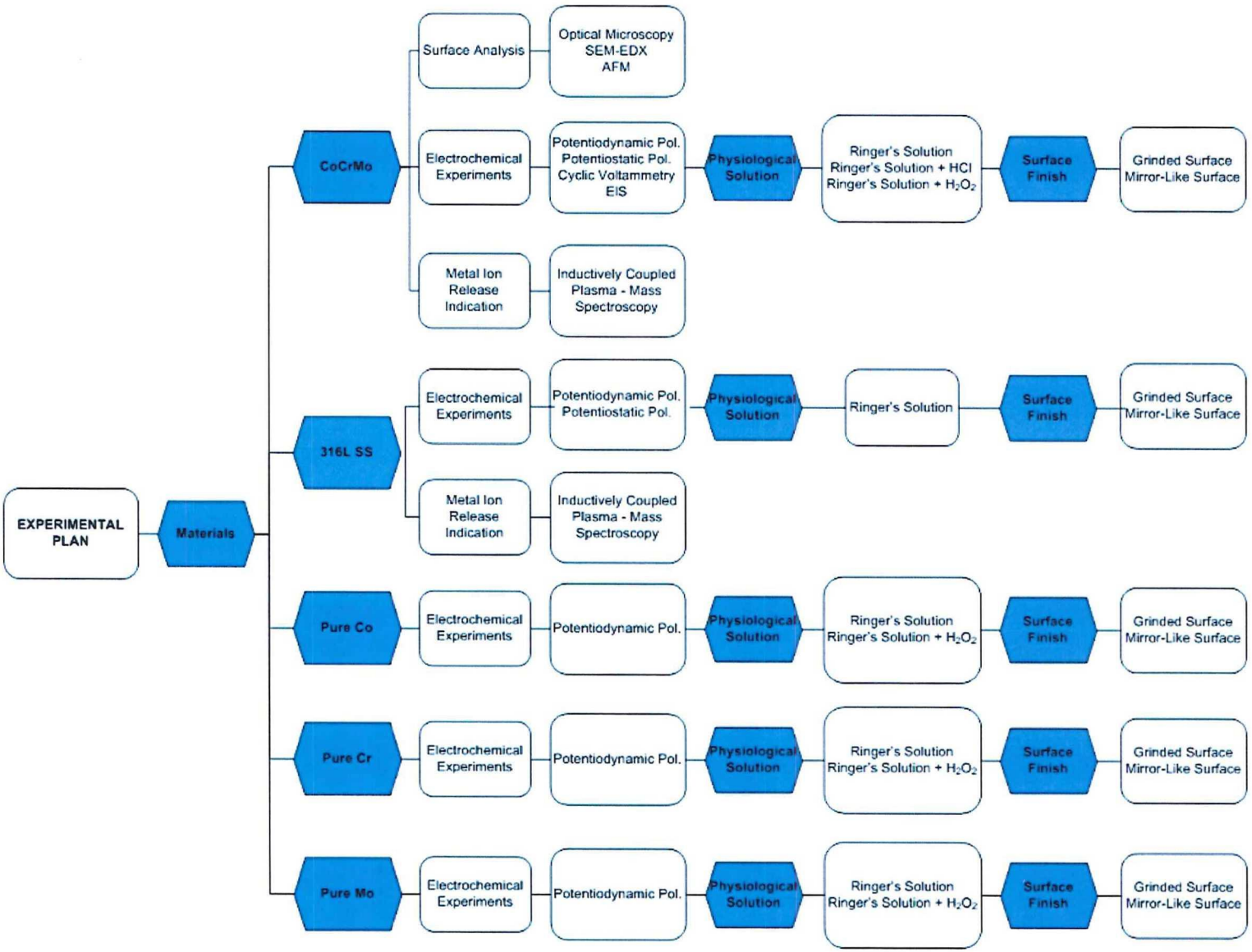
Figure 6.1: Experimental Plan of the Conducted Research
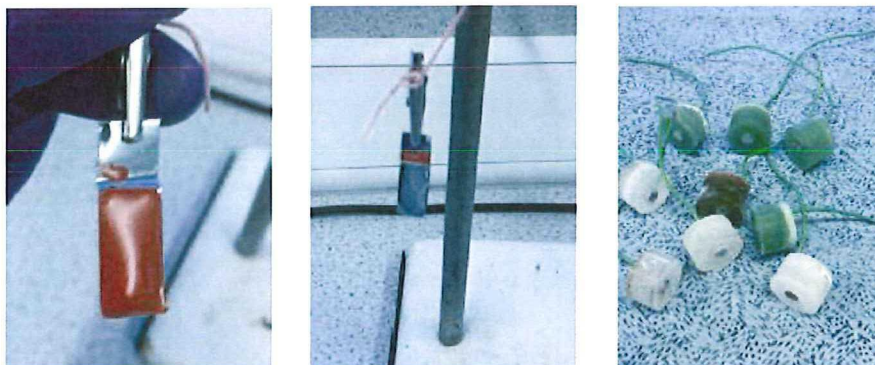
Figure 6.2: Different Steps of Sample Preparation Process

6.2.5 316L Grade Stainless Steel

AISI 316L Temper annealed stainless steel foil was supplied by Advent Research Materials Ltd. and used as a working electrode. Austenic stainless steel is commonly used to manufacture the hip implant prostheses and was considered as a reference materials since countless research has been conducted on this material. The sample chemical composition is reported in Table 6.2. Samples were cut from the foil with the surface area of 3x1 cm^2 and 0.2 mm thick but only 2x1 cm^2 area has been used during the experiments.

Table 6.2: Composition (wt. %) of AISI 316L Stainless Steel

Percent	C	Si	Mn	Ni	Cr	Mo	S	P	Fe
(wt. %)	≤ 0.03	≤ 1	≤ 2	10 - 14	16 - 18	2 - 3	≤ 0.03	≤ 0.045	Balance

6.2.6 Sample Preparation

The test specimens were cut into the size which has been mentioned above. Then, the top part of the cylinder shaped cobalt-chromium-molybdenum alloy, pure cobalt, pure chromium and pure molybdenum samples were soldered to electrical wire. After soldering got stable and the connection was checked by an amperometer, samples were embedded into the cold resin which was conducted at room temperature. The drying time for the resin was approximately 1 hour. Stainless steel samples were connected to the electrochemical cell directly without any soldering is necessary. However backsides of the samples were covered with isolator paint. Then specimens were abraded with SiC emery paper down to 1200-grit for the purpose of rough surface finishing and 2400-grit for the smooth surface finishing samples in Struers Rotopol-31 automatic system. In addition, the smooth surface finishing specimens were polished with the diamond paster down to 0.25 μm and reached a mirror-like surface. After cleaning and rinsing the samples with with water and ethanol in order to get rid of the rough dirt, each specimen were cleaned in the ultrasonic bath with acetone, isopropyl alcohol (2-propanol or the abbreviation IPA) and distilled water respectively and separately for 5 minutes. All specimens were brought in contact with the electrolyte solution after 10 minutes and employed as working electrodes for the research. Preparation of the samples for different materials is shown in Figure 6.2.

51

6.2.7 Electrodes

The potential of the working electrode is measured against a Ag/AgCl reference electrode which was provided by Radiometer Analytical. The electrode functions as a redox electrode and the reaction is between the silver metal and its salt, silver chloride. As counter electrode, platinum gauze was used in three-electrode horizontal cell.

6.3 Electrolytes

6.3.1 Composition

Experiments were carried out at 37°C in Ringer's type solution, a simulated body physiological solution. It was prepared in the laboratory and used for all the electrochemical experiments. Chemical composition of the solution is shown in Table 6.3. In all cases pH values were adjusted to physiological pH 7.8.

Table 6.3: Composition of Ringer's Solution

Composition	NaCl	KCl	CaCl$_2$	NaHCO$_3$
Concentration (gL^{-1})	6	0.075	0.1	0.1

6.3.2 Additive Chemical Solutions

The aim of this study was to examine the different parameters for cobalt-chromium alloys and effect of pH was one of the targets. When, pH falls as consequence of the hydrolysis of the metal ions released, oxygen concentration decreases, while the amount of metal ions and counter-ions such as chloride anion rises. In addition, the concomitant hydrogen evolution reaction and/or oxygen reduction reaction originate reactive species such as nascent hydrogen, nascent oxygen and hydrogen peroxide that may influence the biochemistry involved in biological processes [88].

6.3.2.1 Hydrogen Peroxide

Hydrogen peroxide has been added to Ringer's solutions to simulate the oxygen species which is the case within the human body conditions. In all cases pH values were fixed to pH level of 5.9. Relevant values for the solution are discussed at Chapter 7 under Electrolyte Composition section.

6.3.2.2 Hydrogen Chloride

In order to understand the effect of pH at very low acidic levels, hydrogen chloride was added to Ringer's solution. In all cases pH values were regulated to pH level of 2.4. Relevant values for the solution are discussed at Chapter 7 under Electrolyte Composition section.

6.4 Electrochemical Techniques

Open circuit potential (OCP), potentiodynamic, potentiostatic and cyclic voltammetry measurements were recorded using an Ecochemie Autolab PGSTAT12 PC-controlled poten-

tiostat/galvanostat with GPES Manager computer software program. This is a potentiostat/-galvanostat with a compliance voltage of 12 V, especially dedicated for research in solutions with low resistance, i.e. aqueous solutions. Maximum current is limited to 250 mA and current resolution is 30 fA on the 10 nA current range [89]. Electro-chemical impedance spectroscopy experiments were carried out on Solartron 1286/1287. The model is a research grade, high accuracy, wide bandwidth potentiostat/galvanostat with a full range of DC capabilities. Computer control via an IEEE488 (GPIB) interface is standard, and the instrument is supported by CorrWare and ZPlot software packages [90].

6.4.1 Open Circuit Potential

The open circuit potential is the potential of the working electrode relative to the reference electrode when no potential or current is being applied to the cell. The open-circuit potential is the equilibrium potential. Surface electrochemistry needs to be stable in order to have an healthy result.

6.4.2 Potentiodynamic Polarizations

Potentiodynamic polarization measurements were carried out in a closed three-electrode cell, with a scan rate of 0.1667 mVs^{-1} using an Ecochemie Autolab PGSTAT12. Potentiodynamic curves were examined to assess corrosion resistance by recording anodic and cathodic currents. Both anodic and cathodic polarization curves investigated separately after open circuit potential step. Cathodic polarization curves were recorded starting 1000 mV more negative and finishing 300 mV more positive than the open-circuit potential. For anodic polarization curves, it has been started to record 100 mV more negative and 1000 mV more positive with respect to open circuit potential value.

6.4.3 Potentiostatic Polarizations

As well as potentiostatic polarization experiment were performed via Ecochemie Autolab PGSTAT12. Potentiostatic measurements were carried out in order to evaluate the effect of potential and of mass transport conditions on the corrosion kinetics. Polarization curves were recorded for 30 minutes at different potential values based on the potentiodynamic polarization curves.

6.4.4 Cyclic Voltammetry

Cyclic voltammetry was used to gain further understanding of the mechanisms involved in the transpassive oxidation of CoCrMo. Cyclic voltammetry is the most widely used technique for acquiring qualitative information about electrochemical reactions. It offers a rapid, effective and versatile location of redox potentials of the electroactive species. In a cyclic voltammetry experiment the working electrode potential is ramped linearly versus time [91]. Cyclic voltammograms recorded at different sweep rates which are 1 mV/s, 5 mV/s and 10 mV/s respectively. Start potential was defined as 0.05 V Ag/AgCl. First and second vortex points were selected as 1.5 V and -0.3 V respectively

6.4.5 Electrochemical Impedance Spectroscopy

Electrochemical impedance spectroscopy (EIS) was employed to investigate and monitor in situ changes in the passive film/electrolyte-interface on CoCrMo with time of exposure of the alloy to the electrolyte solution. Solartron 1286 potentiostatgalvanostat, Solartron S1255 frequency response analyzer and National Instruments GPIB-120A bus expander/isolator were used together with a Faraday cage to avoid external interferences. All the experiments has been conducted at 37°C. The traditional EIS three electrode set-up was employed using Ag/AgCl as the reference electrode, platinum gauze as the counter electrode and the cobalt-chromium-molybdenum alloy as the working electrode. The frequency range of study was between 0.01 and 100000 Hz, and the amplitude 10mV. The potentiostat was programmed to perform a 24 hours test, measuring the impedance of the system and open circuit potential (OCP) every hour. Before initiating the impedance test, the system was allowed to stabilize at the OCP for 1 hour.

6.5 Microstructural Investigations

6.5.1 Optical Microscopy

Optical metallography was used to determine the microstructures of the cobalt-chromium-molybdenum alloy. Image analysis of the alloy was performed using a Microscope Leica DMLM which was connected to Olympus analySIS auto image analysis software. Surface of the sample was etched in order to distinguish the carbides and grain boundaries. Chemical composition of the etching solution is shown in Table 6.4.

Table 6.4: Composition of Etching Solution

Composition	HCl	HNO$_3$	FeCl$_3$
Volume (ml) / Weight (g)	200 ml	5 ml	65 gr

6.5.2 Scanning Electron Microscope - Energy Dispersive X-Ray

The specimens were examined using Scanning Electron Microscope (SEM) - JEOL JSM 6500F. Secondary electron imaging and back-scatter electrons were produced by SEM and used as signals. In addition, energy dispersive X-Ray spectroscopy (EDS) analysis was used to study the chemistry of the alloy matrix and the carbides or inclusion particles. The analysis was carried out in a scanning electron microscope with an EDS analyzer.

6.5.3 Atomic Force Microscopy

Atomic Force Microscopy (AFM) is a microscopy technique that can measure the surface characteristics such as topography, elasticity, friction and adhesion. Veeco Digital Instruments Nanoscope IIIa was used to carry out the experiments. Atomic force microscopy uses a microscale cantilever with a sharp tip at its end in order to scan the specimen surface. When the tip is brought into proximity of the sample surface, attractive and repulsive forces arising between the tip and the sample lead to deflection of the cantilever. This deflection is measured using a laser and a photo diode detector, and an image of the samples topography is formed [92]. Tapping mode was applied for topography imaging. Two different pre-electrochemical

process surface finishes of cobalt-chromium-molybdenum alloy were investigated under AFM in order to have an idea about the morphology . Samples were scanned with 0.193 Hz scan rate. Tip velocity was 19.3 m/s. Images were taken by Digital Instruments Nanoscope IIIa, then processed at Image Metrology SPIP software.

6.6   Elemental Analysis of Metal Ion Release

6.6.1   Inductively Coupled Plasma - Mass Spectroscopy

Inductively coupled plasma (ICP) tests were carried out for detecting and measuring released ions during the anodic polarization scan for two materials (Cobalt-chromium-molybdenum alloy and 316L Stainless steel) in Ringer's solution. Measurements were recorded using an iCap 6000 Series ICP-OES Spectrometer with iTEVA Thermo Scientific computer software program. ICP is an analytical technique used for the detection of trace metals in environmental samples. The elements emit light of a characteristic wavelength. Then it converts to an electrical signal which could be measured quantitatively. Different potential values were indicated based on polarization curves. In order to detect the elements in the electrolyte, first ICP standards were introduced. Standards were prepared based on working electrode material chemical composition. Thus, three different 25 ml concentrations (20 ppm, 5 ppm, 1 ppm) plus blank one were prepared by MBH Analytical Ltd. Multielement Plasma Standard - Common Elements Mix II. Certified chemical composition of the plasma is shown in Table 6.5.

Table 6.5: Composition of the Multielement Plasma Standard - Common Elements Mix II

Composition	Ag	Al	B	Ca	Co	Cr	Cu	Fe	K	Mg
	Mn	Na	Ni	P	Pb	Si	Sn	Ti	V	Zn
Concentration (µg/ml)	100									

Results & Discussion

7.1 Electrochemical Procedures

7.1.1 Electrolyte Composition

As mentioned in 6.2.1., Ringer's solution has been used as the main electrolyte in order to simulate body fluid conditions. Furthermore, hydrogen peroxide and hydrogen chloride addition has been investigated during the research. Ad hoc, 100 ml Ringer's solution has been prepared pH level has been fixed to 7.8. Then, different concentration of hydrogen peroxide and hydrogen chloride has been added. Figure 7.1 shows the concentration addition to Ringer's solution versus pH level change.
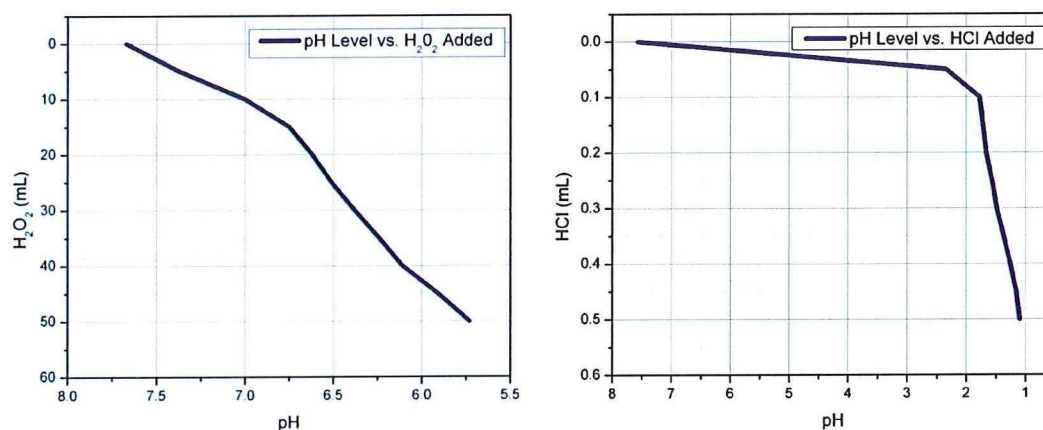
(a) Ringer's Solution pH Level Change in Respect of H_2O_2 Addition

(b) Ringer's Solution pH Level Change in Respect of HCl Addition

Figure 7.1: Electrolyte Composition

It has been decided to add hydrogen peroxide into the electrolyte as it was important to see the effect of this addition. As mentioned in Section 4.3.3., transition metals in toxic doses such as chromium and nickel, alter the bodys oxidationreduction balance. This disturbance damaged redox-sensitive signaling molecules via oxidative stress. Damage to these molecules, prevents normal cell signaling and gene expression, which initiates toxicity and carcinogenicity [82]. By participating in oxidation-reduction reactions, metal ions can cause shifts in the bodys pH [83]. They also cause hydrolysis of oxidehydrates to form metalorganic complexes. Study of Carter shows that iron, copper, chromium and cobalt ions combine with oxygen species, including molecular dioxygen, superoxide and hydrogen peroxide to produce many different redox reactions [83]. In the presence of hydrogen peroxide (H_2O_2), Cr(VI) increases oxidative damage by generating hydroxylradicals (-OH). Furthermore, pH 5.9 was selected since it is not a strong acidic pH level however contained enough amount of hydrogen peroxide

in order to observe the reduction of this additive. Also, pH 2.4 was selected for hydrogen chloride added electrolyte for the further experimental steps since HCl has been used to have a better understanding for an aggressive environment. In addition, some researchers like Contu et al. preferred pH levels close to 2.4 for their conducted studies therefore, pH level was regulated to 2.4 since results could be comparable with the literature afterwards [93].

As a conclusion, oxygen species and low pH level situations were tried to be simulated in vitro condition.

7.1.2 Open Circuit Potential

Corrosion potential in the absence of net electrical current flowing to or from the metal surface is called free corrosion potential (E_{corr}). At E_{corr}, the anodic reaction rate is equal to the cathodic reaction rate and so there is no net current flow to or from the working electrode. It represents a stationary electrochemical process where there is no external polarization of the electrode. The value of E_{corr} is often used to give semi-quantitative indication of the corrosion regimes in which a material resides and it may help to provide a useful tool to differentiate the conditions of active corrosion from passive conditions [94]. The potential evolution indicates the formation of a protecting passivation layer on CoCrMo. This protection layer limits the further dissolution of the alloy and increases the corrosion resistance of CoCrMo.

During the research, different free potential and time scale values for different parameters have been determined. Figure 7.2,Figure 7.3 and Figure 7.4 show the evolution of the open circuit potential (E_{corr}) of CoCrMo with time, when immersed in Ringer's solution and with H_2O_2 or HCl addition.
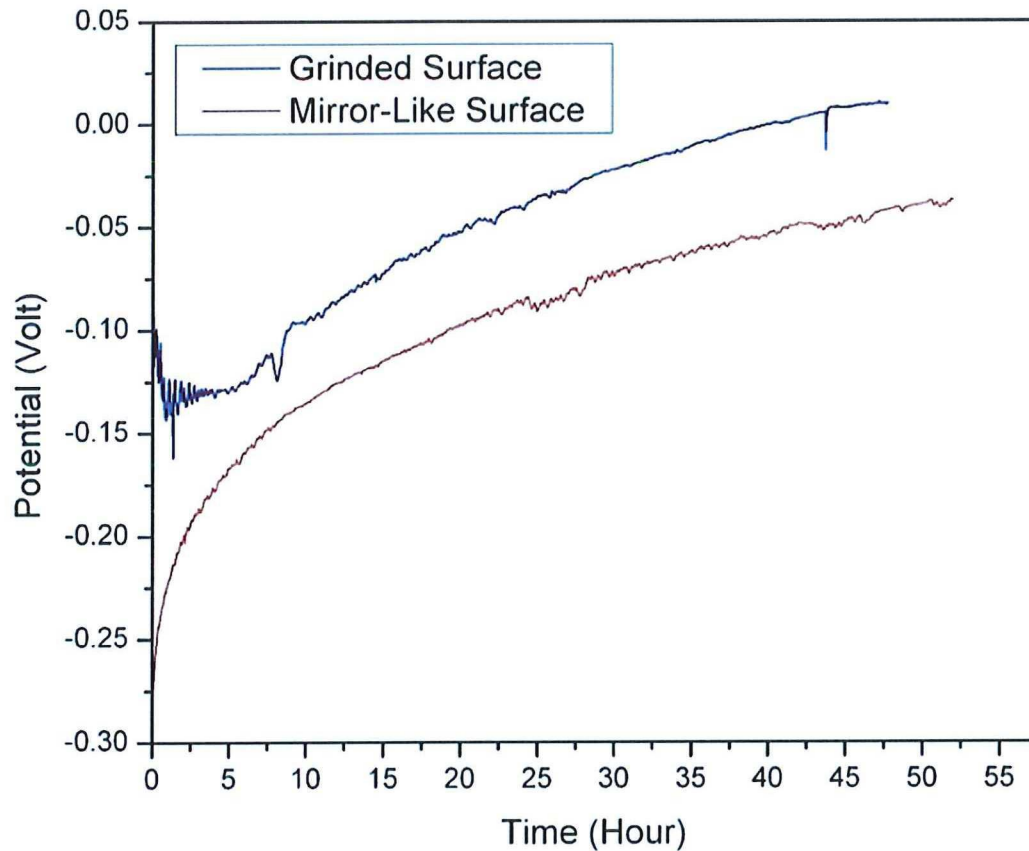
Figure 7.2: Influence of the Ringer's Solution on the Evolution of CoCrMo Alloy Open Circuit Potential with Time

At Figure 7.2 immersed CoCrMo samples show a starting E_{corr}= -0.10 V/AgCl and E_{corr}= -0.25 V/AgCl for grinded and mirror-like surface respectively while reaching values of E_{corr}= 0.01 V/AgCl and E_{corr}= -0.04 V/AgCl after almost 2 days immersion, at which an approximate stationary and steady state electrochemical process was reached. Grinded surface sample become stable at higher potential compare to mirror-like surface one. However the potential difference was almost 50 mV.

For Figure 7.3 immersed samples starts with very close values as E_{corr}= 0.36 V/AgCl and E_{corr}= 0.37 V/AgCl for grinded and mirror-like surface consecutively while reach steady state at values of E_{corr}= 0.33 V/AgCl and E_{corr}= 0.29 V/AgCl respectively after 10 hours immersion. It was observed that, the presence of H_2O_2 in the electrolyte shifts the open circuit potential to the positive direction compare to the value of Ringer's solution itself. The open circuit potential difference between two surface treatments was 5 mV. It is worth mentioning that gas bubbles are observed to evolve constantly on electrode surface during the test. Mirror-like surface finish sample had a low OCP level compare to grinded surface.
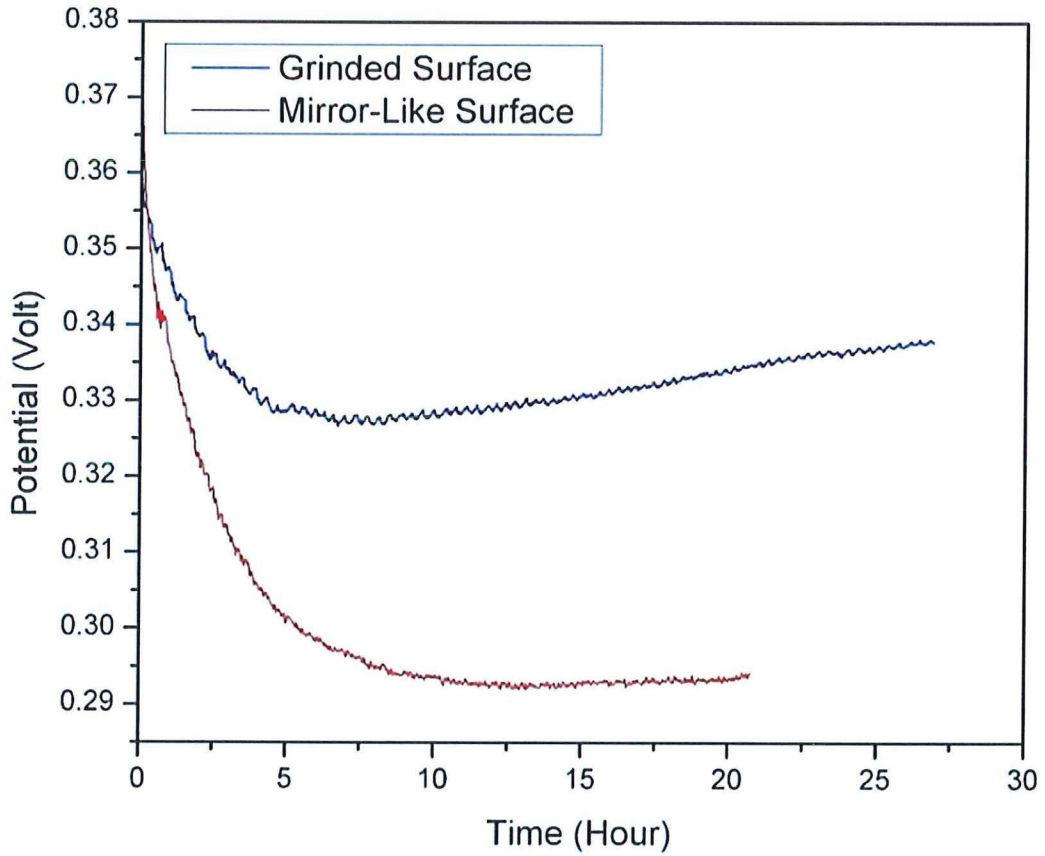
Figure 7.3: Influence of the H_2O_2 Addition to Ringer's Solution on the Evolution of CoCrMo Alloy Open Circuit Potential with Time

Lastly at Figure 7.4 immersed samples initiate at E_{corr}= -0.20 V/AgCl and E_{corr}= -0.05 V/AgCl for grinded and mirror-like surface respectively and stabilize at values of E_{corr}= 0.09 V/AgCl and E_{corr}= 0.17 V/AgCl after 2 days period. There was 70 mV potential difference at the end of two experiments. On contrary of bare Ringer's solution experiment, mirror-like surface sample became stable at higher potential.

As the E_{corr} is determined by both anodic reaction, which possible reactions are the oxidation of cobalt, chromium, molybdenum and the cathodic reaction, which is the hydrogen evolution reaction as in shown Formula 7.1 below [95]. Also the decomposition reactions of the additive chemicals has been introduced in Formula 7.2.

Possible anodic reactions;

$$Co + H_2O \rightleftharpoons CoO + 2\,H^+ + 2\,e^- \tag{7.1a}$$

$$2\,Co^{2+} + 3\,H_2O \rightleftharpoons Co_2O_3 + 6\,H^+ + 2\,e^- \tag{7.1b}$$

$$Mo + 2\,H_2O \rightleftharpoons MoO_2 + 4\,H^+ + 2\,e^- \tag{7.1c}$$

60
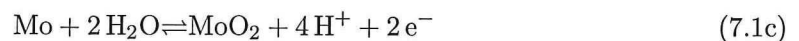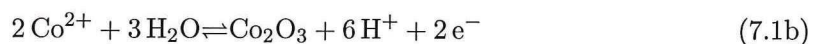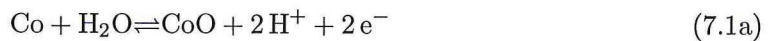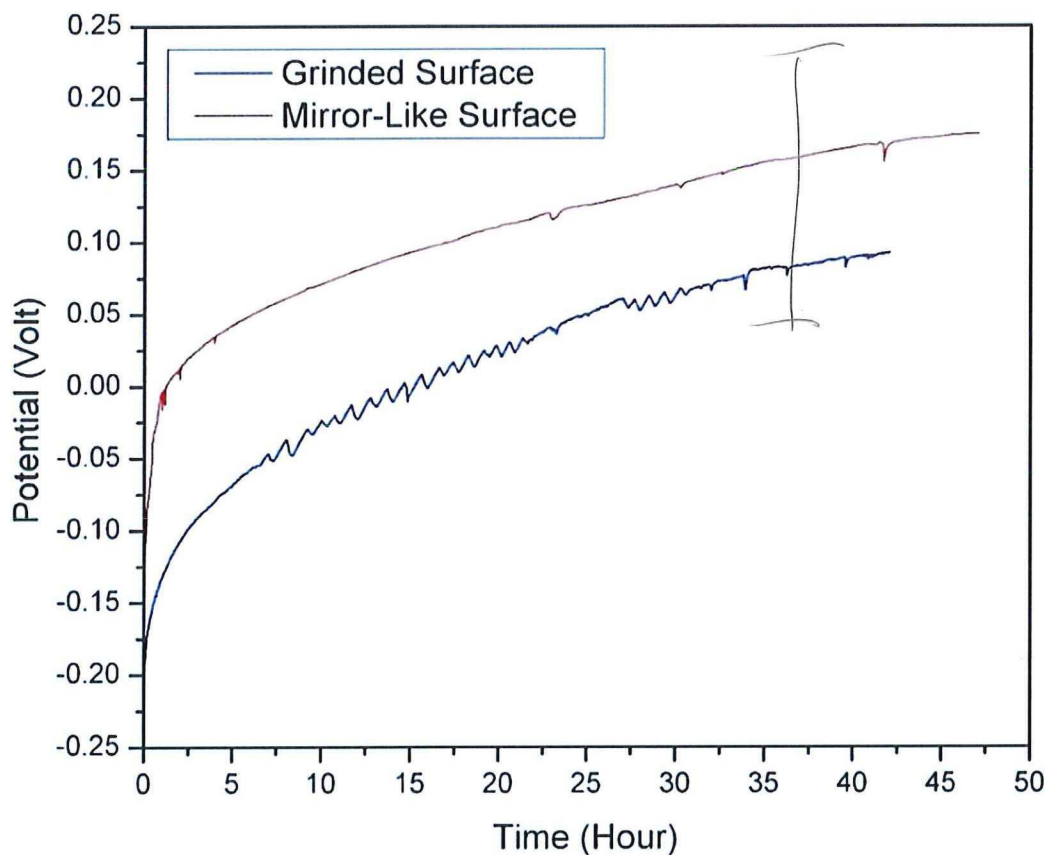
Figure 7.4: Influence of the HCl Addition to Ringer's Solution on the Evolution of CoCrMo Alloy Open Circuit Potential with Time

$$MoO_2 + 2\,H_2O \rightleftharpoons MoO_4{}^{2-} + 4\,H^+ + 2\,e^- \tag{7.1d}$$

$$2\,Cr + 3\,H_2O \rightleftharpoons Cr_2O_3 + 6\,H^+ + 6\,e^- \tag{7.1e}$$

$$Cr_2O_3 + 5\,H_2O \rightleftharpoons 2\,CrO_4{}^{2-} + 10\,H^+ + 6\,e^- \tag{7.1f}$$
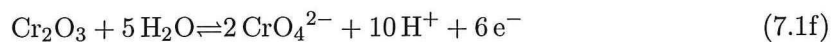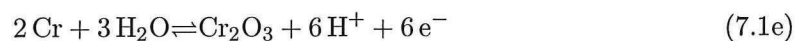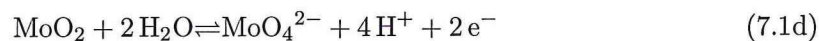
Decomposition reactions of hydrogen peroxide and hydrogen chloride;

$$2\,H_2O_2 \rightarrow 2\,H_2O + O_2 \tag{7.2a}$$

$$HCl + H_2O \rightarrow H_3O^+ + Cl \tag{7.2b}$$

The decrease of the anodic current shifts the E_{corr} progressively in the positive direction as can be see at Figure 7.2 and 7.4 so that the cathodic current can be low enough to balance the

61
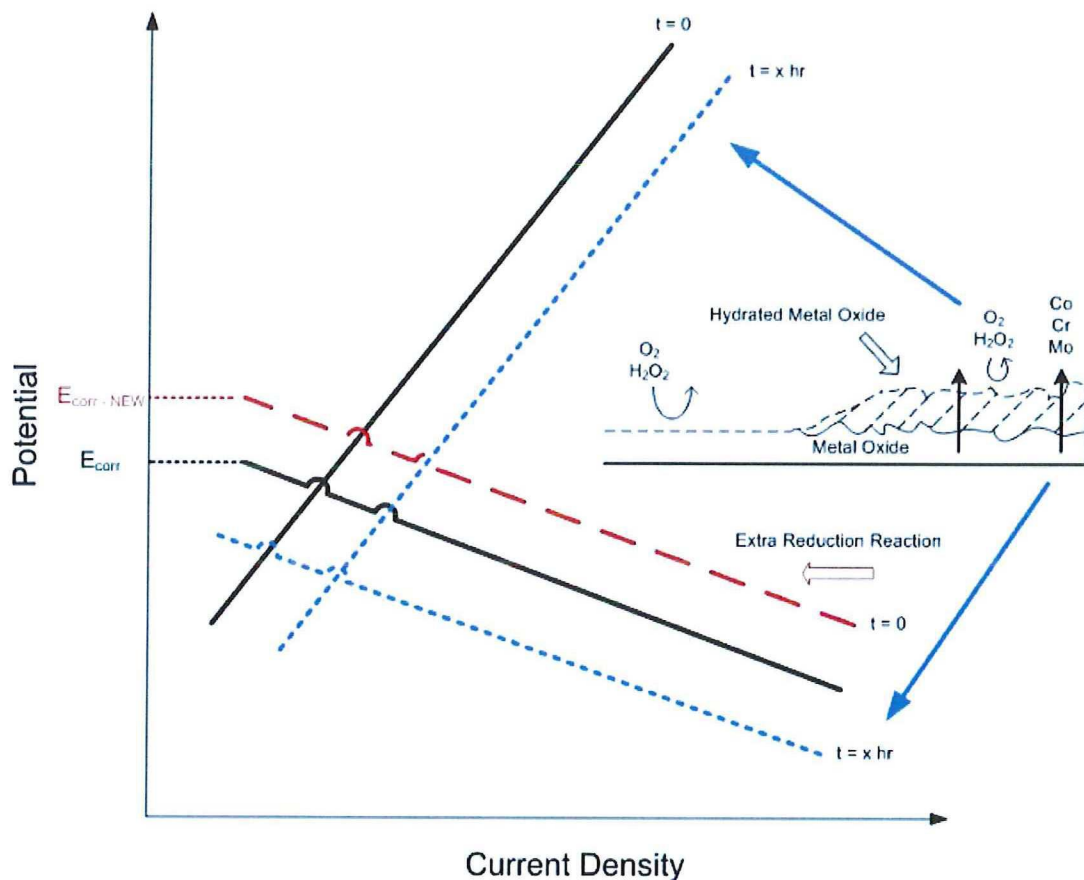
Figure 7.5: Influence of the H_2O_2 Reduction Reaction to Ringer's Solution

decreased anodic current. However, at Figure 7.3 a negative shift has been observed. It can be explained by the influence of autonomous chemical decomposition of hydrogen peroxide. Hydration of the oxide layer occurs at potentials where upon hydrogen is evolved at the metal-hydrated oxide interface.Due either to the decreasing conductivity of the metal because of the formation of that phase or to the increasing anodic reaction rate through the porous, not strongly bonded hydrated metal oxide layer by time could be reasons and hypothesis for a negative shift in the presence of hydrogen peroxide. However, extra reduction reaction gave a positive shift to the steady state potential compare to bare Ringer's solution as schemed in Figure 7.5.

In addition surface finish effect has been observed. For Figure 7.2 and 7.3, mirror-like surface finish samples became stable at lower potentials. However, in hydrogen chloride addition solution it was an opposite behaviour. The reason might be the small pits had been occurred in an aggressive environment which required a a uniform layer in order to repassivate under a constant attack. It was something expectable since mirror-like surface samples had more uniform surface roughness distribution and it is rather easy to form a uniform layer compare to rough surfaces.Therefore mirror-like surface finish samples had a higher OCP value which indicated a better protection on the surface. On the contrast, since the grinded surface samples already had some roughness and surface imperfections, the surface

got stabilized at lower value. But it should be noted without any doubt that, the potential differences between each surface finish were not so high. Therefore the significance of the surface finish was neglectable.

7.1.3 Potentiodynamic Polarizations

Typical polarization curves of 316L Stainless Steel, CoCrMo, pure cobalt, chromium and molybdenum after surface stabilization in different aqueous environment are shown in Figure 7.6, 7.8, 7.10, 7.11, 7.12 and 7.13 respectively. The polarization curves can be divided into two different potential domains which are cathodic and anodic parts. The cathodic domain includes potentials below open circuit potential (E_{corr}), where the current is determined by the reduction of water and partially of dissolved oxygen [96].
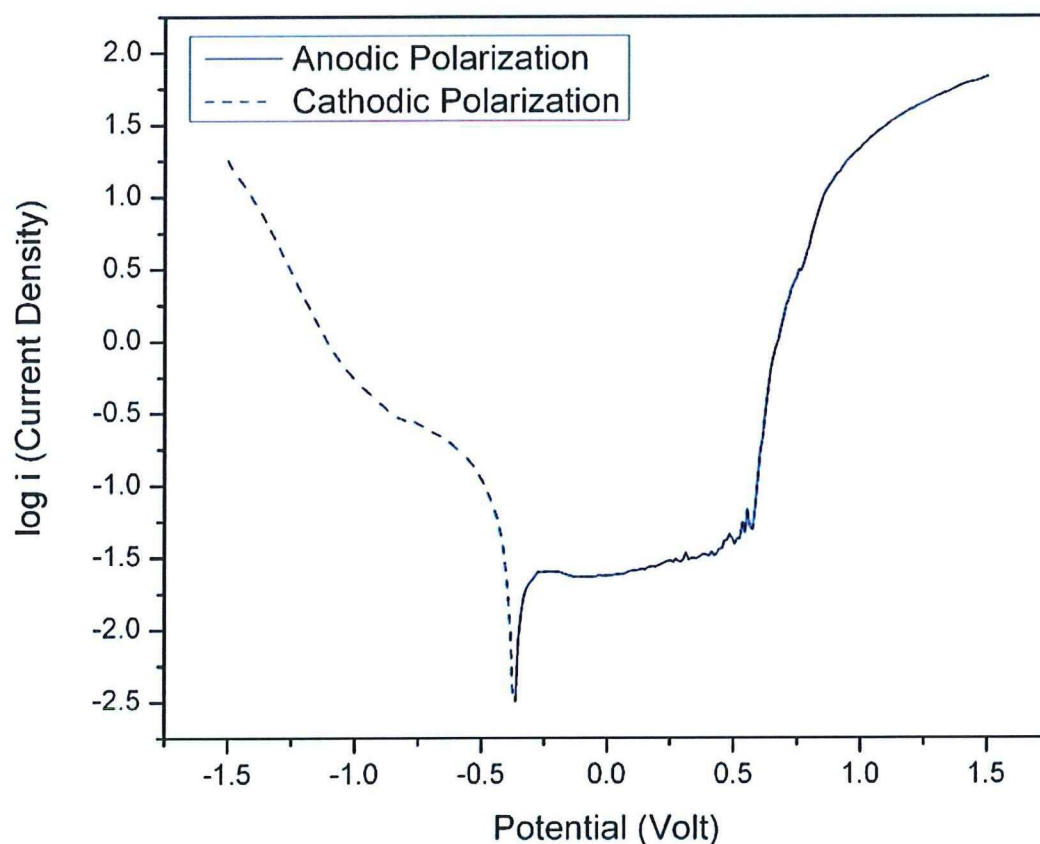
Figure 7.6: Potentiodynamic Polarization Curve of AISI 316L Under Steady-State Conditions

In Figure 7.6, polarization curves of 316L stainless steel are shown. The potential values and behavior of 316L stainless steel polarization curves are in good agreement with recent Hryniewicz et al. study which is shown in Figure7.7 [97].

The anodic polarization curves can be divided into two regions. In the first region, the dissolution of the implanted AISI 316L stainless steel was kinetically limited and the anodic current was increased slowly with the potential showing a passive-like behavior. Finally, there is a transpassive second region beginning at a critical potential, where the rapid increase in

63
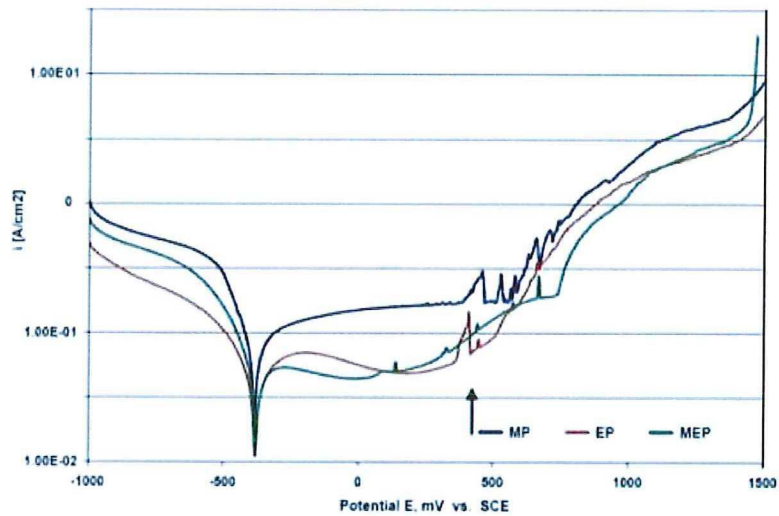
Figure 7.7: Potentiodynamic Polarization Curve of AISI 316L from [97]

the current value occurs due to breakdown of the passive film. This phenomenon is commonly known as pitting corrosion and the potential at which a rapid increase of the current density occurs is usually termed as the pitting potential. The pitting developments could be observed in Figure 7.6 between 300-600 mV range.

Cathodic and anodic polarization curves recorded for three different electrolyte composition are shown in from Figure 7.8, 7.10, 7.11, 7.12 and 7.13.

In Figure 7.8, two different peaks were observed at +0.50 and +0.80 V versus Ag/AgCl preceding a current rise due to the onset of H_2O oxidation may be attributed to the transpassive oxidation of Cr(III) to Cr(VI) as this potential range is in good agreement with previous investigation on transpassive dissolution of chromium oxide films carried out by Hodgson et al. research [99] and is shown in Figure 7.9. As seen in the figure, at 0.4 and 0.7 Volt ranges, transpassive oxidation of chromium can be indicated easily. It should be noted that, since the standard calomel electrode has been used at Hodgson research, approximately 0.2 Volt should be added to those values in order to convert Ag/AgCl electrode values. Furthermore, those peaks were analyzed during the cyclic voltammetry experiment and explained briefly in that section. In addition, surface finish between two samples were compared. It can be easily that, there is not any major difference has been observed between mirror-like and grinded surface.

64
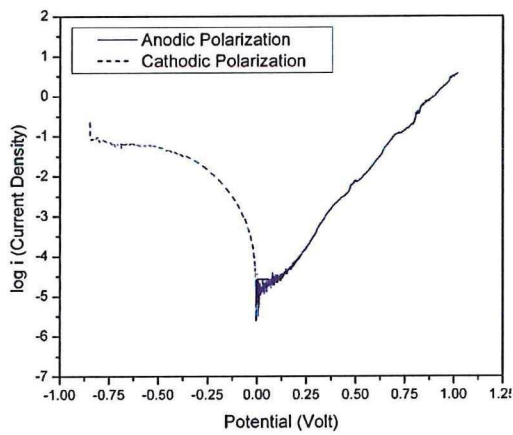
(a) Mirror-Like Surface Finish
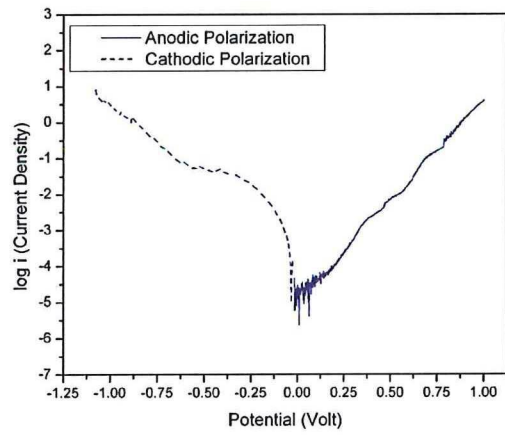
(b) Grinded Surface Finish
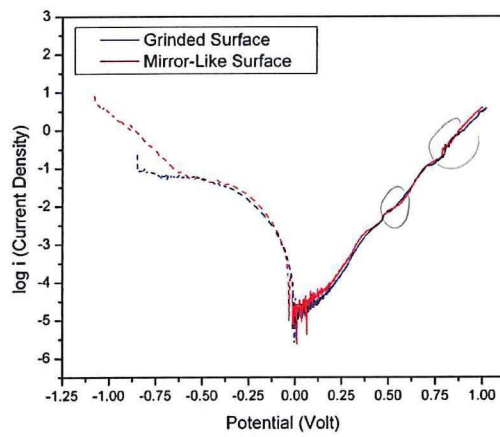
(c) Superposing of Two Curves

Figure 7.8: Potentiodynamic Polarization Curve of ASTM F1537 CoCrMo in Ringer's Solution
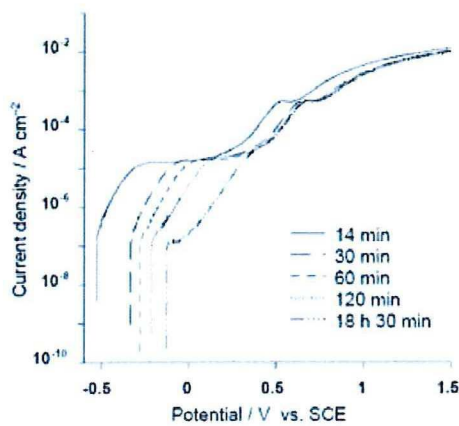
Figure 7.9: Polarisation Curves for CoCrMo Alloy After Different Times at Open-Circuit Potential in Buffered 0.14M NaCl Solution (pH 7.4, 37°C) from [99]

65

(a) Mirror-Like Surface Finish

(b) Grinded Surface Finish

(c) Superposing of Two Curves
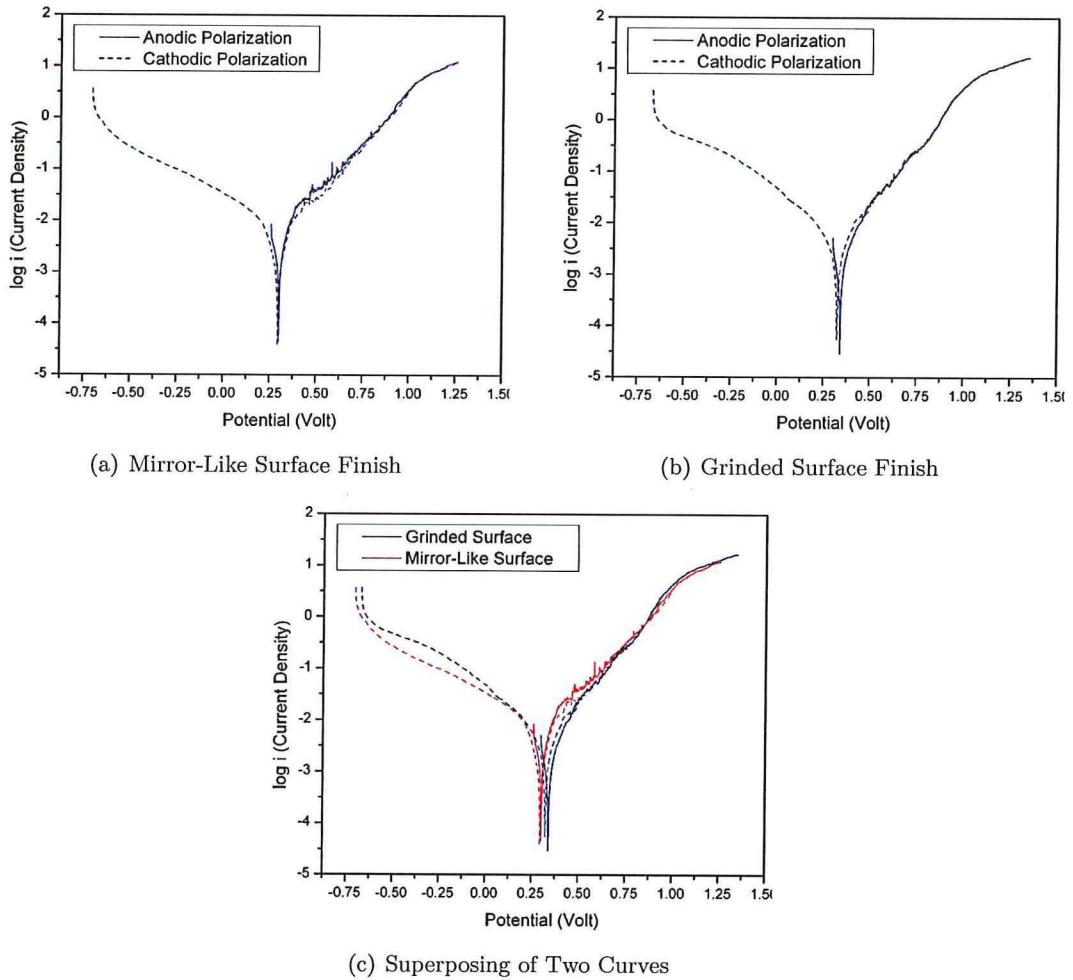
Figure 7.10: Potentiodynamic Polarization Curve of ASTM F1537 CoCrMo in Ringer's Solution with H_2O_2 Addition

In Figure 7.10, there was only one peak indicated close to 0.80 V range. Since there was an extra reduction reaction going as mentioned before,therefore peaks became weaker or even invisible. Further investigation will be conducted at cyclic voltammetry experiment. Moreover, there was 50 mV shift at $E_{c}orr$ between grinded and mirror-like surface finish samples as explained briefly in previous section.
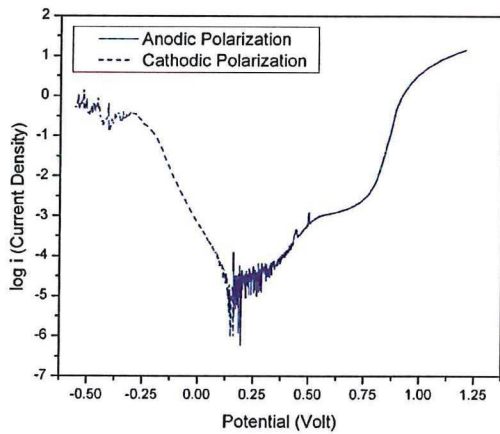
66

(a) Mirror-Like Surface Finish
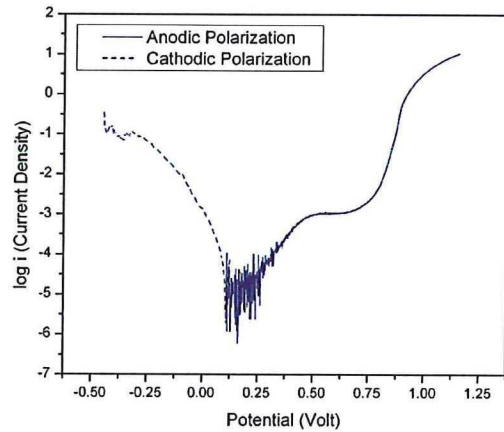
(b) Grinded Surface Finish
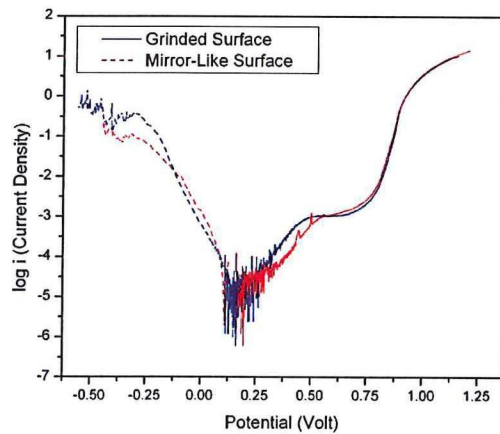
(c) Superposing of Two Curves

Figure 7.11: Potentiodynamic Polarization Curve of ASTM F1537 CoCrMo in Ringer's Solution with HCl Addition

In Figure 7.11, a passive layer formation was observed between 0.40 and 0.60 Volt range. Under aggressive environment attack, material has shown more resistance to the solution compare to other environments. After that passivation layer, transpassive region was started where there was a rapid increase in the current density where the passive film breakdown was initiated.

Potentiodynamic polarisation was also employed to compare the dynamic electrochemical response of the pure metal element components of the alloy itself in order to gain information on the influence and effects that each element plays on the overall behaviour of CoCrMo.
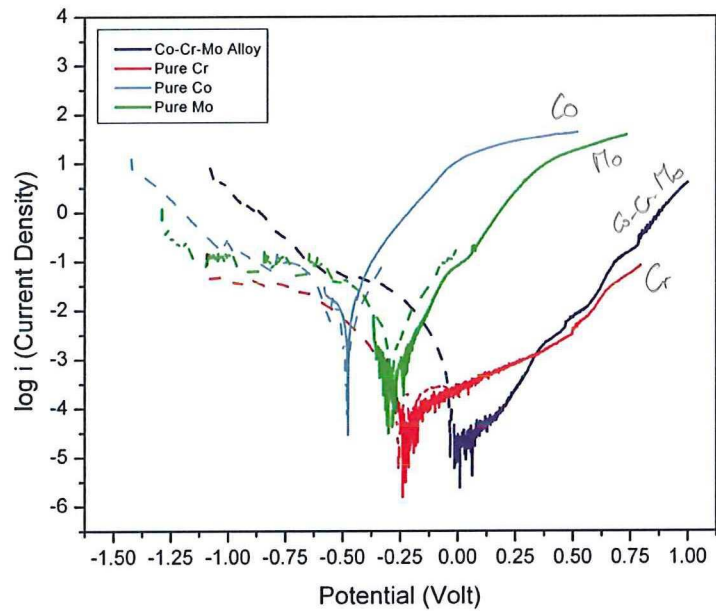
(a) Mirror-Like Surface Finish
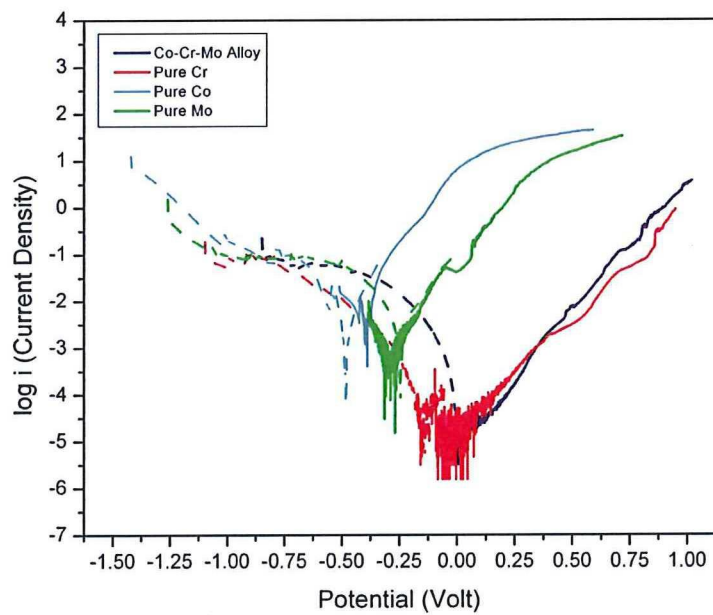
(b) Grinded Surface Finish

Figure 7.12: Potentiodynamic Polarization Curve of ASTM F1537 CoCrMo and Pure Metal Co, Cr, Mo Samples in Ringer's Solution
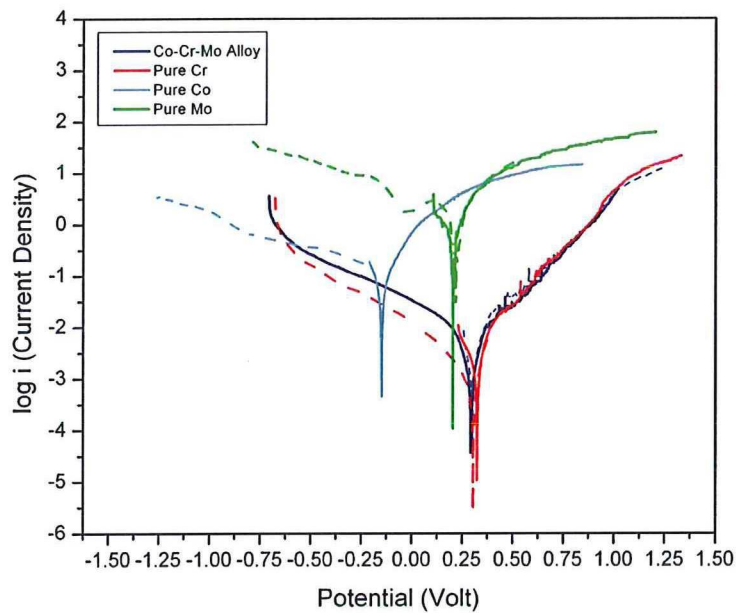
(a) Mirror-Like Surface Finish
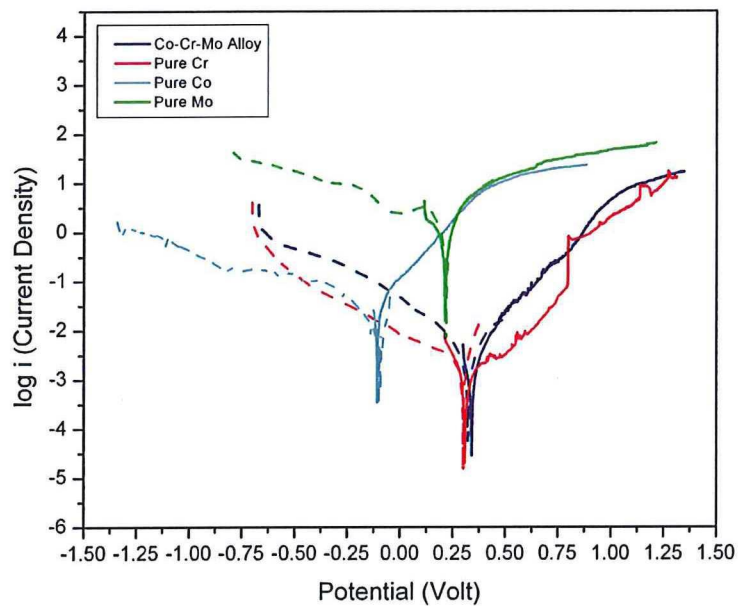
(b) Grinded Surface Finish

Figure 7.13: Potentiodynamic Polarization Curve of ASTM F1537 CoCrMo and Pure Metal Co, Cr, Mo Samples in Ringer's Solution with H_2O_2 Addition

The polarization curves for cobalt, chromium, molybdenum and CoCrMo of the samples in Ringer's solution and hydrogen peroxide addition electrolyte solution are shown in Figure 7.12 and Figure 7.13.
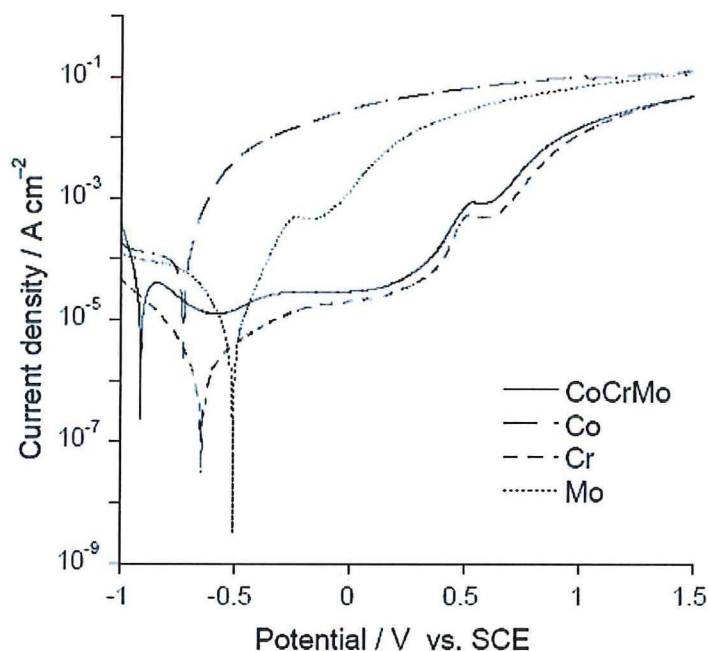
Figure 7.14: Polarisation Curves for CoCrMo Alloy and For Pure Metals Co, Cr and Mo Samples in Buffered 0.14M NaCl Solution (pH 7.4, 37°C) from [95]

In Figure 7.12(a), after stabilization at the open-circuit potential, corrosion potential (E_{corr}) for cobalt in Ringer's solution is -0.47 V, for molybdenum -0.27 V, for chromium -0.21 V and for CoCrMo alloy -0.01 V whereas in Figure 7.12(b) just chromium was shifted into more positive direction, -0.15 V. Thus, influence of surface finish was not a significant parameter. It has been observed that CoCrMo alloy and chromium exhibited passive behaviour under two different surface finish, chromium being spontaneously passive whereas the CoCrMo alloy shows an active to passive transition. Due to the composition of the alloy, which contains high cobalt ratio, that transition was observed at potentiodynamic experiments. Since the cobalt showed an active dissolution and no passive layer formation. Furthermore, those results were supported by Hodgson et al. study one more time and is shown in Figure 7.14 [95]. As seen in the figure, chromium and alloy itself showed same passivity behaviour starting from 0 Volt and whereas cobalt displayed an active dissolution.

In Figure 7.13(a), corrosion potential (E_{corr}) for cobalt in Ringer's solution is -0.15 V, for molybdenum 0.21 V, for chromium 0.32 V and for CoCrMo alloy 0.29 V whereas in Figure 7.13(b) CoCrMo alloy and cobalt were shifted into more positive direction, -0.10 and 0.34 V respectively. In addition, surface finish as well as Figure 7.12 did not play an important role during the experiments besides minor shifts at open circuit potentials. It has been observed that at higher anodic potentials, the polarization curve of the alloy strongly resembles the curve of pure chromium and CoCrMo. Therefore, it was a supporting fact for the indication of the peaks in Figure 7.8 which were assumed as oxidation of Cr(III) to Cr(VI).

70

7.1.4 Potentiostatic Polarizations

Potentiostatic measurements were carried out in order to evaluate the effect of potential and of mass transport conditions on the corrosion kinetics. Based on the polarization curves that have been obtained at Section 7.1.3, CoCrMo and stainless steel samples were polarized 30 minutes for each range and shown in Figure 7.15, 7.16 , 7.17 and 7.18.
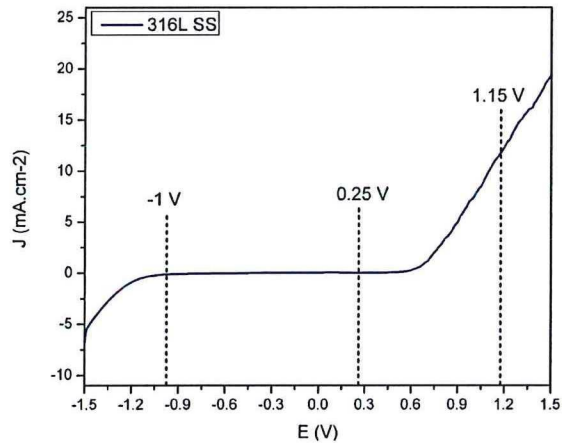
Figure 7.15: Potentiodynamic Polarization Curve of AISI 316L for Potentiostatic Polarization Experiment

In Figure 7.15, it was shown that three different potential values were chosen from three different regimes, which were -1 Volt for the active region, 0.25 Volt for the passive region and 1.15 Volt for the transpassive region.

In Figure 7.16, at -1 Volt range, the overall current was dominated by the cathodic reaction as a consequence of the reduction of water and of dissolved oxygen for both stainless steel. At 0.25 Volt, electrochemical kinetics was determined by passivation. Transpassive region could be determined at 1.15 Volt range for stainless steel whereas anodic dissolution was more important than passivation

In Figure 7.17, four different potential values were chosen from three different regimes, which were -1 Volt for the active region, 0.25 Volt for the passive region, 1 Volt and 1.15 Volt for the transpassive region. An extra high potential region, 1.25 Volt, was chosen in order to observe the metal ion release at a higher value in ICP-MS analysis.

In Figure 7.18, cathodic reaction has the control at -1 Volt since the reduction of water on CoCrMo alloy samples. At 0.25 Volt, passivation was in the charge of kinetics. Furthermore, it was observed that peak was exhibited just after the potential was applied followed by a continuous decrease in current density with time typical for passivation phenomena. Transpassive regions were determined at and 1 and 1.25 Volt. Hodgson stated that for CoCrMo sample, it is possible to have two different reactions at that zone. One might be the passivation, which is indicated by the initial current density peak and the second one could be another anodic reaction, formation of Cr(VI) species, determining the gradual rise in current density after the passivation peak [95].
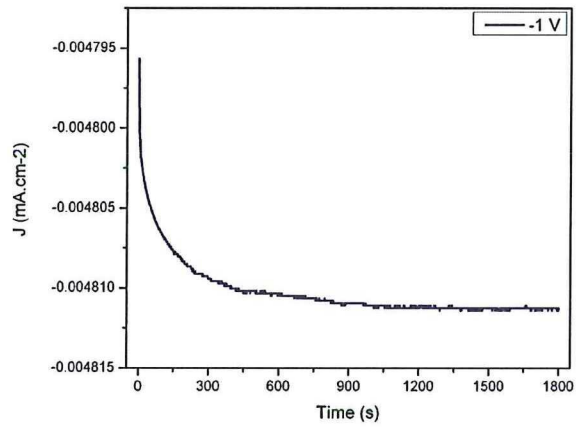
(a) -1 Volt
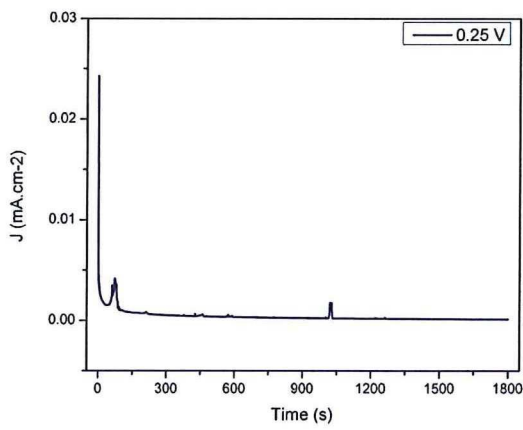
(b) 0.25 Volt
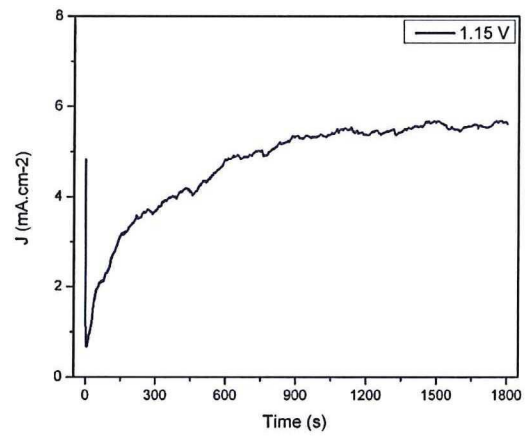
(c) 1.15 Volt

Figure 7.16: Potentiostatic Polarization of 316L Stainless Steel - Current Densities Values for Different Potentials
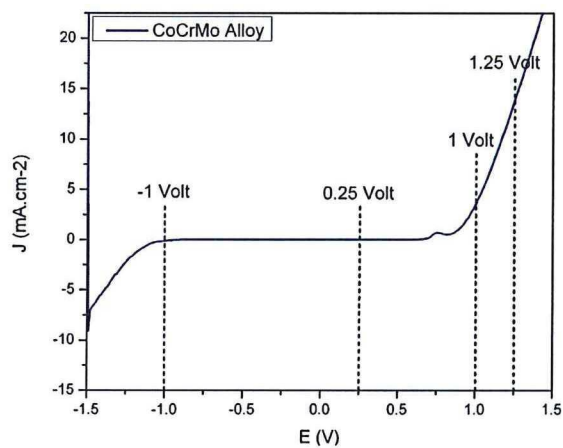
Figure 7.17: Potentiodynamic Polarization Curve of CoCrMo Alloy for Potentiostatic Polarization Experiment

72

(a) -1 Volt

(b) 0.25 Volt

(c) 1 Volt

(d) 1.25 Volt
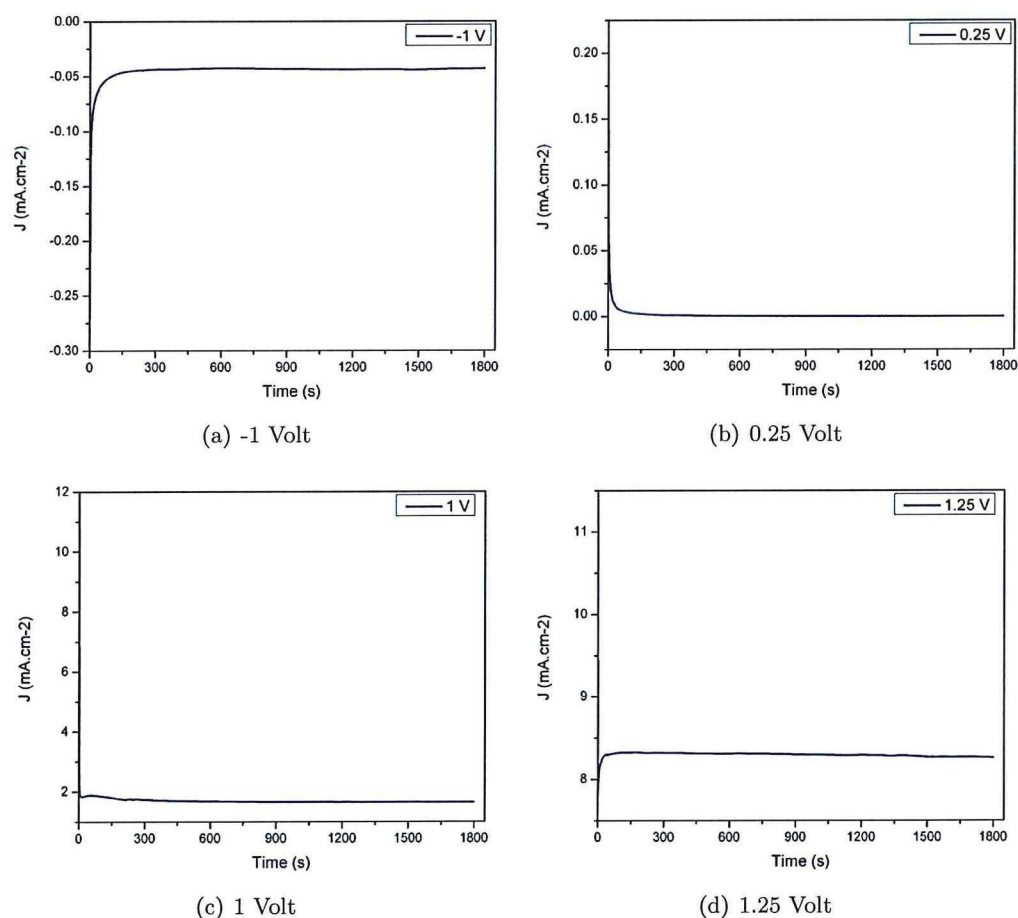
Figure 7.18: Potentiostatic Polarization of CoCrMo Alloy - Current Densities Values for Different Potentials

7.1.5 Cyclic Voltammetry

Cyclic voltammetry was used to gain further understanding of the mechanisms involved in the transpassive oxidation of CoCrMo.

In Figure 7.19 and Figure 7.20, cyclic voltammograms recorded at three different sweep rates starting from 0.05 V Ag/AgCl in different aqueous environment are presented.

There is no anodic peak and the passive range extends from -0.3 to 0.5 V in Figure 7.19(b). However in Figure 7.19(a), mirror like surface finish sample showed small peak between 0.2 - 0.4 V potential range with increasing scan rate. The peak of current density increases and becomes clear starting from 0.5 V, which potential the onset for the oxidation of Cr(III) to Cr(VI) takes place, to 0.8 V potential ranges at 1 mV/s scan rate. Also those results are in good agreement with the data and the assumptions made for potentiodynamic experiments. It is clear that the peak of the current density and the peak of the potential are dependent on the scan rate employed. As be seen in Figure 7.19, for the increasing the scan rate, the current density increases as well as accompanied by a shift for potential in positive direction. In addition that behavior is consistent for irreversible system phenomena [97]. It was noted
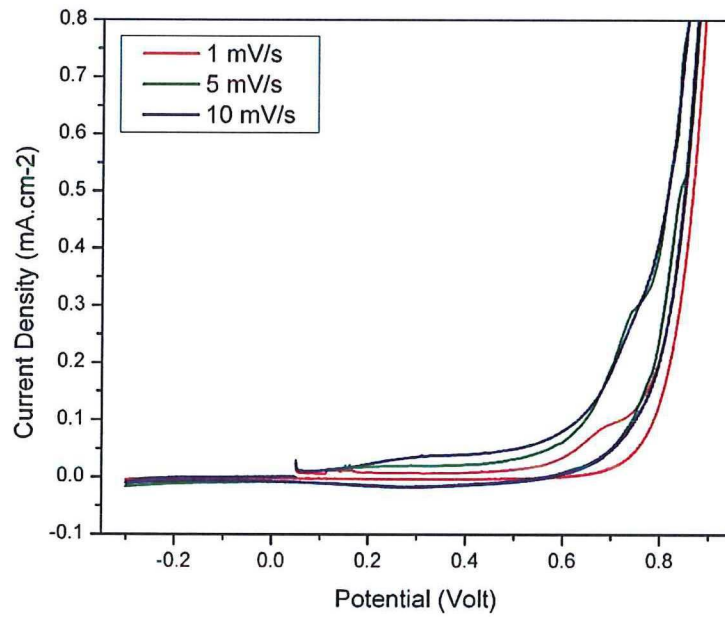
(a) Mirror-Like Surface Finish
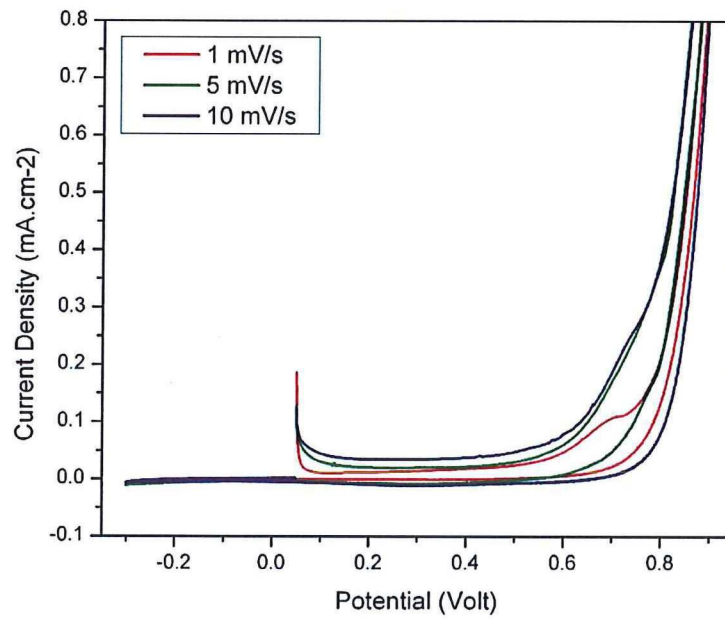
(b) Grinded Surface Finish

Figure 7.19: Cyclic Voltammetry Measurements for CoCrMo Alloy in Ringer's Solution at Different Scan Rates

that peaks belong to reduction of Cr(VI) to Cr(III) were not visible once again for all three scan rates at the reverse potential scan, even with reduced intensity.

The influence of hydrogen peroxide addition on cyclic voltammograms recorded for CoCrMo alloy is shown in Figure 7.20. The results were quite different than those obtained in

pure Ringer's solution since the oxidation and the reduction peaks of chromium were unable to observe.
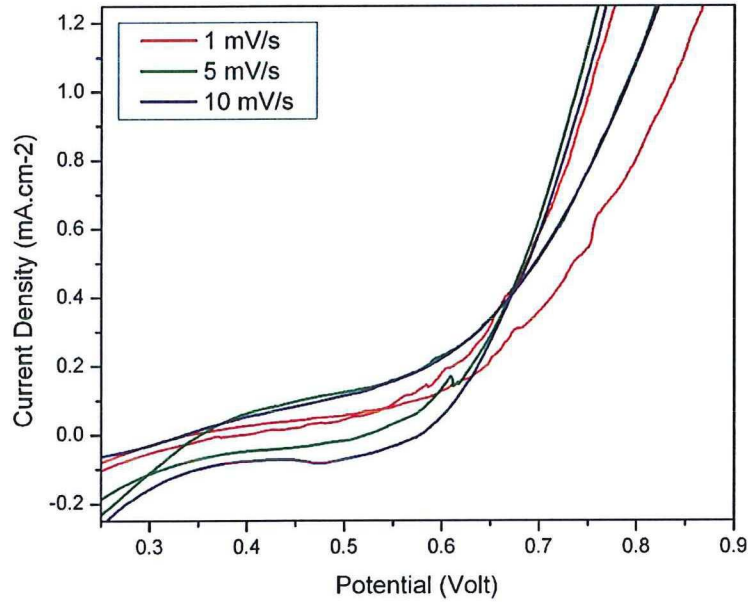
(a) Mirror-Like Surface Finish
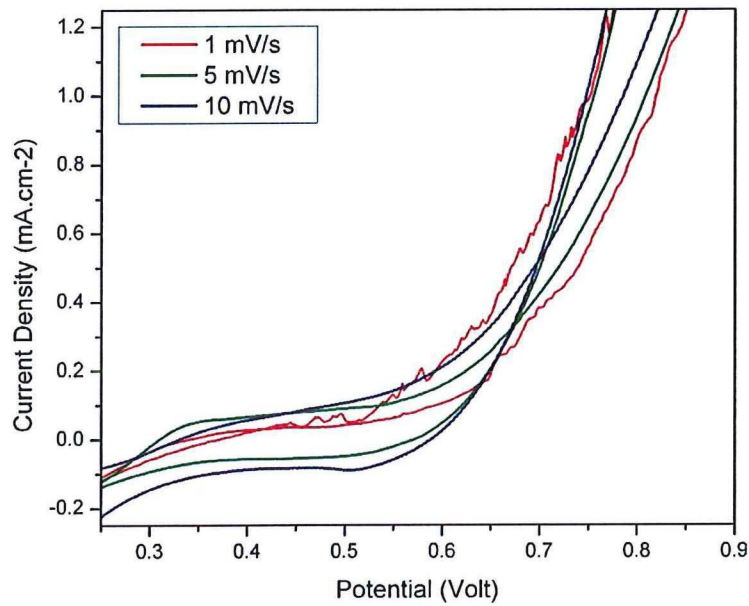
(b) Grinded Surface Finish

Figure 7.20: Cyclic Voltammetry Measurements for CoCrMo Alloy in Ringer's Solution with H_2O_2 Addition at Different Scan Rates

The reason can be expressed by hydrogen peroxide addition. As hydrogen peroxide decomposed into the water and oxygen instantly within the solution, it enhanced the reduction

reaction of hydrogen. Therefore it became much harder to identify the transpassive region in cyclic voltammetry. Furthermore, the current continued to increase as H_2O is oxidized on the surface of the alloy for anodic polarization and helps to enhance transpassive oxidation of chromium. Lastly, the chromium oxidation peaks was found to be independent of the surface finish quality.

Also it has been observed that the current density during the reverse scan is lower as the sweep rate is increased for both figures. The current subsequently returned to zero for Ringer's solution but showed dynamic behaviour for hydrogen peroxide addition.

7.1.6 Electrochemical Impedance Spectroscopy

Electrochemical impedance spectroscopy was employed in order to investigate and monitor in situ changes between the passive film and electrolyte-interface on CoCrMo with respect to immersion time to the electrolyte solution.

In Figure 7.21, 7.22, 7.23 and 7.24, the impedance spectra acquired at 1 hour, 6 hours, 12 hours, 18 hours and 24 hours after immersion in Ringer's solution and with H_2O_2 addition with different surface finish are shown. The CoCrMo samples were left at open circuit potential for an hour between each scans and the spectra were acquired with an amplitude of $\pm 10mV$.
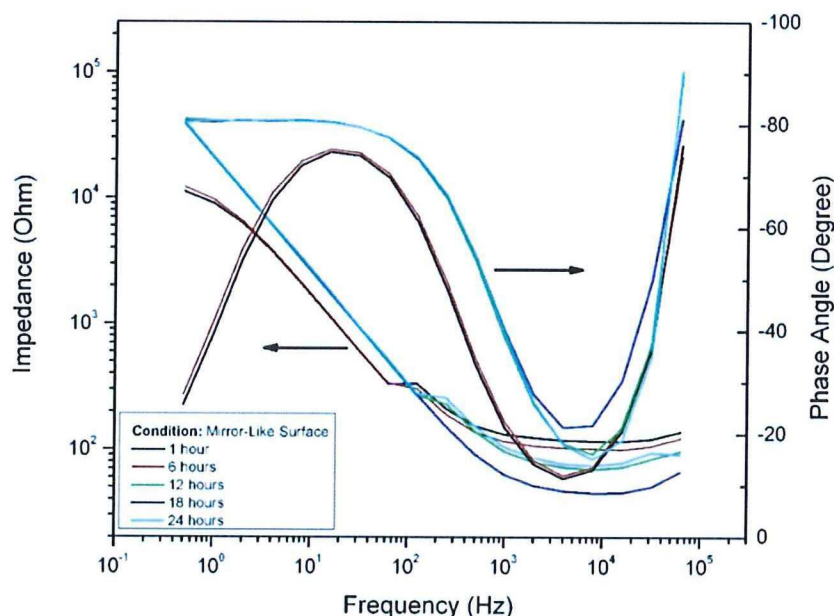
Figure 7.21: EIS Measurements for Mirror Like - Surface Finish CoCrMo Alloy Sample After Various Time Exposure in Ringer's Solution

In Figure 7.21, at the higher frequency impedance value tended to become constant whereas phase angle take its lowest value before to show an increase. This was a response to the environment and corresponded to solution resistance. In medium frequency region, impedance showed a linear behaviour and phase-angle maximum of less than -80°. In low frequency range, impedance value continued to show a linear behaviour and phase angle became constant after 24 hours.

76
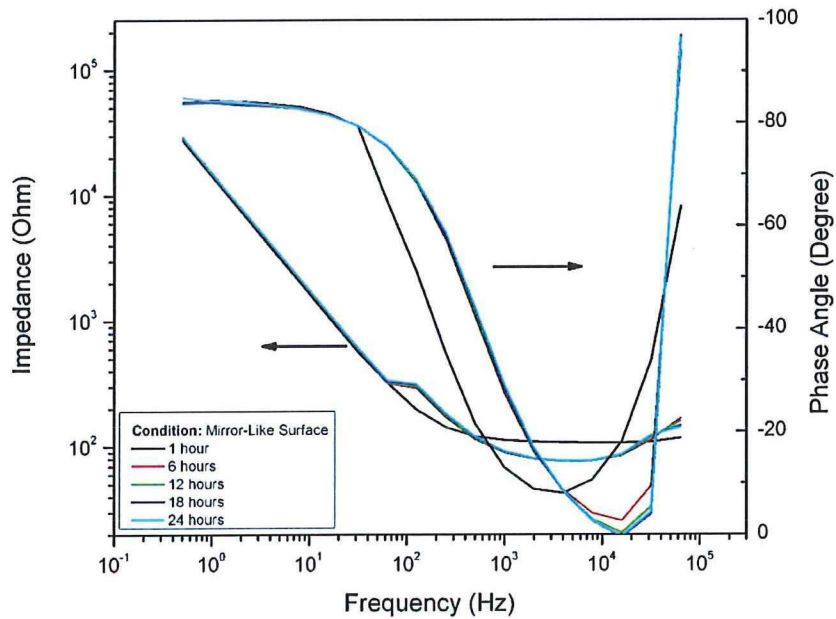
Figure 7.22: EIS Measurements for Grinded Surface Finish CoCrMo Alloy Sample After Various Time Exposure in Ringer's Solution

In Figure 7.22, at the higher frequency impedance value tended to become constant and phase angle take its lowest value around 0°. However after 1 hour, phase angle became more consistent with time. In medium frequency range, impedance showed a linear behaviour and phase angle had a maximum value around -80°. In low frequency range, impedance value continued to show a linear behaviour and phase angle became constant around -85°.

Also for Figure 7.21 and 7.22, some dramatic time-dependent changes can be observed and it can be explained as change of the passive film properties in the time range studied.
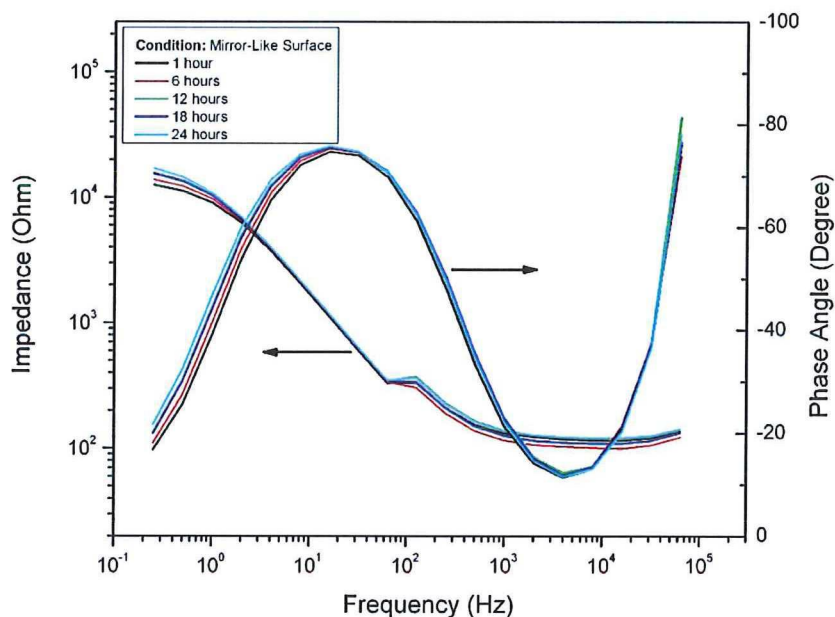
Figure 7.23: EIS Measurements for Mirror Like - Surface Finish CoCrMo Alloy Sample After Various Time Exposure in Ringer's Solution with H_2O_2 Addition

In Figure 7.23, at the high frequency range impedance value became constant and phase angle take its lowest value around -10°. In medium frequency region, impedance showed a linear behaviour and phase angle had its maximum value around -80°. In low frequency range, impedance value continued to show a linear behaviour and became stable at the end and phase angle decreased until -20°.

Lastly in Figure 7.24, impedance acted to become constant and phase angle take its lowest value around -10° at the higher frequency zone. However after 1 hour, phase angle became more consistent with time. In medium frequency range, impedance showed a linear behaviour and phase angle had a maximum value around -80°. In low frequency region, impedance value almost became stable at the end whereas phase angle decreased rapidly until -20°.

It is clear from the Figure 7.21, 7.22, 7.23 and 7.24, the impedance values in the medium to lower frequency regions increased with time of exposure to Ringer's solution. As the time of exposure to the solution increased, the capacitive behaviour, which was a indicator of corrosion resistance, expanded to a larger frequency range. The increase in the low frequency impedance values together with a more ideal capacitive behaviour with time indicated that the passive film on CoCrMo became more protective. The increase in corrosion resistance was again accompanied by a shift in the open circuit potential to more anodic values.

Figure 7.25 and 7.26 has shown the influence of surface finish and pH changes on the passive behavior of CoCrMo at the same diagram. An example of such experiments for in order to understand the surface topography influence after 24 hours exposure is shown in Figure 7.25. As can be seen in Bode plot, the impedance spectra recorded in the Ringer's solution showed difference in amplitude between two samples at high frequency region. At medium and low frequency regions, different surface finish samples behaved almost same. Also, it should be noted that at low frequency range, impedance value stayed constant in Ringer's solution whereas it dropped in hydrogen peroxide addition. Lastly, it was noted
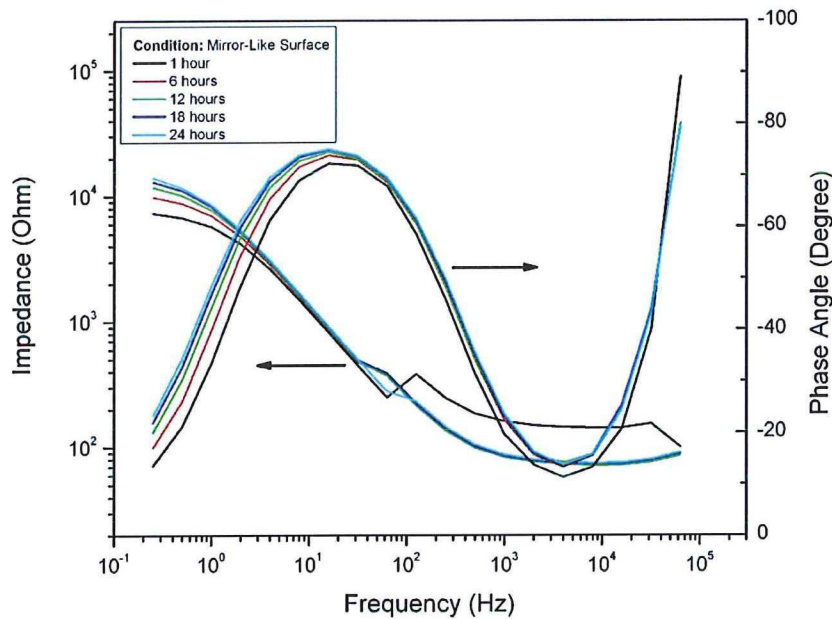
Figure 7.24: EIS Measurements for Grinded Surface Finish CoCrMo Alloy Sample After Various Time Exposure in Ringer's Solution with H_2O_2 Addition

that, mirror-like surface formed stronger passive layer than the one grinded.

In Figure 7.26, effect of pH level change has been observed. At high frequency values, impedance value stayed constant whereas phase angle for Ringer's solution almost dropped to zero. Medium frequency zone, impedance and phase angle acted almost same. However at low frequency, presence of hydrogen peroxide dropped phase angle whereas for Ringer's solution it became constant. Besides, it can be said that after 24 hours exposure, the passive film in Ringer's solution showed more corrosion resistance compare to the one in hydrogen peroxide addition. The reason for that behavior can be explained once more by presence of hydrogen peroxide addition since it will increase the rate of hydrogen reduction. So it will become harder to passivate the surface. Therefore there was a decrease in impedance so on resistance range of the surface. Solution chemistry modifies passive film properties thus modifying the corrosion resistance behavior.
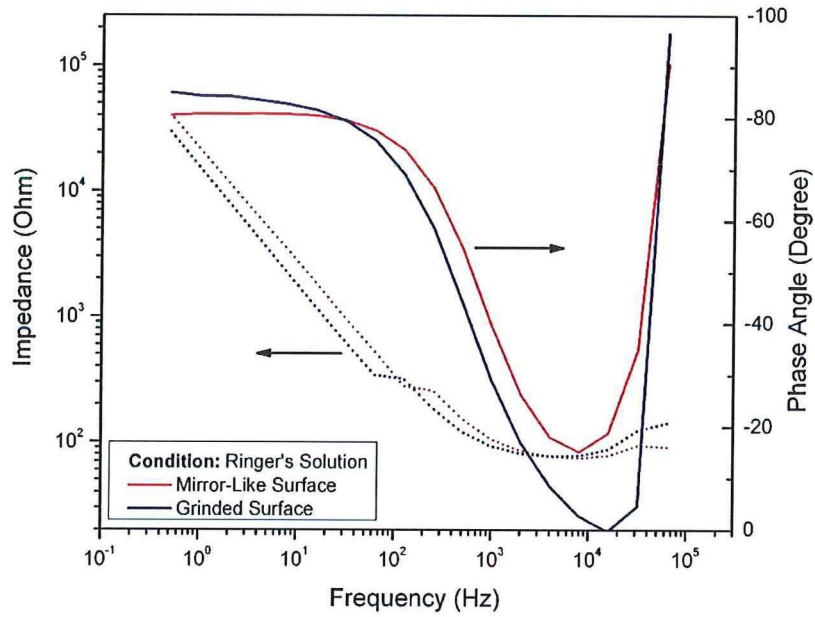
(a) Ringer's Solution
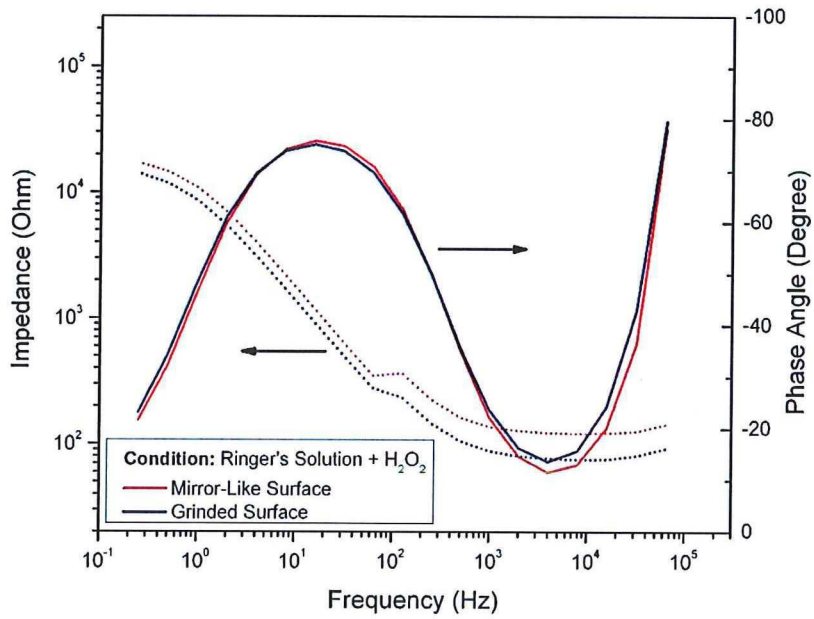
(b) Ringer's Solution with H_2O_2 Addition

Figure 7.25: EIS Measurements Comparison for Grinded and Mirror-Like Surface Finish CoCrMo Alloy Samples After 24 hours Exposure in Same Aqueous Environments
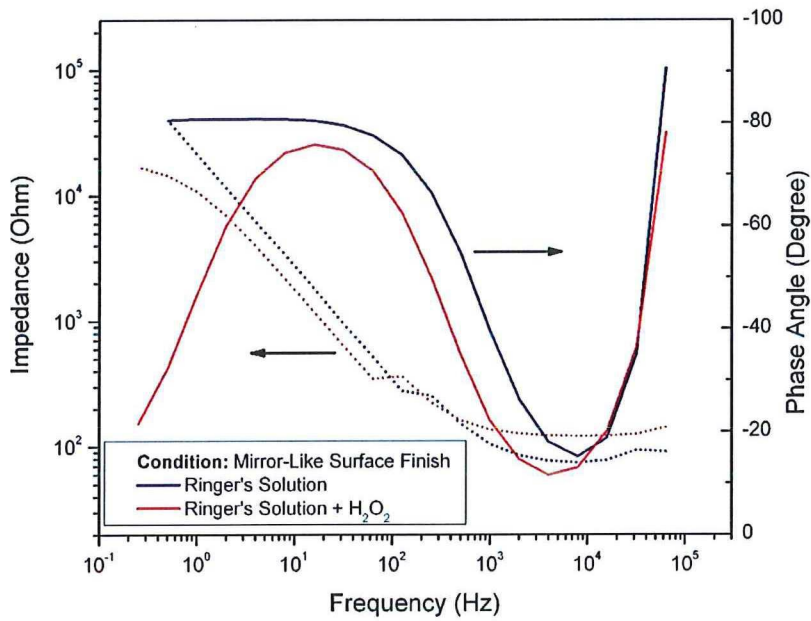
(a) Mirror-Like Surface
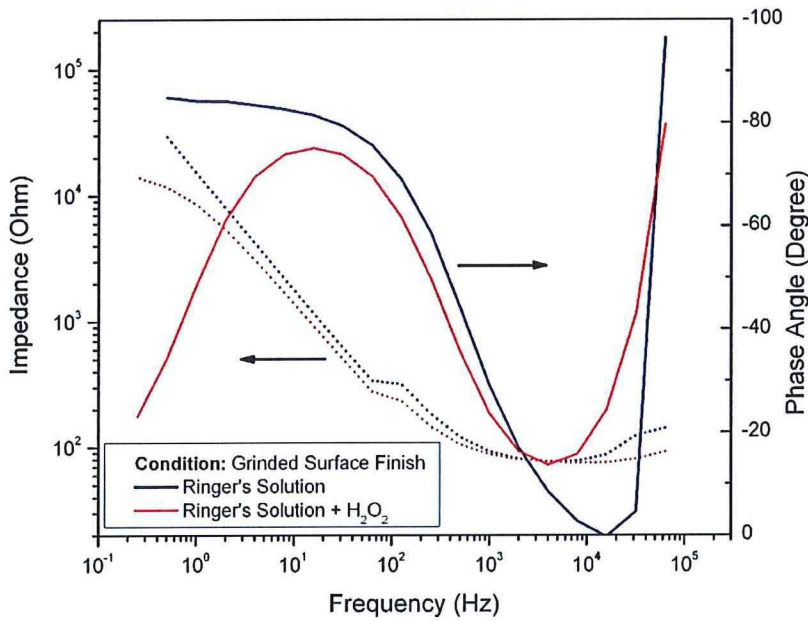
(b) Grinded Surface

Figure 7.26: EIS Measurements Comparison for Different Aqueous Environments Exposed CoCrMo Alloy Samples After 24 hours Exposure with Same Surface Finishes

7.2 Surface Analysis

7.2.1 Optical Microscopy

In order to observe the microstructure of the alloy, optical microscopy investigation is employed and shown in Figure 7.27. As shown below, carbides appeared as discrete particles

(a) 10X Magnification   (b) 20X Magnification

(c) 50X Magnification   (d) 100X Magnification
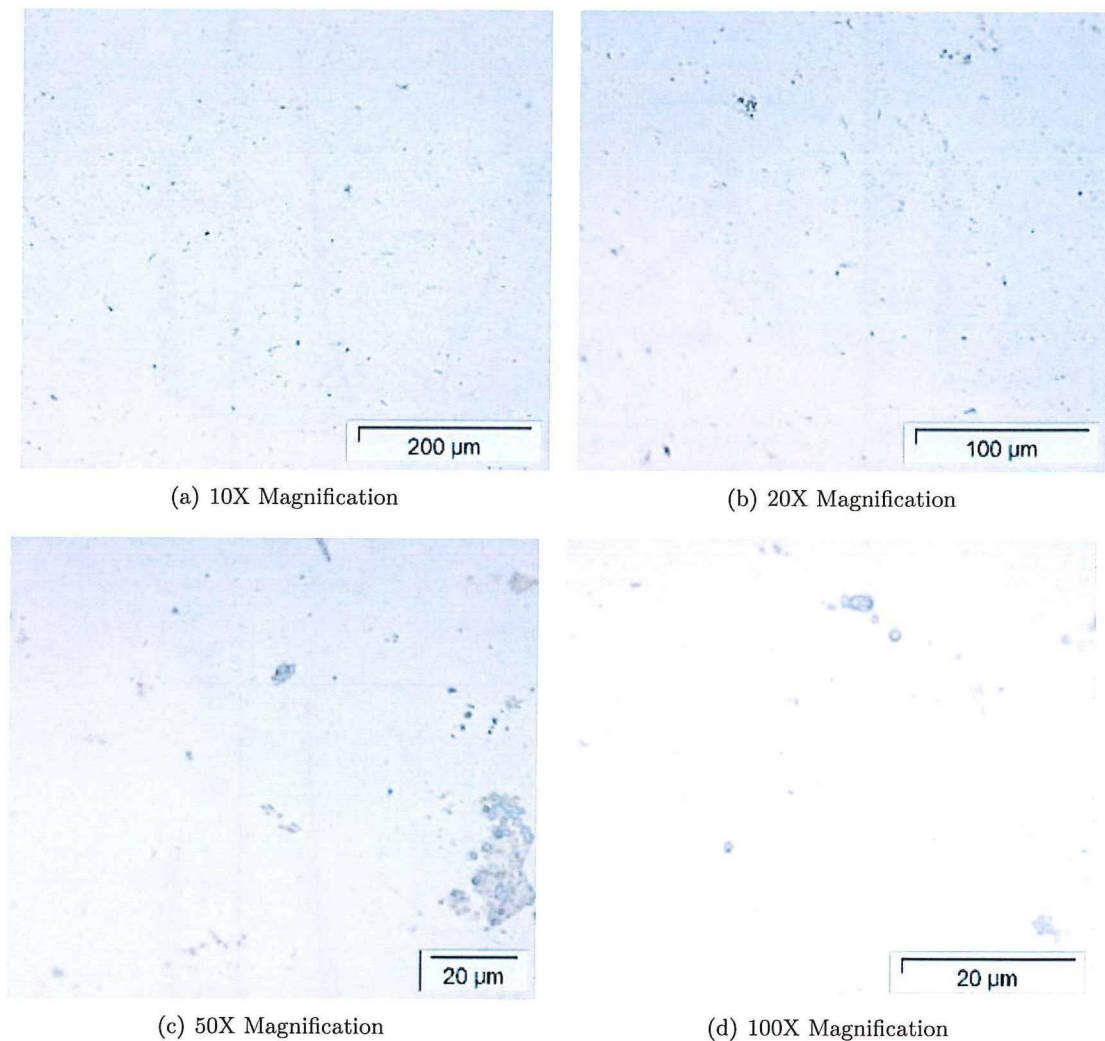
Figure 7.27: Microstructure of F1537 CoCrMo Low Carbon Alloy - Optical Micrographs

with a circular morphology. As in shown in Chapter 6.2.1., their chemical compositions revealed the presence of cobalt, chromium, molybdenum and they were distributed within the structure. The carbides can be in various types such as $M_{23}C_6$ or M_6C as mentioned in study of Varano [101]. It is expectable to see very weak images since the low carbon concentration so carbide formation.

It is a well-known fact that carbide precipitation has a major effect on the corrosion behaviour [100]. In literature, it has been reported that high cobalt contents increase the chromium content in the passivation layer, which increase the oxide stability and subsequently improves the corrosion resistance [101]. At the same time cobalt enforces the carbide formation, which might cause a decrease of the corrosion resistance. Therefore, a major effect of cobalt on corrosion resistance can be expected, irrespective whether it is beneficial or detrimental since corrosion properties are not only linked to chemical composition but to a high extent to the applied heat treatment. For instance, chromium and molybdenum can improve

the corrosion resistance unless portions of these elements are precipitated as carbides since only the dissolved content in the matrix is effective. In addition, the higher the tempering temperature the lower is the corrosion resistance. Because of secondary hardening carbides are rich in chromium which results a decrease of the corrosion resistance [100].

7.2.2 Scanning Electron Microscope - Energy Dispersive X-Ray

The specimens were examined using scanning electron microscope (SEM) for further investigation of microstucture.

| (a) Back-scatter Electrons | (b) Secondary Electron Imaging |
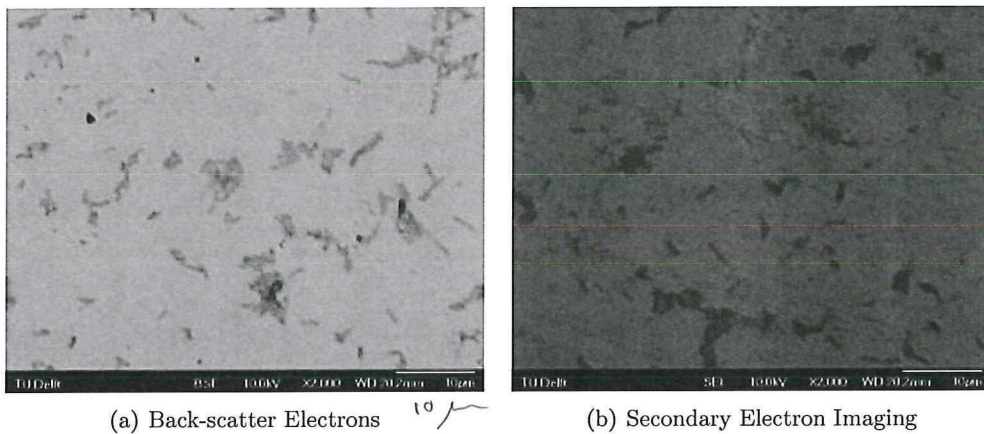
Figure 7.28: Microstructure of F1537 CoCrMo Low Carbon Alloy - SEM Images

In Figure 7.28, carbides become more visible under SEM imaging. Carbides had been considered to be very important second-phase materials with respect to wear owing to their relatively hard nature. In terms of wear resistance, carbides might influence the wear of materials not only because of their high hardness characteristics but also as a protective barrier against matrix delamination [100].

As mentioned before, carbides can be formed in different variations. In order to understand those formations and investigate the surface composition, energy dispersive X-Ray spectroscopy (EDS) analysis is employed and shown in Figure 7.29 for both matrix and carbides sites. In Figure 7.29(a), matrix composition analysis has been run and gives quiet accurate result parallel to composition of the alloy. Based on surface composition metal carbides may change thus they are shown as $M_{23}C_6$ or M_6C. Therefore random carbide is chosen and EDS analysis is employed and showed in Table 7.1. In Figure 7.29(b), it may be seen that, cobalt based carbide formation as well as chromium and molybdenum based carbides in the structure are possible.
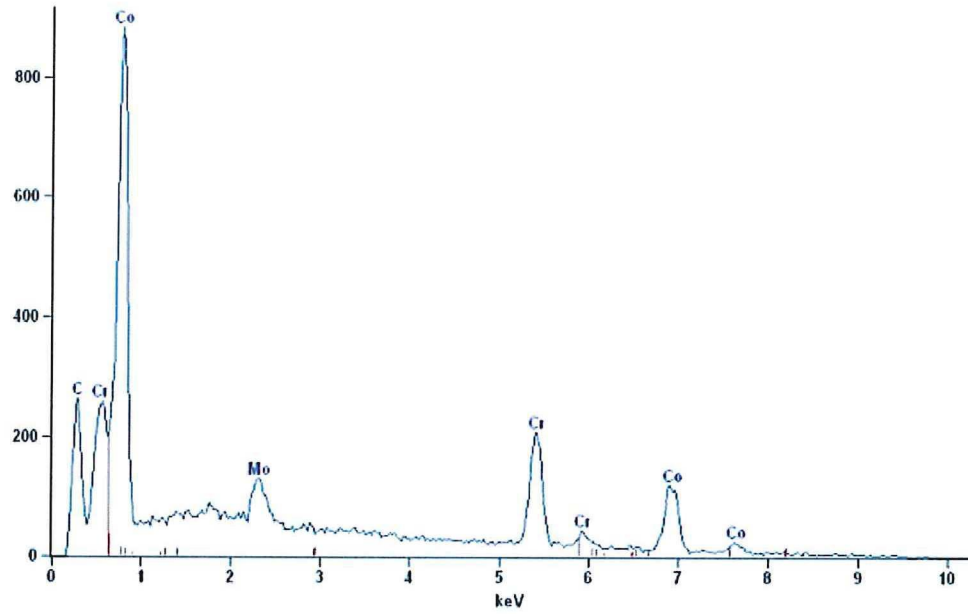
(a) CoCrMo Alloy Matrix
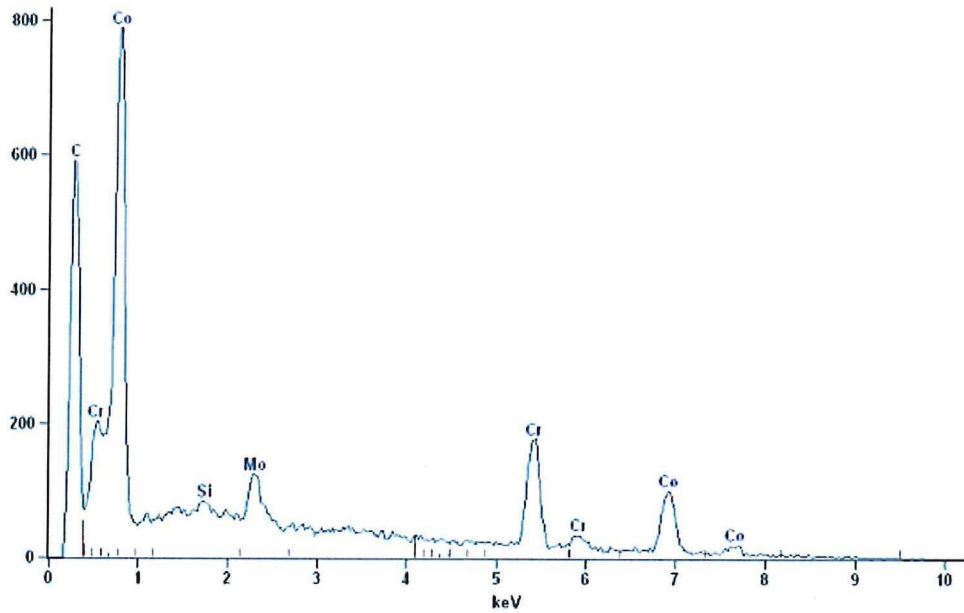
(b) CoCrMo Alloy Carbide (Possibly $M_{23}C_6$ or M_6C)

Figure 7.29: EDS Analysis Results of CoCrMo Alloy

84

Table 7.1: Quantitative Results of CoCrMo Alloy EDS Analysis

Element Line	Net Counts	Weight %	Weight % Error	Atom %	Atom % Error
CoCrMo Carbide					
C K	5265	22.35	±0.27	57.79	±0.70
Si K	240	0.31	±0.06	0.34	±0.07
Cr K	2839	24.32	±0.93	14.53	±0.56
Co L	9657	50.05	±0.98	26.38	±0.52
Mo L	1438	2.98	±0.21	0.96	±0.07
Total	——	100.00	——	100.00	——
CoCrMo Matrix					
C K	2136	10.37	±0.21	35.62	±0.72
Cr K	3122	27.62	±1.03	21.90	±0.81
Co L	10722	58.63	±1.03	41.02	±0.72
Mo L	1544	3.38	±0.35	1.45	±0.15
Total	——	100.00	——	100.00	——

7.2.3 Atomic Force Microscopy

Surface topography and roughness were selected as parameters in the experimental plan. Thus, atomic force microscopy (AFM) has been used in order to have a good understanding of that phenomena and shown in Figure 7.30 and 7.31.

In Figure 7.30, sample shows very smooth surface and well peak distribution. Rms value, which is the root mean square average of the profile height deviations from the mean line recorded within the evaluation length, was 10.811 nm. Also Ra value, which is the arithmetic average of the absolute values of the profile height deviations from the mean line recorded within the evaluation length, was 8.202 nm. In addition, surface are were calculated as 2.503×10^{-3} μm^2.

However in Figure 7.31, grinded sample until 1200 SiC grit has a rough surface and a large quantity of scratches. Rms value was 64.163 whereas Ra was 50.051 nm. Also, calculation of the surface area gave the value of 2.511×10^{-3} μm^2.

When two different surface finish qualities has been compared, it can be seen that mirror-like surface finish sample have a very smooth and uniform surface where grinded surface finish samples six times rougher in a quantitative manner. But at the same time, it came out that, both surface finish qualities have the same surface area. It can justify the results that came from electrochemical characterization since the transpassive and the passive regions of the both variables were close to each other.

Surface roughness is an important factor for corrosion resistance. Since the rough surfaces have bigger surface area compare to the smooth ones and imperfections on the surface that make it harder to penetrate beneath it, inhibit an uniform layer formation. Therefore, it has a surface finish qualities play significant role on the formation of the passive film and its quality in general. However, it came out it was not the case for this conducted research since the surface areas were close to each other.
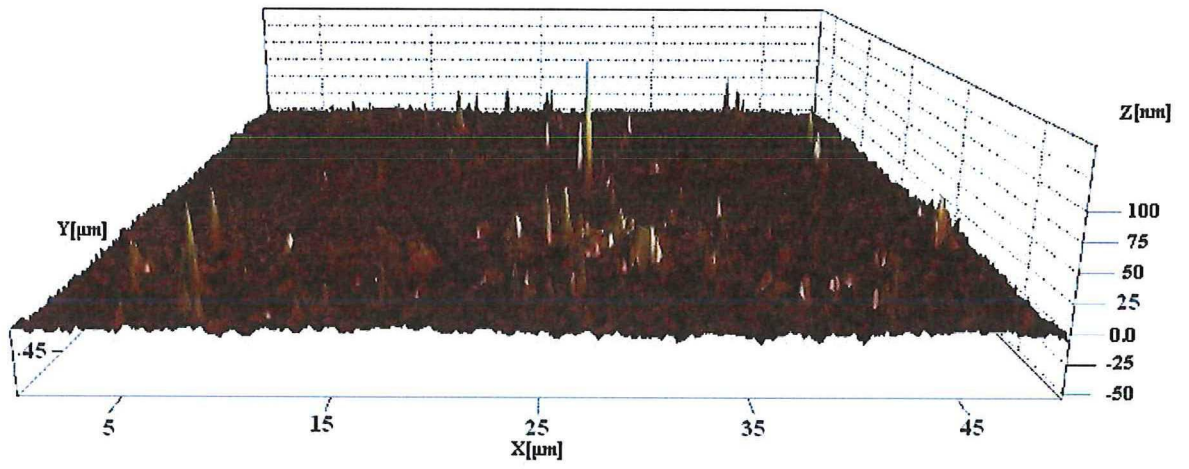
(a) 3D Topography
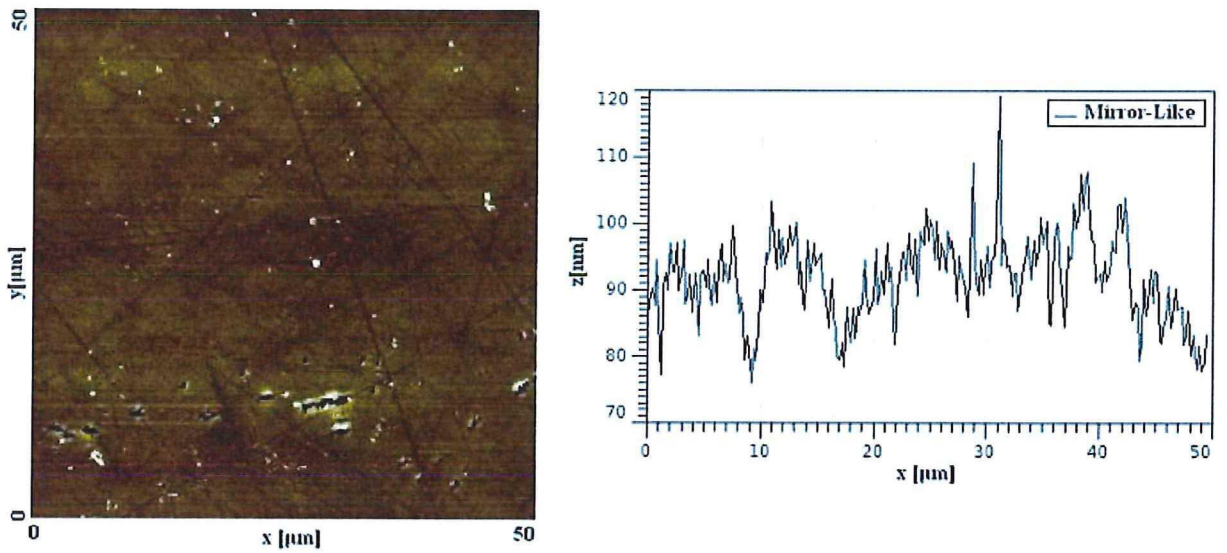
(b) 2D Topography

Figure 7.30: Surface Topography Analysis of F1537 CoCrMo Mirror-Like Surface Finish Samples
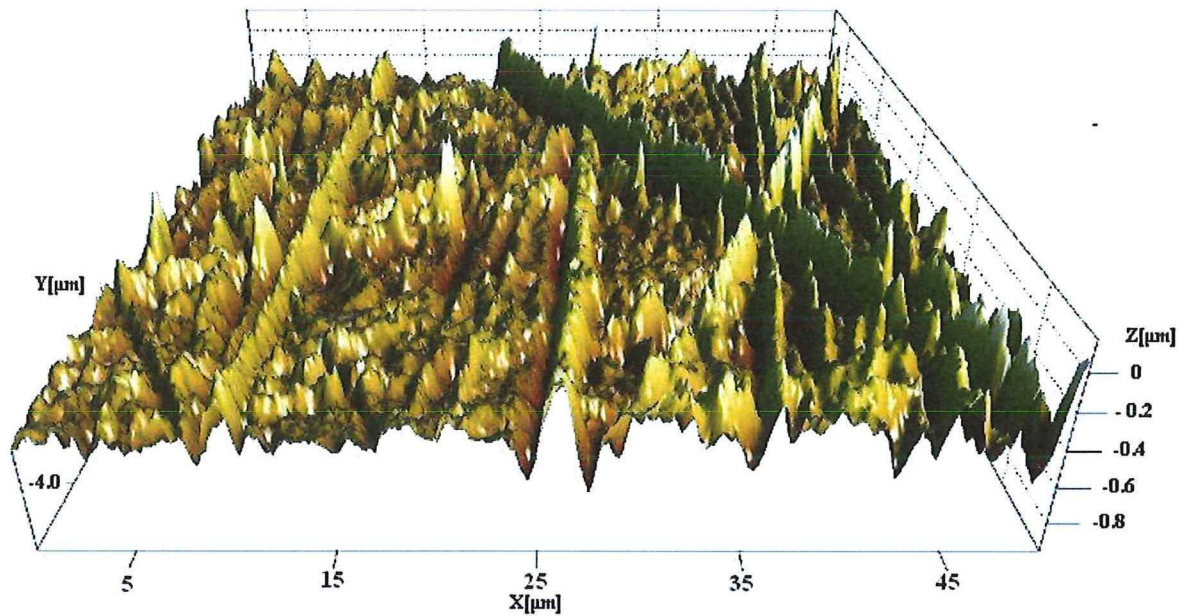
(a) 3D Topography
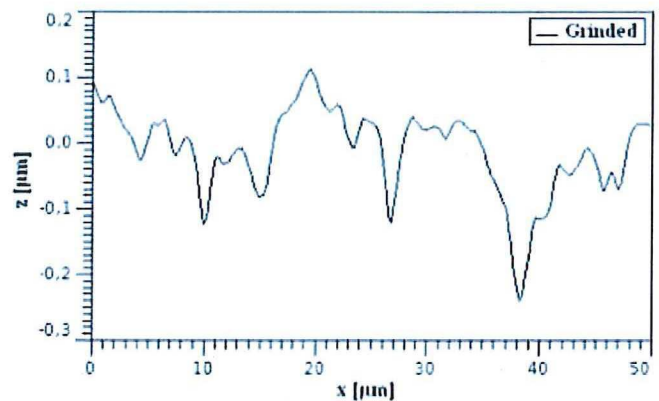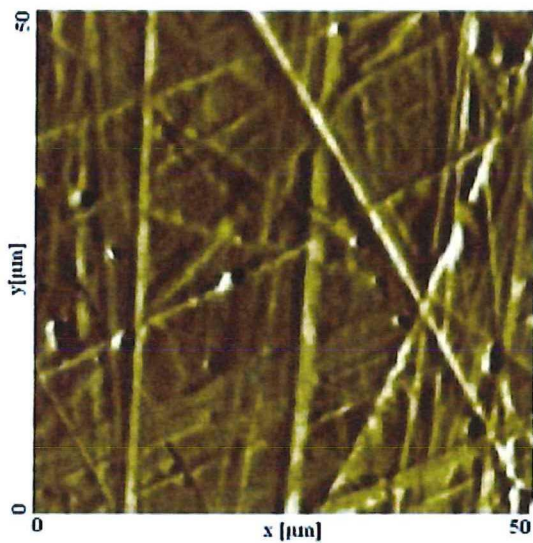
(b) 2D Topography

Figure 7.31: Surface Topography Analysis of F1537 CoCrMo Grinded Surface Finish Samples

7.3 Elemental Analysis of Metal Ion Release

7.3.1 Inductively Coupled Plasma - Mass Spectroscopy

Inductively Coupled Plasma Mass Spectrometry or ICP-MS is an analytical technique which has been used for elemental determinations for CoCrMo alloy and 316L stainless steel in this

research . Firstly, 200 milliliter electrochemical cell was employed for the each potentiostatically controlled polarisation of the samples. After each experiment, the solution was collected in small plastic bottles. As mentioned Section 6.5.1., ICP standards were prepared after the poteniostatic experiments in order to make a comparison with the electrolyte and have quantitative results for tracing the elements. Standards were prepared based on working electrode material chemical composition. Thus, three different 25 ml concentrations (20 ppm, 5 ppm, 1 ppm) plus blank one were prepared. Calculation has been estimated as the following;

- 100 g/ml = 100 mg/L = 100 ppm

- 20 ppm $\Rightarrow$ 25 * (20/100) = 5 ml Plasma + 20 ml Electrolyte (Ringer's Solution)

- 5 ppm $\Rightarrow$ 25 * (5/100) = 1.25 ml Plasma + 23.75 ml Electrolyte (Ringer's Solution)

- 1 ppm $\Rightarrow$ 25 * (1/100) = 0.25 ml Plasma + 24.75 ml Electrolyte (Ringer's Solution)

- Blank $\Rightarrow$ 25 ml Electrolyte (Ringer's Solution)

Quantitative elemental analysis of collected electrolyte solutions for evidence of cobalt, chromium and other various metals were subsequently performed via the use of ICP-MS. Results from the solution analysis carried out after different polarizations are shown in Table 7.2 and Figure 7.32.

Table 7.2: Quantitative Results of CoCrMo Alloy ICP-MS Analysis

Potential	Ion Concentration								
	ppm								
Volt	AISI 316L Stainless Steel			ASTM F1537 CoCrMo Alloy					
	Cr	Fe	Ni	Co	Cr	Mn	Ni	P	Si
-1	0.0037	0.0137	0.0049	0.0093	-0.0359	-0.0085	0.2385	-0.2773	-0.0664
0.25	-0.0015	-0.0057	0.0088	-0.0155	-0.0341	-0.0102	0.0825	-0.2834	-0.1863
1	N/A	N/A	N/A	0.6986	0.1926	-0.0032	3×10^{-4}	-0.2798	-0.1887
1.15	1.356	6.106	1.263	N/A	N/A	N/A	N/A	N/A	N/A
1.25	N/A	N/A	N/A	3.202	1.08	0.0276	0.1615	-0.084	-0.075

In passive region polarization, small amount of cobalt and nickel are detected in the Ringer's solution for CoCrMo alloy whereas the concentrations of chromium, manganese, phosphorus and silicon are below the detection limit and therefore are given negative values. In addition for stainless steel sample; chromium, iron and nickel are indicated by ICP-MS in passive region again in small amounts. As be seen in Figure 7.32, transpassive region polarization accelerates dissolution with a very rapid ration for both materials. In that region, all the target alloying elements are detected in the electrolyte for stainless steel. However, phosphorus and silicon cannot be detected at any potential range since release of those elements are below the detection limit. It has been observed by the outcome of ICP-MS data, the major species dissolving for CoCrMo is cobalt and for stainless steel is iron. It is important to mention that electrochemical parameters have a big influence on the dissolution mode such as stoichiometric or selective way and the kinetics of dissolution of the materials.

Besides electrochemical mechanism that can trigger metal release into environment also mechanical properties play an important role. Since the break down of the passive film can
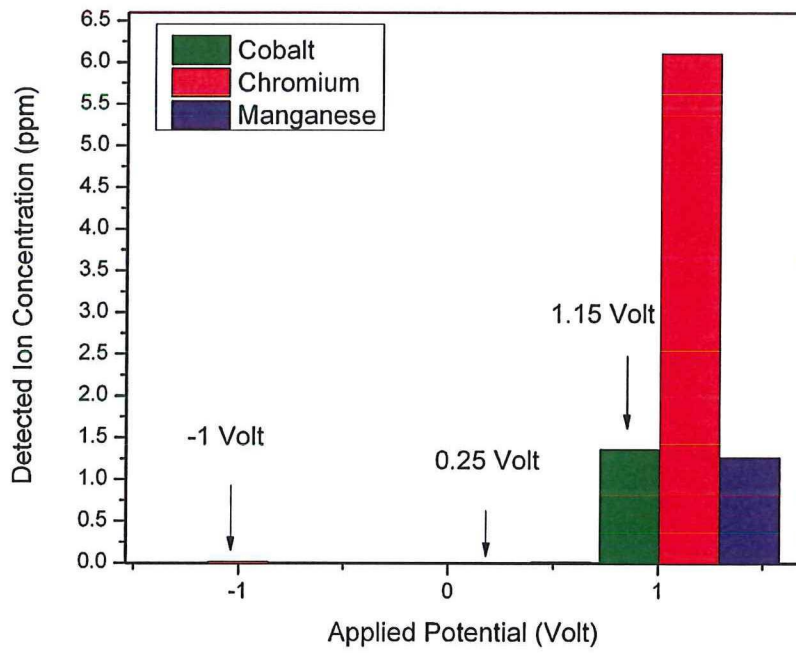
(a) AISI 316L Stainless Steel
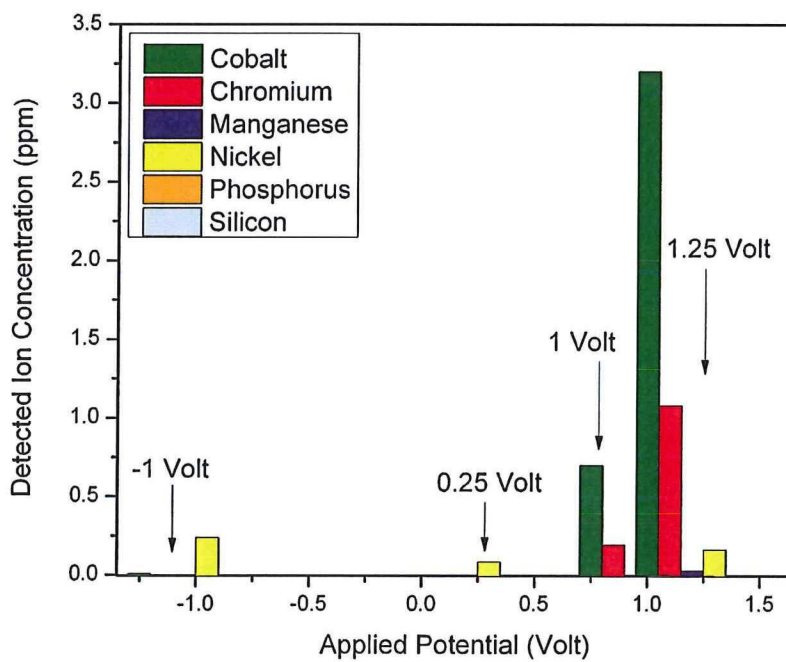
(b) ASTM F1537 CoCrMo Alloy

Figure 7.32: Ion Concentration Release after Potentiostatic Experiment

accelerate the corrosion process, it is crucial to be aware of what can be the causes for that kind of a distortion. For metal-on-metal design hip implants, the main mechanism is abrasive wear. In this mechanism, the asperities from each surface, which are peaks of material protruding from the bulk material, contact each other under an applied load and this causes some asperities to break off. Adhesive wear is a secondary wear mechanism that may occur to a lesser extent. In tribological theory, if the lubrication between two identical metal surfaces is insufficient, asperities from both surfaces could potentially bond. Though this process does not occur when proper lubrication is present, adhesive wear is a potential wear mechanism in metal-on-metal implants since both surfaces are identical.

Conclusions & Recommendations

<div style="text-align: right">8</div>

8.1 Conclusion

ELECTROCHEMICAL behaviour investigation of the CoCrMo alloy has been performed using different techniques and control parameters.

It is a well known fact that the passive and transpassive behaviour of the CrCrMo alloy is formed and dominated by the formation an oxide film which is highly enriched with chromium on the alloy surface.

The open circuit potential situation initiates and enhances the protectiveness of the passive film, by a shift of the open circuit potential into more positive potential region towards to the anodic direction. The potential evolution creates formation of a protecting passivation layer on CoCrMo which limits the further dissolution of the alloy CoCrMo. This behavior is clearer in Figure 8.1.
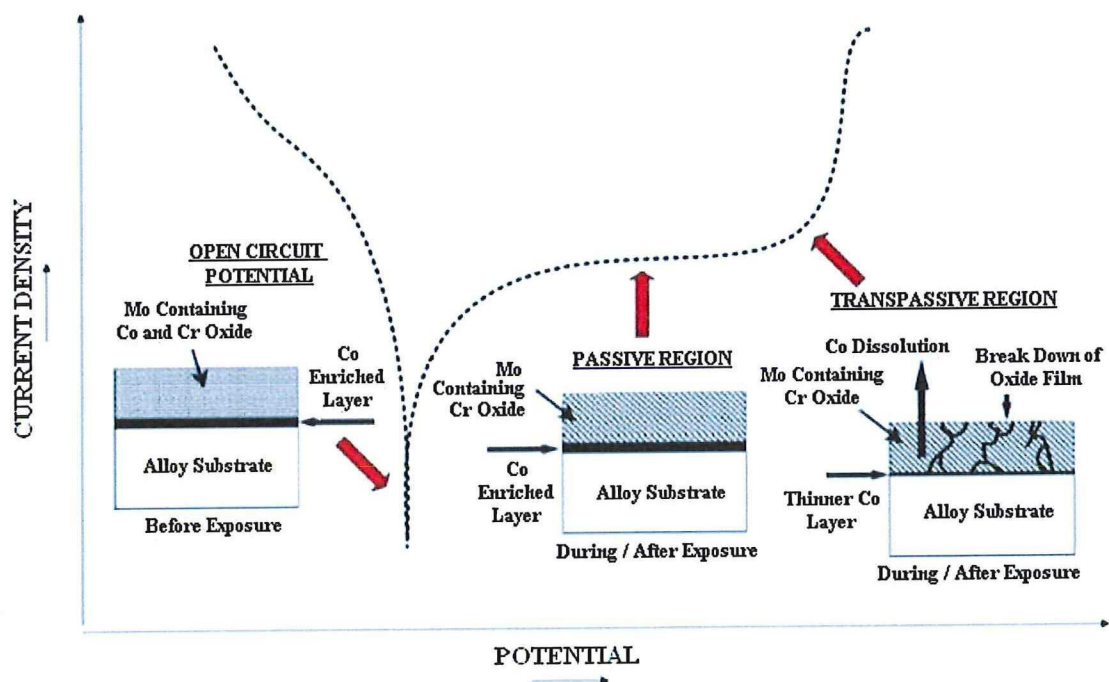
Figure 8.1: Schematic Reconstruction of Surface Oxide Film on a CoCrMo Alloy

It has been observed by the polarization curves, at higher potentials values, the passive and the transpassive regions are protected by chromium oxide film. Based on ICP-MS results, that is the zone of peak metal ion release due to oxidative dissolution of chromium oxide film. Furthermore, elemental analysis of the Ringer's solution after different potential levels shows that the highest ion release from the alloy into the electrolyte belongs to cobalt. This data is

consistent with the electrochemical behaviour of pure cobalt. Pure cobalt dissolves actively at higher anodic potential since there is no passivation layer. During the formation of the passive film, the oxidized chromium mostly forms the passive film, whereas the oxidized cobalt species dissolve. Cathodic zone polarization curves initiate an active/passive transition. The reason for that transition might be reductive dissolution of the passive film. Chromium and molybdenum show stable passivity at the active/passive transition zone, whereas cobalt shows active dissolution. Thus, on the cathodically activated surface, oxidized chromium remains on the surface forming the passive film, whereas oxidized cobalt is dissolved at repassivation reaction as shown in Figure 8.2.
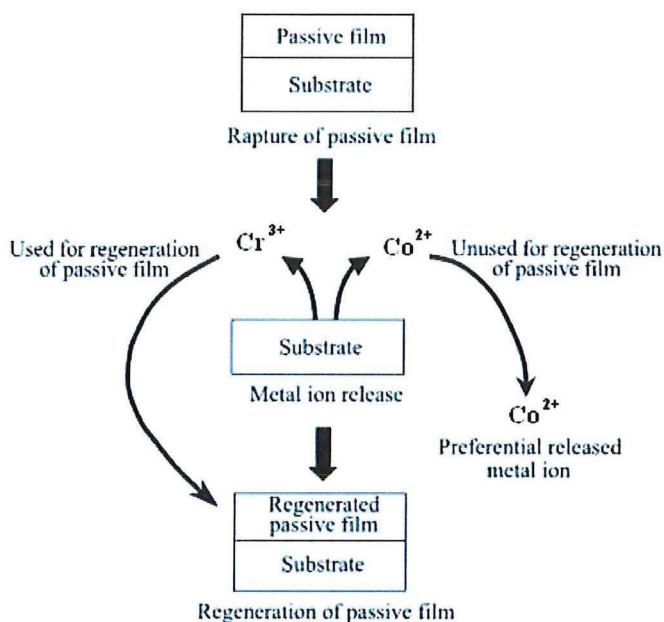
Figure 8.2: Mechanism of Preferential Metal Ion Release

Potentiostatic polarisation experiments show that in the cathodic range, mass transport is controlled by O_2 reduction. For the transpassive region, the chromium oxidation rate is mass transport dependent. It is also in good agreement with the cyclic voltammetry graphs. It shows higher current density levels for the chromium oxidation reaction at higher scan rates which is an inevitable behavior for a mass transfer controlled reaction since there are not any spontaneous transfer of the electroactive species from higher concentrations to lower concentrations. Thus, it can be said that the metal ion release is very strongly influenced by oxidizing conditions leading to transpassive dissolution.

Electrochemical impedance spectroscopy outputs show that as the time of exposure to the solution increases, the capacitive behaviour expands to a larger frequency range. The increase in the low frequency impedance values together with a more ideal capacitive behaviour with time indicate that the passive film on CoCrMo becomes more protective and corrosion resistant behavior. Also it has been observed after 24 hours exposure, the passive film in Ringer's solution itself shows more corrosion resistance compared to the one in hydrogen peroxide addition due to solution chemistry modifies passive film properties since the passive
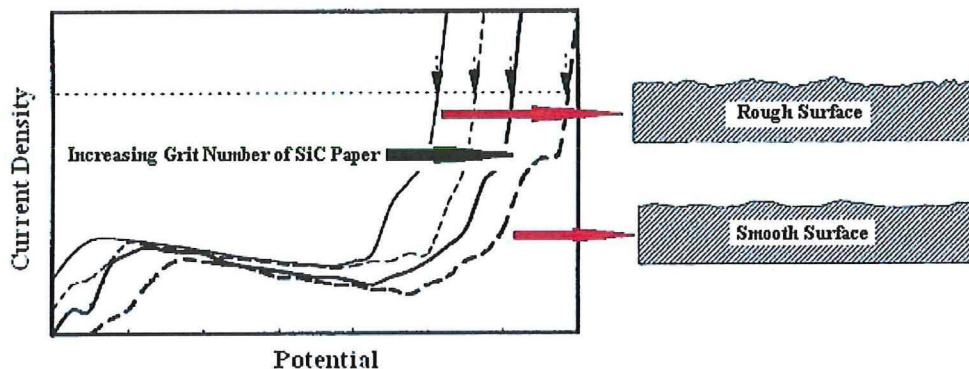
Figure 8.3: Difference Between the Surface Morphologies

films are constantly changing and adapting to the environment based on the parameters such as kinetics, pH level, conductivity and concentration.

The OCP and potentiodynamic behavior of CoCrMo alloy used for hip implants has been studied in different aqueous environments. From the results it can be concluded that pH level change can have a big influence on the electrochemical behavior of the material. Ringer's solution with hydrogen peroxide additive, which is added to the electrolyte in order to understand the oxygen species influence on the material, showed a negative shift with respect to time. It was explained by due either to the decreasing conductivity of the metal because of the formation of that phase or to the increasing anodic reaction rate through the porous, not strongly bonded hydrated metal oxide layer. However, extra reduction reaction gave a positive shift to the steady state potential compare to bare Ringer's solution at the beginning. Also hydrogen chloride addition shows that aggressive environment can affect the surface composition and the electrochemical behaviors adversely.

In addition difference at surface finish techniques has been investigated. The results show that the surface finish is an important parameter that should take in consideration at the design. Even though for potentiodynamic experiments that difference does not show a major influence, it has been observed at EIS experiments, mirror-like surface forms stronger passive layer than the one grinded. The reason for that might be, grinded surface finish samples are more vulnerable for local corrosion at local imperfections of the oxide film since the surface area differences and scratches that can initiate preferential corrosion attacks. The methods of sample preparation have major effect on surface roughness and chemistry. The chemistry of the surface layer is dependent on method of preparation since surface chemistry plays a major role in corrosion and other reactions with the environment. It should be noted that, potentiodynamic experiment curves showed almost same behaviour since the difference between two morphologies were not so dramatic. But EIS experiment data gave an inspiration that if the surface roughness difference was higher, the characteristics of the passive layer region would be different in potentiodynamic experiments as shown in Figure 8.3 since the passive films formed on smooth polished surfaces are superior compared to those on rough surfaces [57].

During this research, activation of the surface was purely caused by electrochemical manners. However, when the implant itself is assumed within the body, there might be different reason to trigger the surface activation such as interaction between the hip implant and the

94

surrounding material based on the design such as fretting corrosion possibility as shown in Figure 8.4. That phenomenon can create continuous activation and repassivation cycles on the surface of the material. It can initiate selective dissolution of cobalt in high ratio and therefore an accumulation of cobalt ions in the tissue can be a matter of question. As mentioned in degradation phenomena section, release and accumulation of cobalt ions in the tissues have a dramatic effect on the performance of a CoCrMo implant system and on the human immune system.
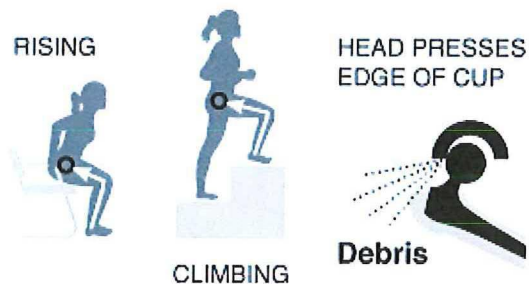
Figure 8.4: Friction Between the Components of THR [104]

8.2 Recommendations and Future Research

Future research on CoCrMo alloy used for hip implant will focus on the design parameter and possible surface modifications. Therefore material, which is the most common used alloy especially for hip implants, still needs to be improved in order to resolve different problems. Long-term corrosion protection can be achieved by hard thin film coatings since wear is one of the major problems for implants. Thus, different deposition techniques should be investigated in order to minimize wear debris particles and formation of uniform passivation layers. Also it can be helpful to work with actual hip implants components rather than prepared specimens since the behavior of the material can be investigated in real scale.

It is recommended that also working on tribocorrosion setup may give useful outputs and can simulate electrochemical and mechanical behaviors much better. Degradation results from the combined action of corrosion and mechanical loading and it is well-known that synergistic effects can accentuate the wear-corrosion rate. To observe the repassivation behavior under a constant mechanical motion can mimic the human body behaviour in much real situation.

With respect to simulate the body conditions it might be necessary to add chemical components such as proteins, enzymes, oxide species, complexing agents and vitamins into the electrolyte. Therefore influence of those additives can be observed.

Also, characterization via X-ray photoelectron spectroscopy (XPS) can give some crucial hints to analyze the surface properties such as elemental composition, empirical formula, chemical state and electronic state of the element before and after each electrochemical treatment.

Possible synchrotron experiments can give a chance to see the reactions going on during the polarization or transition between active, passive and transpassive regions simultaneously. It is important to understand the role of each element within the alloy especially cobalt and chromium since the release of those metal particles within the body can cause some serious

side effects such as cytotoxicity, genotoxicity, and carcinogenicity.

It is furthermore highly recommended that also work on high carbon version of CoCrMo alloy and investigate the electrochemical behavior of the alloy with high carbide percentage on the surface.

Bibliography

[1] Park, J.B., Bronzino, J.D. (2003) *Biomaterials - Principles And Applications*, (Boca Raton: CRC Press), Preface

[2] Black, J. (1992) *Biological Performance of Materials*, 2nd ed. (New York: Marcel Dekker)

[3] Bruck, S.D. (1980) *Properties of Biomaterials in the Physiological Environment* (Boca Raton: CRC Press)

[4] Williams, D.F. (1987) *Definition in Biomaterials. In: Progress in Biomedical Engineering* (Amsterdam: Elsevier), p. 67

[5] Black, J., Hastings, G.W. (1998) *Handbook of Biomaterials Properties* (London: Chapman and Hall)

[6] Wintermantel, E., Mayer, E. (1995) *Encyclopedic Handbook of Biomaterials and Bioengineering: Anisotropic Biomaterials Strategies and Developments for Bone Implants*, (New York: Marcel Dekker), p. 3-42

[7] Ramakrishna, S. Huang Z. (2004) *An Introduction to Biocomposites* (London: Imperial College Press), p. 3

[8] Park, J.B. (1984) *Biomaterials Science and Engineering* (New York: Plenum Press)

[9] Hench, L.L. (1985) *Inorganic Biomaterials* (Washington DC: American Chemical Society) p. 523

[10] Park, J.B., Young, K.K. (2003) *Biomaterials - Principles And Applications: Metallic Biomaterials* (Boca Raton: CRC Press), p. 1-3

[11] Williams, D. F. (1982) *Biocompatibility in Clinical Practice* (Boca Raton, FL: CRC Press)

[12] Kingery, W.D., Bowen, H.K., Uhlmann, D.R. (1976) *Introduction to Ceramics*, 2nd ed. (New York: Wiley), p. 368

[13] Park, J.B., Lakes, R.S. (1992) *Biomaterials - An Introduction*, 2nd ed. (New York: Plenum Press)

[14] Janssen, M., Zuidema, J. (2004) *Fracture Mechanics*, 2nd ed. (Oxford: Spon PR)

[15] Billotte, W. G. (2003) *Biomaterials - Principles And Applications: Ceramic Biomaterials* (Boca Raton: CRC Press), p. 22

[16] Hench L.L. (1993) *Bioceramics: From Concept to Clinic* (Ohio: American Ceramic Society Bulletin), p. 72:93-96

[17] Lee, H.B. (1989) *Application of Synthetic Polymers in Implants* (Oxford: Blackwell Scientific), p. 579-582

[18] Lee, H.B., Khang, G., Lee, J.H. (2003) *Biomaterials - Principles And Applications: Polymeric Biomaterials* (Boca Raton: CRC Press), p. 55

[19] Lakes, R.S. (2003) *Biomaterials - Principles And Applications: Composite Biomaterials* (Boca Raton, FL: CRC Press), p. 79

[20] Lakes, R. S. (1993) *Materials with Structural Hierarchy* (London: Nature Publish Group), p. 361

[21] Rabiei, A. (2009) *Biomedical Materials: Hip Prosthesis* (New York: Springer), p. 349

[22] Ducheyne, P. (1988) *Encyclopedia of Medical Devices and Instrumentation: Prosthesis Fixation For Orthopedics* (New York: Wiley-Interscience), p. 2146-2149

[23] Harris, W. H. (1995) *The Problem is Osteolysis* (Clin. Orthop. Rel. Res.) Vol. 311, p. 46-51

[24] Park, J.B. (2003) *Biomaterials - Principles And Applications: Hip Joint Prosthesis Fixation* (Boca Raton: CRC Press), p. 219-223

[25] Kossowsky, R., Kossovsky, N. (1995) *Advances in Materials Science and Implant Orthopedics* (Dordrecht: Kluwer Academic Publishers), p. 103-105

[26] http://www.disabled-world.com/health/orthopedics/hip-replacement.php#ixzz1JmR3mS3K

[27] Hallab, N., Jacobs, J., Black, J. (2000) *Hypersensitivity to Metallic Biomaterials: A Review of Leukocyte Migration Inhibition Assays*, p. 21

[28] Dumbleton, J.H., Manley, M.T. (2005) *Metal-on-Metal Total Hip Replacement: What Does the Literature Say?*, p. 175

[29] Hughes, S., McCarthy, I. (1998) *Science Basic to Orthopaedic* (Philadelphia: WB Saunders Company Ltd)

[30] Davis, J.R. (2003) *Handbook of Materials for Medical Devices* (ASM International)

[31] Bisno, A.L., Waldvogel, F.A. (1994) *Infections Associated with Indwelling Medical Devices* (Washington: ASM Press), p. 259

[32] Malchau, H., Herberts, P. (1996) *Prognosis of Total Hip Replacement: Surgical and Cementing Technique in THR* (63rd American Academy of Orthopedic Surgeons, Atlanta)

[33] Williams, D.F. (1984) *Biocompatibility of Orthopedic Implants* (Boca Raton: CRC Press)

[34] Schoen, F.J. (1996) *Biomaterials Science - An Introduction to Materials in Medicine: Host Reactions to Biomaterials and Their Evaluation* (San Diego: Academic Press), p. 165

[35] Anderson, F. M. (1993) *Mechanisms of Inflammation and Infection with Implanted Devices* (Cardiovascular Pathology Vol:2 No:3), p. 33-36

[36] Hutchings, I.M. (2003) *Friction, Lubrication, and Wear of Artificial Joints* (Bury St Edmunds: Professional Engineering Publishing), p. 1-6

[37] Wang, A. (1998) *Lubrication and Wear of Ultra-High Molecular Weight Polyethylene in Total Joint Replacement* (Tribology International), p. 31-33

[38] Devine, T. M., Wulff, J. (1975) *Cast vs. Wrought Cobalt-Chromium Surgical Implant Alloys* (Journal Biomedical Materials Vol. 9), p. 151-157

[39] ASTM: Annual Book of ASTM Standards (1992) (Philadelphia: American Society for Testing and Materials), F75-87 p.42, F90-87, p.47; F562-84, p.150

[40] Kilner, T., Laanemae, W.M., Pilliar, R.M. (1986) *Static mechanical Properties of Cast and Sinter-Annealed Cobalt-Chromium Surgical Implants* (Journal of Materials Science), p. 1349-1352

[41] Taylor, R.N.J., Waterhouse, R.B. (1983) *A Study of Aging Behaviour Of a Cobalt Based Implant Alloy* (Journal of Material Science), p. 3265

[42] Mishra, A.K., Hamby, M.A. (1999) *Cobalt-Base Alloys for Biomedical Applications: Metallurgy, Microstructure, Chemistry and Mechanical Properties of a New Grade of Cobalt-Chromium Alloy Before and After Porous-Coating* (West Conshohocken: ASTM), p. 71-88

[43] Kilner, T., Pilliar, R.M., Weatherly, G.C. (1982) *Phase Identification and Incipient Melting in a Cast Co-Cr Surgical Implant Alloy* (Journal of Biomedical Materials), p. 63-65

[44] Wang, K.K. (1999) *Cobalt-Base Alloys for Biomedical Applications: A Dispersion Strengthened Co-Cr-Mo Alloy for Medical Implants* (West Conshohocken: ASTM), p. 89-97.

[45] http://calphad.com/cobalt-chromium.html

[46] Pilliar, R.M. (2009) *Biomedical Materials: Metallic Biomaterials* (New York: Springer), p. 41-67

[47] Nevelos, J. (2004) *Metal Ion Release from Metal on Metal Hip Replacement Implants* (Hip International 14), p. 1-20

[48] Kamachi Mudali, U., Sridhar, T.M., Raj, R. (2003) *Corrosion of Bio-implants* (Sadhana Vol. 28), p. 601-637

[49] Williams, D.F. (1981) *In Fundamental Aspects of Biocompatibility: Electrochemical Aspects of Corrosion in the Physiological Environment* (Boca Raton: CRC press), p. 11-20

[50] Okazaki, Y., Gotoh, E. (2008) *Metal Release From Stainless Steel, CoCrMoNiFe and NiTi Alloys in Vascular Implants* (Journal of Corrosion Science, Elsevier), p. 3429-3438

[51] Von Recum,A.F. (1999) *Handbook of Biomaterials Evaluation Scientific, Technical and Clinical Testing of Implant Materials* (Philadelphia: Taylor & Francis)

[52] Manivasagam, G., Dhinasekaran, D., Rajamanickam, A. (2010) *Biomedical Implants: Corrosion and its Prevention - A Review* (Recent Patents on Corrosion Science), p. 40-54

[53] Dee, K.C., Puleo, D.A., Bizios, R. (2002) *An introduction to Tissue-Biomaterial Interactions* (New York: Wiley-Liss); p. 53-88

[54] Williams, D.F. (2003) *Biomaterials and Tissue Engineering in Reconstructive Surgery* (Sadhana Vol.28), p.563-574

[55] Aksakal, B., Yildirim, .S., Gul, H. (2004) *Metallurgical Failure Analysis of Various Implant Materials Used in Orthopedic Applications* (Journal of Failure Analysis and Prevention, Springer), p. 17

[56] Shreir, L.L., Jarman, R.A., Brustein, G.T. (1994) *Corrosion. Vol.1: Metal/Environment Reactions* (London: Butterworth Heinemann)

[57] Jones, D.E. (1996) *Principles and Prevention of Corrosion* (2nd Edition) (London: Macmillan Pub. Co)

[58] Kamachi Mudali, U. (1993) *Studies on Pitting, Intergranular Corrosion and Passive Film of Nitrogen Bearing Austenitic Stainless Steels* (PhD Thesis, University of Madras)

[59] Sivakumar, M., Kamachi Mudali, U., Rajeswari, S. (1994) *A Investigation of Failures in Stainless Steel Orthopaedic implant Devices*, Steel Res. 65: 76-79

[60] Bates, J.B. (1973) *Cathodic Protection to Prevent Crevice Corrosion of Stainless Steel in Halide Media* (Journal of Corrosion Science, Elsevier), p. 28-32

[61] Hu, J., Zhano, Z.J., Li, L.X. (1993) *Corrosion Fatigue Resistance of Surgical Implant Stainless Steels and Titanium Alloys* (Journal of Corrosion Science, Elsevier), p. 587-597

[62] Syrett, B.C., Wing, S.S. (1978) *An Electrochemical Investigation of Fretting Corrosion of Surgical Implant Materials* (Journal of Corrosion Science, Elsevier), p. 379-386

[63] Blackwood D.J. (2003) *Biomaterials: Past Successes and Future Problems* (Corrosion Reviews), p. 97-124

[64] Dong, H., Nagamatsu, Y., Chen, K.K. (2003) *Corrosion Behavior of Dental Alloys in Various Types of Electrolyzed Water* (Dental Materials Journal), p. 482-493

[65] Anusavice, K.J. (2003) *Phillips Science of Dental Materials* (London: Saunders), p. 411-434

[66] Sargeantm A, Goswami, T. (2006) *Hip implants: Physiological Effects* (Materials and Designs, Elsevier), p. 287-292

[67] Sachiko, H., Onodera, E., Akihiko, C., Katsuhiko, A., Hanawa, T. (2005) *Microstructure and Corrosion Behaviour in Biological Environments of the New Forged Low-Ni Co-Cr-Mo Alloys* (Biomaterials, Elsevier), p. 4912-4923

[68] Howling, G.I., Barnett P.I., Tipper, J.L., Stone, M.H., Fisher, J., Ingham, E. (2001) *Quantitative Characterization of Polyethylene Debris Isolated From Periprosthetic Tissue in Early Failure Knee Implants and Early and Late Failure Charnley Hip Implants* (Journal of Biomedical Materials Research), p. 415-420

[69] MacDonald, S.J., McCalden, R.W., Chess, D.G., Bourne, R.B., Rorabeck, C.H., Cleland, D. (2003) *Metal-on-Metal vs. Polyethylene in Hip Arthroplasty: A Randomized Clinical Trial* (Journal of Clinical Release Research), p. 282-296

[70] Schaffer, A.W., Pilger, A., Engelhardt, C., Zweymueller, K., Ruediger, H.W. (1993) *Increased Blood Cobalt and Chromium After Total Hip Replacement* (Journal of Clinical Toxicology), p. 839-844

[71] Shrivastava, R., Upreti, R.K., Seth, P.K., Chaturvedi, U.K. (2002) *Effects Of Chromium On The Immune System* (Immunology and Medical Microbiology, Elsevier), p. 1-7

[72] Kerger, B.D., Paustenbach, D.J., Corbett, G.E. and Finley, B.L. (1996) *Absorption and Elimination of Trivalent and Hexavalent Chromium in Humans Following Ingestion of a Bolus Dose in Drinking Water* (Journal of Toxicol. Appl. Pharmacol), p. 145-158.

[73] Bagchi, D., Stohs, S., Downs, B., Bagchi, M., Preuss, H. (2002) *Cytotoxicity and Oxidative Mechanisms of Different Forms of Chromium* (Journal of Toxicology), p. 5-22

[74] Granchi, D., Ciapetti, G., Savarino, L., Stea, S., Filippini, F., Sudanese, A. (2000) *Expression of CD69 Activation Antigen on Lymphocytes of Patients With Hip Prosthesis* (Journal of Biomaterials), p. 2059-2065

[75] Chen, F., Ding, M., Castranova, V., Shi, X. (2001) *Carcinogenic Metals and NF-κB Activation* (Journal of Molecular Cellular Biochemical), p. 159-171

[76] Dayan, A., Paine, A. (2001) *Mechanisms of Chromium Toxicity, Carcinogenicity and Allergenicity: Review of the Literature From 19852000* (Journal of Human and Experimental Toxicology), p. 439-445

[77] Plaper, A, Jenko-Brinovec, S., Premzl, A., Kos, J., Raspor, P. (2002) *Genotoxicity of Trivalent Chromium in Bacterial Cells Possible Effects on DNA Topology* (Journal of Chemical Research Toxicology), p. 943-949

[78] Vasant, C., Balamurugan, K., Rajaram, R., Ramasami, T. (2001) *Apoptosis of Lymphocytes in the Presence of Cr(V) Complexes: Role of Cr(VI)-induced Toxicity* (Journal of Biochemical & Biophysical Research Community), p. 1354-1360

[79] Kawanishi, S., Hiraku, Y., Murata, M., Oikawa, S. (2002) *The Role of Metals in Site-Specific DNA Damage with Reference to Carcinogenesis* (Radic Biol Med), p. 822-832

[80] Catelas, I., Petit,. A, Zukor, D., Antoniou, J., Hu,K. (2003) *TNF-α Secretion and Macrophage Mortality Induced by Cobalt and Chromium Ions in Vitro Qualitative Analysis of Apoptosis* (Journal of Biomaterials), p. 383-391

[81] Jones, D., Lucas, H., ODriscoll, M., Price, C., Wibberley, B. (1975) *Cobalt Toxicity After McKee Hip Arthroplasty* (Journal of Bone Joint Surg Br), p. 389-396

[82] Buzard, G., Kasprzak, K. (2000) *Possible Roles of Nitric Oxide and Redox Cell Signaling in Metal-Induced Toxicity and Carcinogenesis: A Review* (Journal of Environ Pathol Toxicol Oncol), p. 179-199

[83] Carter, D.E. (1995) *OxidationReduction Reactions of Metal Ions* (Environ Health Persp), p. 17-19

[84] Harris, G., Shi, X. (2003) *Signaling by Carcinogenic Metals and Metal-Induced Reactive Oxygen Species* (Mutat Res), p. 183-200

[85] Donati, M.E., Savarino, L., Granchi, D., Ciapetti, G., Cervellati, M., Rotini, R. (1998) *The Effects of Metal Corrosion Debris on Immune System Cells* (Chir Organi Mov), p. 387-393

[86] Yang, J., Merritt, K. (1994) *Detection of Antibodies Against Corrosion Products in Patients After CoCr Total Joint Replacements* (Journal of Biomedical Materials Research), p. 1249-1258

[87] Sargeantm, A., Goswami, T. (2007) *Hip implants: Ion concentrations* (Materials and Designs, Elsevier), p. 155-171

[88] Golub, E.S., Green, D.R. (1992) *Immunology: A Synthesis*, 2nd ed. (Sunderland: Sinauer Associates), p. 21-41

[89] http://www.ecochemie.nl/Products/Echem/PGSTAT128N.html

[90] http://www.solartronanalytical.com/Pages/Electrochemistry.htm

[91] Kissinger, P., William R. (1996) *Laboratory Techniques in Electroanalytical Chemistry*, 2nd ed. (Boca Raton: CRC Press)

[92] http://www.nrc-cnrc.gc.ca/eng/facilities/imaging/surface-morphology.html

[93] Contu, F., Elsener, B., Bohni H. (2005) *Corrosion Behaviour of CoCrMo Implant Alloy During Fretting in Bovine Serum* (Journal of Corrosion Science), p. 1863-1875

[94] Yan, Y., Neville, A., Dowson, D. (2005) *Tribo-Corrosion Properties of Cobalt-Based Medical Implant Alloys in Simulated Biological Environments* (Journal of Wear), p. 1105-1111

[95] Kocijan, A., Milosev, I., Merl, D.K., Pihlar, B. (2004) *Electrochemical Study of Co-Based Alloys is Simulated Physiological Situation* (Journal of Applied Electrochemistry), p. 517-524

[96] Contu, F., Elsener, B., Bohni H. (2003) *Electrochemical Behaviour of CoCrMo Alloy in the Active State in Acidic and Alkaline Buffered Solutions* (Journal of Electrochemical Society), p. 419-424

[97] Hryniewicz, T., Rokosz, K., Filippi, M. (2009) *Biomaterial Studies on AISI 316L Stainless Steel after Magnetoelectropolishing* (MDPI-Materials), p. 129-145

[98] Hodgson, A., Kurz, S., Virtanen, S., Fevrel, V., Olsson, C., Mischler, S. (2004) *Passive and Transpassive Behaviour of CoCrMo in Simulated Biological Solutions* (Journal of Electrochemical Society), p. 2167-2178

[99] Southampton Electrochemistry Group (1990) *Instrumental Methods in Electrochemistry* (Chichester: Ellis Horwood Ltd), p. 185-192

[100] Peissl, S., Mori, G., Leitner, H., Ebner , R., Eglsaer, S. (2006) *Influence of Chromium, Molybdenum and Cobalt on the Corrosion Behaviour of High Carbon Steels in Dependence of Heat Treatment* (New York: Wiley-Interscience), p. 759-765

[101] Campbell, C., Olso, G. (2001) *Systems Design of High Performance Stainless Steels I. Conceptual and Computational Design* (Journal of Computer-Aided Materials Design), p.145-170

[102] Varano, R. (2004) *Wear Behaviour of CoCrMo Alloys Used in Metal-on-Metal Hip Implants* (Montreal: PhD Thesis, McGill University)

[103] Shetty, H. R., Kosel, T. H., and Fiore, N. F. (1982) *A Study of Abrasive Wear Mechanisms Using Diamond and Alumina Scratch Tests* (Journal of Friction, Lubrication and Wear), p. 347-376

[104] http://www.nytimes.com/imagepages/2010/03/04/health/04metalhipGraphic.html?ref=health